IMPACTS OF CLIMATE CHANGE AND ANTHROPOGENIC ACTIVITIES ON CATCHMENT WATER BALANCE AND HYDROLOGIC EXTREMES

Maochuan Hu

2016

IMPACTS OF CLIMATE CHANGE AND ANTHROPOGENIC ACTIVITIES ON CATCHMENT WATER BALANCE AND HYDROLOGIC EXTREMES

(流域水収支と水文極値に対する気候変動及び人間活動の影響)

by

Maochuan Hu

A dissertation
Submitted in partial fulfillment of the requirements for the
Degree of Doctor of Engineering

Department of Civil and Earth Resources Engineering

Kyoto University, Japan

2016

Acknowledgements

Time flies! It is my fourth year in Professor Takara's Laboratory, Disaster Prevention Research Institute (DPRI), Kyoto University. I gained a great deal of knowledge and various skills in these more than 3 years. There were pleasures and pains during the PhD study, which are unforgettable experiences in my whole life. I would like to acknowledge all the people giving helps to me.

I would like to express my deepest appreciation to my supervisor Professor Kaoru Takara. Without his help, I would not have the chance to study in Kyoto University. Also, he gave me guidance, encouragement and faith towards my research. He provided me many chances to attend international conferences and activities to communicate and study with other researchers. Moreover, He cared for my life conditions, held birthday party for me and other members and gave us feelings of family. I am proud of a member of Takara's family.

I would also like to give my great gratitude to Associate Professor Takahiro Sayama. It is lucky for me to have the chance to study from him in my last year of PhD course study. He taught me how to do research and write papers. He also helped me to collect data and modify my thesis. We had many pleasant discussions on my research.

In addition, I would like to express my appreciation to Professor Bin He for his help for my study. He guided and supported my research and gave me much help on the life when he was a projected associate professor in DPRI. He also supported and gave me the chance to study from him when he has become a professor in China.

I would also like to give my thanks to my sub-supervisors Professor Yasuto Tachikawa and Professor Eiichi Nakakita. Appreciations and acknowledgements are also towards Professor Yosuke Yamashiki, Professor Tetsuya Sumi, Professor Kenji

Tanaka, Professor Tomoharu Hori, Professor Srikantha Herath, Associate Professor Masahito Ishihara and Assistant Professor Keisuke Himoto for their kind suggestions and comments on my research.

Also, I would like to give my gratitude to the Ms. Sono Inoue, Ms. Kaori Saidera, Ms. Mayumi Nishimura, Ms. Saho Matsuda and Ms. Yoko Yonekawa for their kind assistance for me and the other members.

Lovely thanks are also for my dear members. They are Dr. Apip, Dr. Luo, Dr. Emmanuel, Dr. Maja, Dr. Nga, Dr. Teramoto, Dr. Alias, Dr. Duan, Dr. Khang, Mr. Vilaysane, Mr. Josko, Mr. Hendy, Mr. Xue, Ms. Eunbi, Ms. YongA, Mr. Azuma, Mr. Sasaki, Mr. Kurokawa, Mr. Tien, Mr. Loi, Mr. Adnan, Mr. Goto, Ms. Chong, Ms. Siska, Ms. Shi, Ms. Karlina, Ms. Jamila, Mr. Toma, Mr. Takahashi, Mr. Ushiro, Mr. Kobayashi and Mr. Yamamoto.

The appreciations are also to my darling wife for her sacrifices, patience and care towards me and our son. In addition, I would like to give thanks to my grandfather for his encouragement for my study. He left me forever last year. Hope him well in heaven. “Grandfather, I miss you.” Also, I wish to thank my grandmother and father for their love and support.

Finally, I gratefully acknowledge the financial support from the China Scholarship Council (CSC) and Murata Overseas Scholarship Foundation. Moreover, this thesis is supported by the Kyoto University Global COE Program: “Sustainability/Survivability Science for a Resilient Society Adaptable to Extreme Weather Conditions” (Program Leader: Kaoru Takara).

DPRI, Kyoto University

November, 2015

Abstract

In the last decades, the relentless usage of fossil fuel, growth of population, migration to urban areas, land use transition and consequent global climate change have altered water cycle, which might increase the risk of water-related disasters and bring challenges to water resource management. Water planning has to consider not only disaster management but also the multi-purposes of water facilities in hydro-power, irrigation, water supply, environment, etc. Understanding hydrological processes and predicting the variations in water cycle in the context of climate change, land use change and current water management are necessary for sustainable water resources management. The Kamo River is an important culture carrier in Kyoto-city, the historical capital of Japan. There are many landscapes distributed along the river. Also, the river bank is a famous place for sightseeing and attracts many tourists and local inhabitants every year to visit. The variations of the Kamo River discharge have significant impact on the water-related landscapes including freshwater habitat. Due to Baiu front and typhoons, the Kamo River basin has been vulnerable to floods and suffered from disastrous floods in the history. This study conducts integrated impact analysis of climatic variability, land use change and water management on the water resource distribution in the Kamo River basin. The main purpose is to assess the changes in long-term average conditions and extreme events of hydro-climatic variables from 1962 to 2014 and find the reasons and contributions to these changes.

Firstly, homogeneity is tested in all observed data using the family of Levene's F tests to adjust the non-homogeneities. Homogeneity test is an important step in hydrological statistical analysis, especially for this study in the Kamo River basin. This is because the observed river discharge shows unrealistic high values in some years.

After the homogeneity test, trend analysis is conducted in precipitation, temperature, river discharge and potential evapotranspiration at different time scales to detect the modifications in water cycle and potential probability in the future, which is useful for water resource management and planning. In order to reduce the uncertainties from statistical methods, the parametric linear regression t-test is used to detect the no data missing variables with normal distribution. Non-parametric Mann-Kendall test and Sen's Slope estimator are also used to test for the other variables. Normality of variables is analyzed by Shapiro-Wilk test. The results show that there was a statistically significant downward trend in river discharge at both annual and seasonal scales. The changes in potential evapotranspiration are related to changes in temperature. All the temperature and evapotranspiration variables increased significantly from 1962 to 2014. For the basin average precipitation, a significant upward trend was observed in winter, actually in February and December. In addition, the change in precipitation at a location is likely to be not in correspondence with basin average precipitation variations.

The dominant cause of the decreasing trend in the river discharge at the outlet of the Kamo River basin was investigated by using water balance analysis and hydrological simulation. First, the "natural streamflow" from 1989 to 2010 is estimated to calibrate and validate a hydrological model (Hydrological Predictions for the Environment model) by excluding the impact of water management from observed discharge based on water balance analysis. Then, the "natural streamflow" (no effects from water management) and "climatic streamflow" (no effects from land use change) from 1962 to 2010 are generated by hydrological simulation using the calibrated and validated model. Finally, the contributions of precipitation, evapotranspiration, land use and water resource management are evaluated by comparing the differences in average values of observed streamflow, "natural streamflow" and "climatic streamflow" from

the period 1962-1976 to the period 1996 to 2010 at annual, seasonal and monthly scales. It was estimated that the decreasing trend in river discharge was primarily caused by the increase of drainage areas of the sewer system in Kyoto city and the reduction of intake from Lake Biwa canal to the Kamo River. These effects, which resulted in a decrease of 502.5 mm in annual average river discharge, diminish the effect of slight increase in the annual precipitation and suppress the increase in evapotranspiration in the Kamo River basin. The combined impact of precipitation and evapotranspiration resulted in a slight increase in annual river discharge (about 32.3mm) and varied at seasonal and monthly scales. The impact of land use is small.

Lastly, a variety of extreme indices of precipitation, temperature and river discharge are analyzed based on observed and simulated records. The changes of hydrological extremes (100-year events) in magnitude and frequency from the period 1962-1988 to the period 1989-2014 are quantified by inverse cumulative distribution functions using the defined extremes indices. Three probability distributions (Log-normal 3p, generalized extreme-value and Gamma 3p) are used in this study. The distribution with the best fit to extreme indices is selected by four criteria based on goodness of fit test. The results show that generalized extreme-value distribution is adequate for most of extreme indices. In the Kamo River basin, maximum temperature have increased over 1962-2014. The changes in extreme streamflow are highly correlated with the changes in extreme precipitation and there was an increase in the occurrence of flood and a decrease in the occurrence of drought. The magnitude of 100-year events of annual hourly maximum precipitation and annual hourly peak flow increased by 41% and 23%, while 100-year events of annual maximum consecutive dry days (daily precipitation$<$1 mm) and annual maximum consecutive low flow days (daily

streamflow＜the value of 10^{th} percentile in the period 1981-2010) decreased by -22% and -34%, respectively.

In general, it was estimated that the decreasing trend in river discharge was dominantly caused by water management, which diminished the effect of slight increase in the annual precipitation and suppressed the effect of the increase in evapotranspiration. In addition, the occurrences of floods and extreme heat events have increased while the occurrence of droughts has decreased. The knowledge of integrated impacts of climate change and anthropogenic activities and information of potential changes in hydrological extremes are useful for the sustainable water resource management and planning in the Kamo River basin. Moreover, the defined extreme indices can be future used in other areas for hydrological extreme analysis. Furthermore, the coupled methods of water balance analysis and hydrological simulation are transferable to the basins which are highly managed and affected by human activities.

Contents

List of Figures

List of Tables

Chapter 1 Introduction

1.1 Background

The importance of water is self-evident. It is the source of life, essential of social-economic development and cornerstone of environment. Water is not stationary and it is a cycle related to climatic system (e.g. precipitation and temperature), land cover system (e.g. land use) and water resource management system (e.g. canals and reservoirs). The growth of population and development of industrialization bring larger demand of water. The changes in climatic system, especially in extremes events are likely to result in the increase of disaster occurrences. In addition, due to urbanization, a mass of population and treasure are concentrated in cities. Urban vulnerability becomes higher. All of these bring challenges to water resource management. The current water management constructions like dams and urban sewage systems may not adapt to the new uncertainties. It is necessary to assess and predict the variations in water cycle and plan measures to adapt future potential uncertainties in the context of climate change, land use change and the current water management.

IPCC AR5 concluded that “warming of the climate system is unequivocal” and “heavy precipitation events are very likely to increase in the frequency and intensity over most of the mid-latitude land masses and over wet tropical regions”. The changes in climatic system will affect the spatiotemporal distribution of river discharge (Takara and Kojiri, 1993; Parr and Wang, 2014). The uneven distributed and irregular extreme precipitation events at global resulted in large floods and caused tremendous damage in

different regions, such as 2011 Thailand floods, 2011 Tohoku tsunami and 2015 Kinugawa river floods in Japan, etc. It is essential to assess the potential changes and impacts of climatic system on water resources at basin scale.

As we know, current extents and intensities of land cover and land use change are great due to industrialization and population dynamics. For example, urban population in Japan increased about 10% from 1960 to 1970 and in China increased from about 36% to 47% in the period 2000-2010. Land cover and land use play a major role in hydrological cycle. The changes in land use will cause changes in hydrological variables like runoff, groundwater and evapotranspiration. For instance, the increase of impervious lands due to urbanization results in earlier and higher peak flow, which bring in great pressure on urban sewer system and the risk of sewer floods increasing (Braud et al., 2013). It is evidence that the frequently occurred urban waterlogging events in recent years in China are due to extreme precipitation and low drainage capacity of sewer system (Zhang et al., 2012; Zhang et al., 2014). It is merit to evaluate the impact of land use change on water source at regional scale.

Water resource management in Japan has begun from thousands years ago. There are many dams and canals over Japan with multi-purposes like disaster control, hydropower and irrigation. The water cycle is affected by the operation of these constructions. It is of significance to estimate the effects of water resource management and plan sustainable water management to face a series of uncertainties due to the increase demand of water, land use change and climatic variability.

Kyoto city was the capital of Japan since 794 and has more than 1200 years' history. Due to Baiu front and typhoons, the basin of the Kamo River flowing through Kyoto city has been vulnerable to floods and suffered from some disastrous floods in the history. Table 1-1 shows the number of floods in the Kamo River basin from 1000 to

2000. Recently largest flood occurred in 1935. 27% of flat land was inundated and there were about 160 victims and hundred thousand affected persons. The number of floods in the period 1951-2000 was relatively lower than previous 50 years. There were also some extreme events occurring in recent 10 years. For example, during typhoon No. 11 in 2015, the highest water level at the Kojinbashi station in the Kamo River was more than the danger level of flood by 0.1 m. This thesis focuses on the integrated impact of climatic variability, land use change and water management on water cycle and the changes in extreme events in the Kamo River basin.

Table 1-1 Number of floods in the Kamo River basin in the history

Period	1000 | 1100	1101 | 1200	1201 | 1300	1301 | 1400	1401 | 1500	1501 | 1600	1601 | 1700	1701 | 1800	1801 | 1900	1901 | 1950	1951 | 2000
Number	11	7	7	4	34	13	15	26	11	10	6

Data source: Nakajima (1983) and Uemura (2011)

1.2 Problem statement

The topic of trend analysis is popular and important in hydrological sciences. Understanding the changes in hydro-meteorological variables is useful for regional water resource applications, basin water management and hydraulic structure deign (Bae et al., 2008). Using GCM data, Kurihara et al. (2005) concluded that increased daily precipitation will be seen from June to September in the period 2081-2100 in the western part of Japan. Based on 51 weather stations over Japan, Duan et al. (2015) reported annual and seasonal precipitation exhibited a decrease at 49 stations from 1901 to 2012. In addition, trend detection was conducted in precipitation in Miyazaki

(Takeshita, 2010) and Tokyo (Kanae et al., 2004), and in river discharge in the Mogami and Yoshino River basins (Tachikawa et al., 2009). From these studies, it was found that the changes at different stations and different spatial scales were different. It is necessary to conduct research on each basin with local historic data. To date, there is no study on the changes in precipitation, temperature and river discharge in the Kamo River basin.

The impact of climate change is of a high degree of regional dependence due to the spatial variability of climate change. Many studies have been conducted on climate change impact in Japan (Kameyama, 2002). Fujihara et al. (2006) presented that annual river discharge in the Tone River basin increased by about 160 mm from the period 1981-2000 to the period 2081-2100. Wada et al. (2005) estimated the effects of global warming on flood and drought risk over Japan using MRI-RCM20 data. However, there are few studies that estimate the impact of climate variability in recent years in the Kamo River basin. In addition, most of studies are taken using daily or monthly data. The applications at hourly scale are not abundant.

Japan is a country with high vulnerability to water-related disasters and there are many water management structures over Japan. It is of importance to monitor and evaluate the variations of water resource under water management. Yoshimura and Koike (2015) evaluated dam volume reallocation under climate change in the Kono River basin. Satoh et al. (2015) reported that effective water management could mitigate natural variability of drought and alleviate the increasing rate of the drought days due to global climate change. Also, Sayama et al. (2008) reported that the frequency of emergency operation by the Hiyoshi dam in Katsura River basin seemed to increase in the period 2031-2050. In the Kamo River basin, water resource is related to the operation of Lake Biwa canal and Kamo river canal which exist more than 100 years.

And few studies have been considered the impact of them and the combined effects with climate and land use changes.

Land cover and land use change impacts are conducted in many basins of Japan including the Kamo River basin (Fan and Shibata, 2015; Ishida and Miyamoto, 2012). Luo et al. (2014) evaluated the impact on peak flow by palaeo-flood simulation using historic land use data at 1902. However, the integrated impact of land use change, climate variability and water resource management is not studied in the Kamo River basin.

Extreme events and their changes are of particular crucial for society and ecosystems due to their potentially severe impacts (Special Report on Extreme Events of IPCC, 2012). Plentiful studies have reported the evidence of extreme changes over the world including Japan (Borth et al., 2015; Ohba et al., 2015; Saidi et al., 2015). Most notably, Fujibe et al. (2005, 2006) argued that the extreme daily precipitation, four-hourly and hourly precipitation increased over Japan in the past century. Tachikawa et al. (2011) found that there was an increase in the means of annual maximum hourly discharge from the period 1979-2003 to the period 2075-2099 over south regions of Kinki, Japan. However, to date extreme analysis in small river basins is less done and most of studies focus on large regional and national scales. The indices of precipitation and temperature have been widely used in extreme analysis. Few studies evaluated hydrological extremes using a series of indices of river discharge.

1.3 Research objectives and scopes

Based on the problems mentioned in the above section, the overall purpose of this research is to assess the changes of hydro-climatic variables in long-term average

conditions and extreme events from 1962 to 2014, and to find the reasons and contributions to these changes in the context of climatic variability, land use change and water resource management. The main objectives are as follows:

(1) **To detect the monotonic trends in precipitation, temperature, potential evapotranspiration and streamflow at different time scales and to quantify the magnitude of trend slope and significance of trends.** First, the non-homogenies in the data are removed based on homogeneity test. Then, potential evapotranspiration is generated using the equation of Penman-Monteith FAO 56. Finally, according to the results of normality test, the trends and slopes in annual, seasonal and monthly variables with normal distribution are detected using linear regression t-test, while the trends and slopes in the variables without normality are detected using non-parametric Mann-Kendall test and Sen's Slope estimator.

(2) **To investigate the dominant reasons for the streamflow changes and to estimate the relative contributions of the changes in precipitation, evapotranspiration, land use and water resource management to the changes of streamflow.** First, the "natural streamflow" from 1989 to 2010 is estimated by excluding the impact of water management from observed discharge based on water balance analysis. Then, the "natural streamflow" and "climatic streamflow" (no changes in land use) from 1962 to 2010 are calculated by HYPE-model simulation, which are calibrated and validated using the water balance-generated 1989-2010 "natural streamflow". Finally, the changes in annual, seasonal and monthly average values of water balance variables from the period 1962-1976 to the period 1996 to 2010 are discussed and the contributions of precipitation, evapotranspiration, land use and water resource management are evaluated.

(3) **To develop indices for hydro-climatic extremes analysis and to estimate the**

changes of extreme hydro-climatic events which are defined by extreme indices. First, a series of extremes indices of precipitation, temperature and river discharge are defined or referred by literature review, which can be future used in other regions of Japan. Then, the extreme indices are fitted for three probability distributions and the distribution with the best fit is selected for frequency analysis according to the results of goodness of fit test. Finally, the changes of extreme indices from the period 1962-1988 to the period 1989-2014 are quantified in magnitude and frequency using inverse cumulative distribution functions.

1.4 Thesis Organization

Figure 1-1 shows the framework of the thesis. There are seven chapters and each chapter is outlined as follows:

Chapter 1 describes the background, the scientific problems the study wishes to assess, the objectives and scopes, the organization and framework of the dissertation.

Chapter 2 gives the detailed information of the Kamo River basin characteristics and the database used for the research including meteorological data, topographic data and water management data.

Chapter 3 introduces the Hydrological Predictions for the Environment model including general structure, partial important components used for the simulation in this study and the methods of model calibration and validation.

Chapter 4 evaluates the monotonic trends in precipitation, temperature, river discharge and potential evapotranspiration at annual, seasonal and monthly scales from 1962-2014. Before trend detection, homogeneity check by Levene's test and normality analysis by Shapiro-Wilk test are conducted. No data missing variables with normal

distribution are detected by linear regression t-test, others are tested by Mann-Kendall test and Sen's Slope estimator. The results show the decreasing river discharge is not dominantly caused by climatic variability, which requires future studies on the reasons of the decrease in river discharge.

Chapter 5 presents the contribution of water resource management, land use, precipitation and evapotranspiration (temperature) to the changes of river discharge by applying calibrated and validated HYPE model over the Kamo River basin. The impact of water resource management on streamflow is separated by water balance analysis. And the impact of climatic variability and land use changes are divided based on HYPE model-simulation by controlling the land use data during simulation. After the long-term changes of average conditions and the reasons for these changes are known, it is necessary to discuss the changes of extremes which are of high important to basin disaster management.

Chapter 6 investigates the changes of extreme events from the period 1962-1988 to the period 1989-2014 by frequency analysis using a series of extreme indices of precipitation, temperature and river discharge. The changes of extreme indices are quantified in magnitude by the changes of 100-year event and in frequency by the changes of return period with the value of 100-year event in the period 1962-1988 using inverse cumulative distribution functions which are selected by goodness of fit test.

Chapter 7 summaries the important conclusions presented in the previous chapters. The limitations of this thesis and future concerns are also discussed in this chapter.

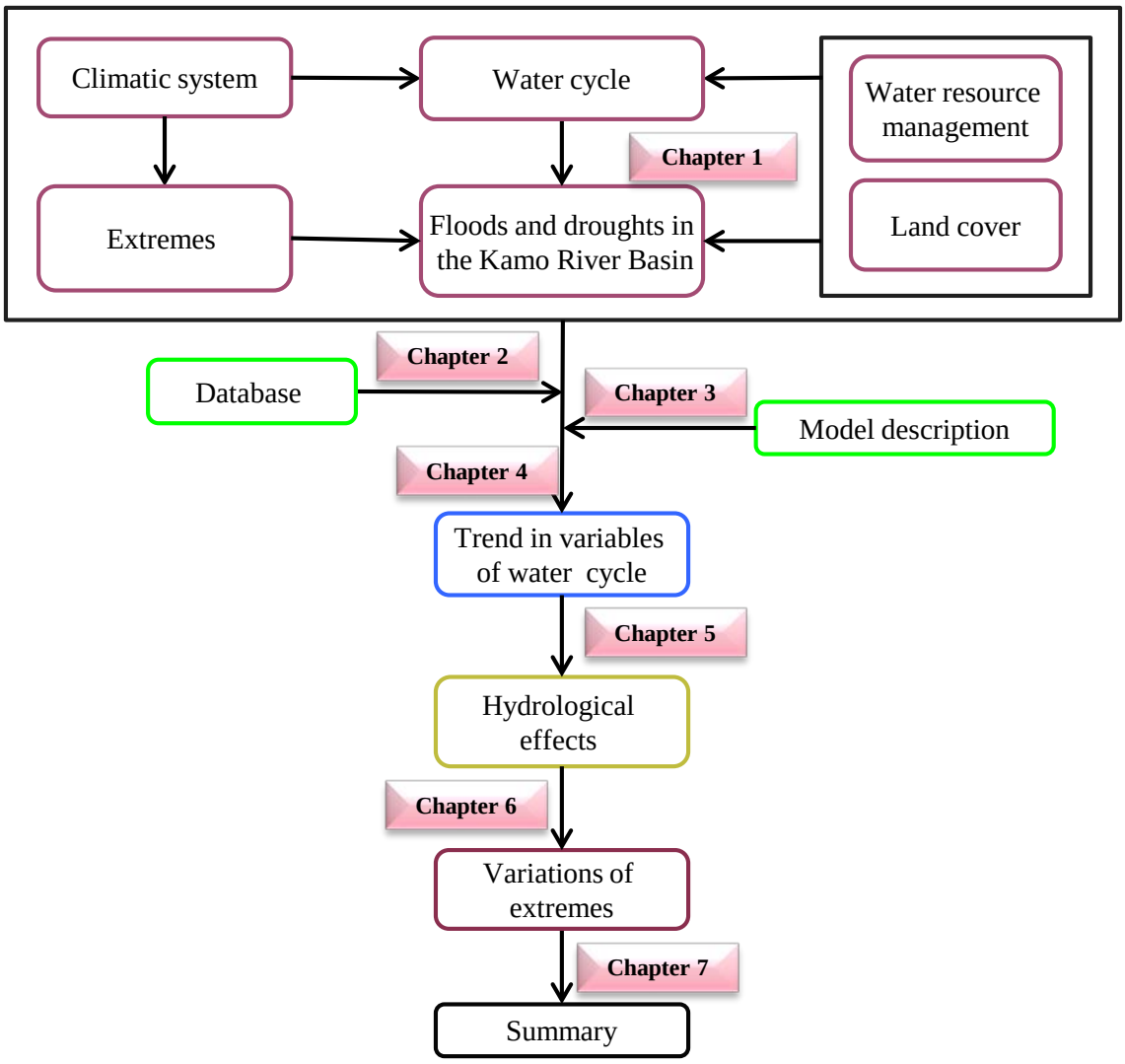

Figure 1-1 Framework of the thesis

Reference

Bae DH, Jung IW and Chang H, 2008. Long‐term trend of precipitation and runoff in Korean river basins. *Hydrological Processes* 22, 2644-2656.

Borth H, Tao H, Fraedrich K, Schneidereit A and Zhu X, 2015. Hydrological extremes in the Aksu-Tarim River Basin: Mid-latitude dynamics. *Climate Dynamics*, 1-12.

Braud I, Breil P, Thollet F, et al., 2013. Evidence of the impact of urbanization on the hydrological regime of a medium-sized periurban catchment in France. *Journal of*

Hydrology 485, 5-23.

Duan W, He B, Takara K, et al., 2015. Changes of precipitation amounts and extremes over Japan between 1901 and 2012 and their connection to climate indices. *Climate Dynamics* 45, 2273-2292.

Fan M and Shibata H, 2015. Simulation of watershed hydrology and stream water quality under land use and climate change scenarios in Teshio River watershed, northern Japan. *Ecological Indicators* 50, 79-89.

Fujibe F, Yamazaki N, Katsuyama M and Kobayashi K, 2005. The increasing trend of intense precipitation in Japan based on four-hourly data for a hundred years. *Sola* 1, 41-44.

Fujibe F, Yamazaki N and Kobayashi K, 2006. Long-term changes of heavy precipitation and dry weather in Japan (1901-2004). *Journal of the Meteorological Society of Japan* 84, 1033-1046.

Fujihara Y, Ode M, Kojiri T, Tomosugi K and Irie H, 2006. Effects of Global Warming on the Water Resources of the Tone River Basin. *J. Japan Soc. of Civil Eng.* 50, 367-372. [In Japanese]

Ishida K and Miyamoto H, 2012. Flow Regime Estimation in River networks Using Link Magnitudes with Climate, Geology and Land Use Conditions. *J. Japan Soc. of Civil Eng.* 68, I_487-I_492. [In Japanese]

Kameyama Y, 2002. Climate change and Japan. *Asia Pacific Review* 9 (1), 33-44.

Kanae S, Oki T and Kashida A, 2004. Changes in hourly heavy precipitation at Tokyo from 1890 to 1999. *Journal of the Meteorological Society of Japan*, Ser. II 82, 241-247.

Kurihara K, Ishihara K, Sasaki H, et al., 2005. Projection of climatic change over Japan due to global warming by high-resolution regional climate model in MRI. *Sola* 1,

97-100.

Luo P, Takara K, Apip, He B and Nover D, 2014. Palaeoflood simulation of the Kamo River basin using a grid-cell distributed rainfall run-off model. *Journal of Flood Risk Management* 7, 182-192.

Nakajima C, 1983. Historical Review of the Floods Of the Kamo River in Kyoto (1). *Disaster Prevention Research Institute Annuals* 26B, 75-92. [In Japanese]

Ohba M, Kadokura S, Yoshida Y, Nohara D and Toyoda Y, 2015. Anomalous Weather Patterns in Relation to Heavy Precipitation Events in Japan during the Baiu Season. *Journal of Hydrometeorology*, 688-701.

Parr D and Wang G, 2014. Hydrological changes in the U.S. Northeast using the Connecticut River Basin as a case study: Part 1. Modeling and analysis of the past. *Global and Planetary Change* 122, 208-222.

Saidi H, Ciampittiello M, Dresti C and Ghiglieri G, 2014. Assessment of Trends in Extreme Precipitation Events: A Case Study in Piedmont (North-West Italy). *Water Resources Management* 29, 63-80.

Satoh Y, Yoshimura K, Kim H, and Oki T, 2015. Study on Impact of the Water Resources Management on Projected Future Change of Drought. *J. Japan Soc. of Civil Eng.* 59, I_391-396. [In Japanese]

Sayama T, Tachikawa Y, Takara K, Masuda A and Suzuki T, 2008. Evaluating the impact of climate change on flood disasters and dam reservoir operation in the Yodo river basin. *Journal of Japan Society of Hydrology and Water Resources* 21, 296-313. [In Japanese]

Tachikawa Y, Takino S, Ichikawa Y and Shiiba M, 2009. Study on the Impact of Climate Change on River Flow Regime in the Mogami and Yoshino River Basins, . *J. Japan Soc. of Civil Eng.* 53, 475-480. [In Japanese]

Tachikawa Y, Takino S, Fujioka Y, Yorozu K, Kim S and Shiiba M, 2011. Projection of river discharge of Japanese river basins under a climate change scenario. *J. Japan Soc. of Civil Eng.* 67, 1-15. [In Japanese]

Takara K and Kojiri T, 1993. Numerical experiments on effects of global warming on catchment response change. *J. Japan Soc. of Civil Eng.*, 1-10. [In Japanese]

Takeshita S, 2010. Influence on precipitation and the distribution in Miyazaki [Japan] Prefecture with climate changes. *Bulletin of the Faculty of Agriculture, Miyazaki University*, 73-78. [In Japanese]

Uemura Y, 2011. Flood Control of Kyoto Basin and the 1935 Biggest Flood Damage of Kyoto in the Showa Era. Bunrikaku, Kyoto. [In Japanese]

Wada K, Murase M and Tomizawa Y, 2005. Study on the Variation of Rainfall Characteristic and Flood and Drought Risks Assessment of Global Warming. *J. Japan Soc. of Civil Eng.*, 23-37. [In Japanese]

Yoshimura K and Koike T, 2015. Dam Volume Reallocation between Flood Control and Water Use as an Adapting Policy under Climate Change in Kino River Basin. *J. Japan Soc. of Civil Eng.* 59, I_385-390. [In Japanese]

Zhang X, Hu M, Chen G and Xu Y, 2012. Urban Rainwater Utilization and its Role in Mitigating Urban Waterlogging Problems—A Case Study in Nanjing, China. *Water Resources Management* 26, 3757-66.

Zhang XQ and Hu MC, 2014. Effectiveness of Rainwater Harvesting in Runoff Volume Reduction in a Planned Industrial Park, China. *Water Resources Management* 28, 671-82.

Chapter 2 Study Area and Data

2.1 Study area

The study site is the upstream of Fukakusa station (34.9661N, 135.7592E) in the Kamo River basin, located in Kyoto (Figure 2-1). The area is 180km^2, with mountain terrain comprising about 70% of the surface, ranging in elevation from 17 m to 888 m. The river, about 31 km, flows through Kyoto city, eventually empties into the Katsura River, supporting about 1.5 million residents. The annual rainfall is about 1491 mm and more than 80% of precipitation is concentrated from March to October. The daily mean air temperature is about 16°C, ranging from -3°C to 33°C.

Kyoto is a historical city famous for many cultural heritages and also water-related landscapes, whose large part of water is distributed through the Kamo River. The water terrain of Kamo River is a popular sightseeing place for local residents and tourists. There are open pathways along or across the river and abundant freshwater fish in the river. The variations of the Kamo River discharge have significant impact on the water-related landscapes including freshwater habitat. Modern water management in Kyoto has begun about hundreds of years ago. Most notably, Lake Biwa canal, a waterway to transport water from Lake Biwa to Kyoto city, has also more than 100 years history. The water from Lake Biwa is used for potable water, uptake to the Matsugasaki filtration plant, Keage filtration plant and Shin-Yamashina filtration plant. The left water flows through Kamo River Canal into the Uji River. Also, there are some human controlled outlets along Kamo River Canal connected to the Kamo River, e.g.

Reizei outlet, Nioumo outlet and Shiokouji outlet shown in Figure 2-2. In some special time, water in Kamo River Canal also flows into the Kamo River through these outlets under water management. In addition, rainwater, flows into urban sewerage system, is treated at the Toba treatment plant and eventually empties into the downstream of Fukakusa station in the Kamo River basin. The location of Toba is shown in Figure 2-1 and the sewage map is displayed in Figure 2-3.

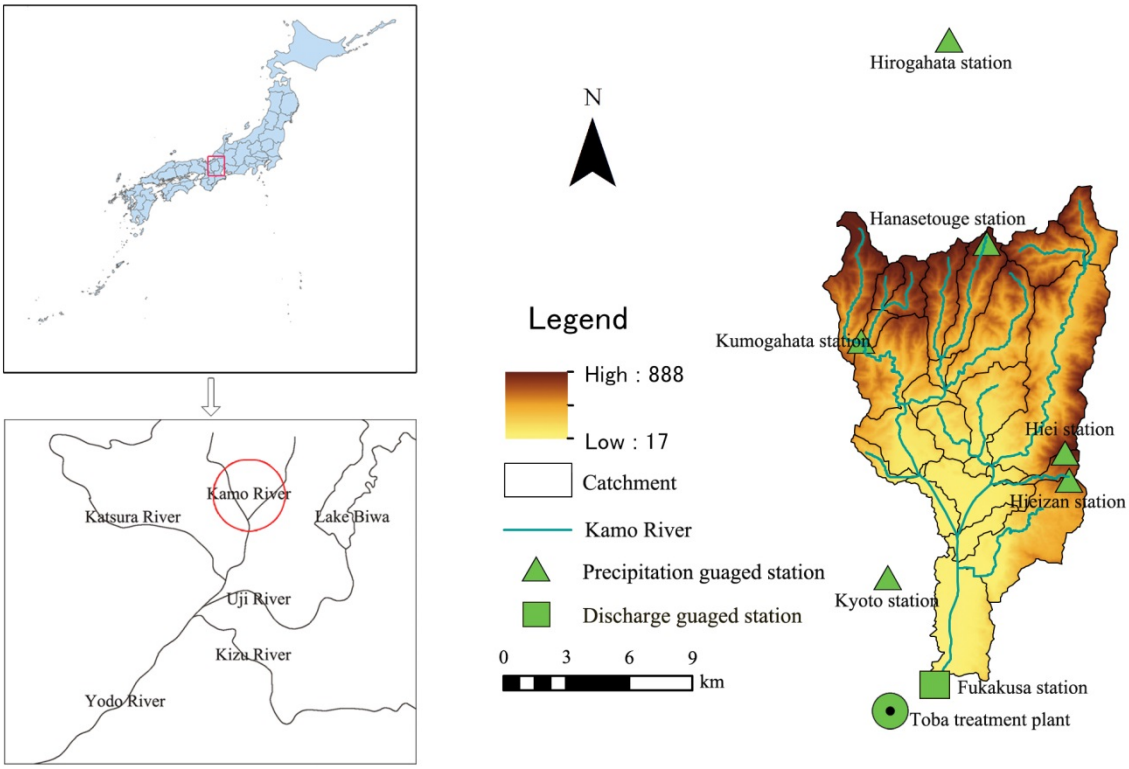

Figure 2-1 Location of the study area

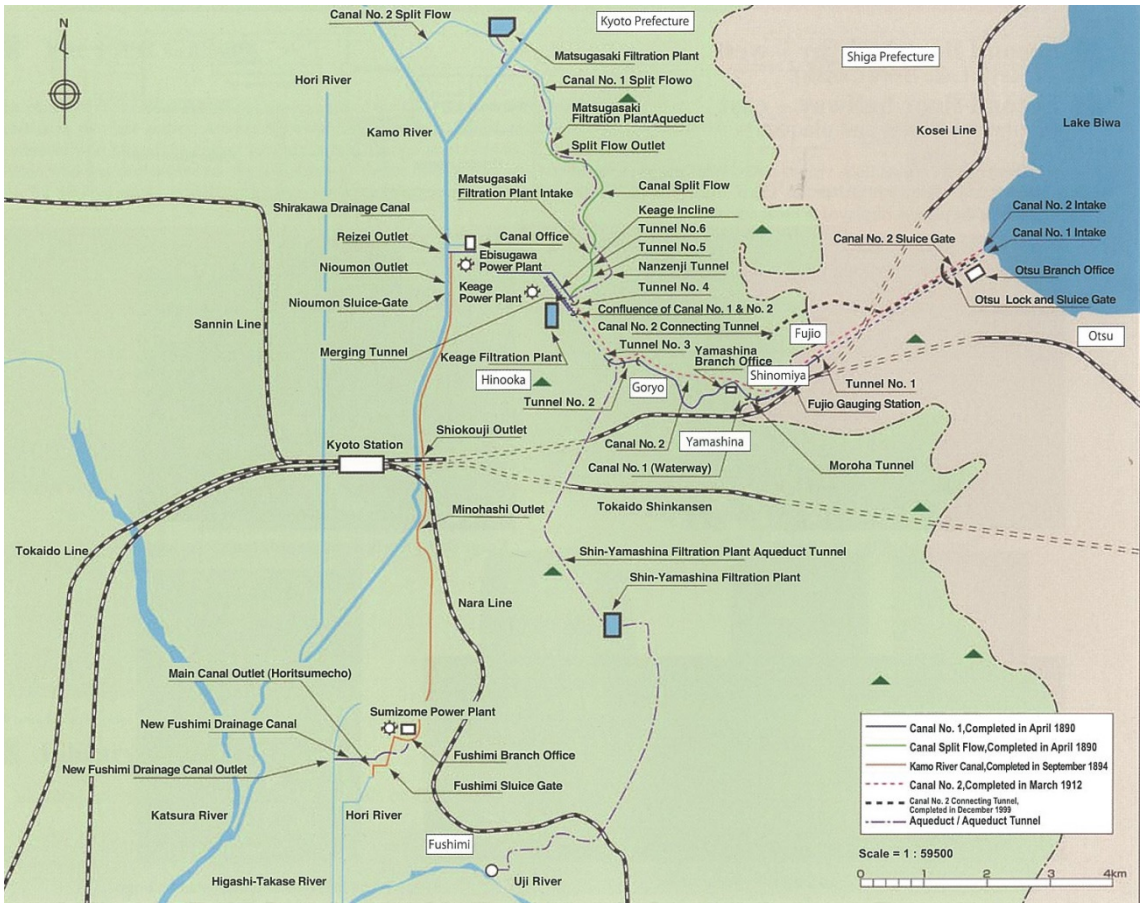

Figure 2-2 Map of the Lake Biwa Canal area (from Lake Biwa Canal Museum of Kyoto)

2.2 Data source

The data used in this study is listed in Table 2-1, including meteorological data, water resource management related data and geographical data. Kyoto station has the longest data series with best data quality. Except hourly temperature and precipitation, the daily data of wind speed, humidity, actual duration of sunshine and shortwave radiation at Kyoto station are also collected and used for potential evapotranspiration estimation. Excluding Kyoto station, there are five precipitation gauged stations in or around the Kamo River basin. The periods of data series and missing records vary at different stations. For instance, the records of daily precipitation at Kumogahata are from 1942 to 2014 and hourly records started in 1964 until 2009. While hourly records

at Hiezan station are from 1963 to 2000. Basin average precipitation of the Kamo River basin is calculated with Thiessen polygon interpolation. Observed daily long-term river discharge data from 1962 to 2010 (hourly records in the period from 1970 to 2010) is obtained from the Japan Ministry of Land, Infrastructure, Transport and Tourism (MLIT).

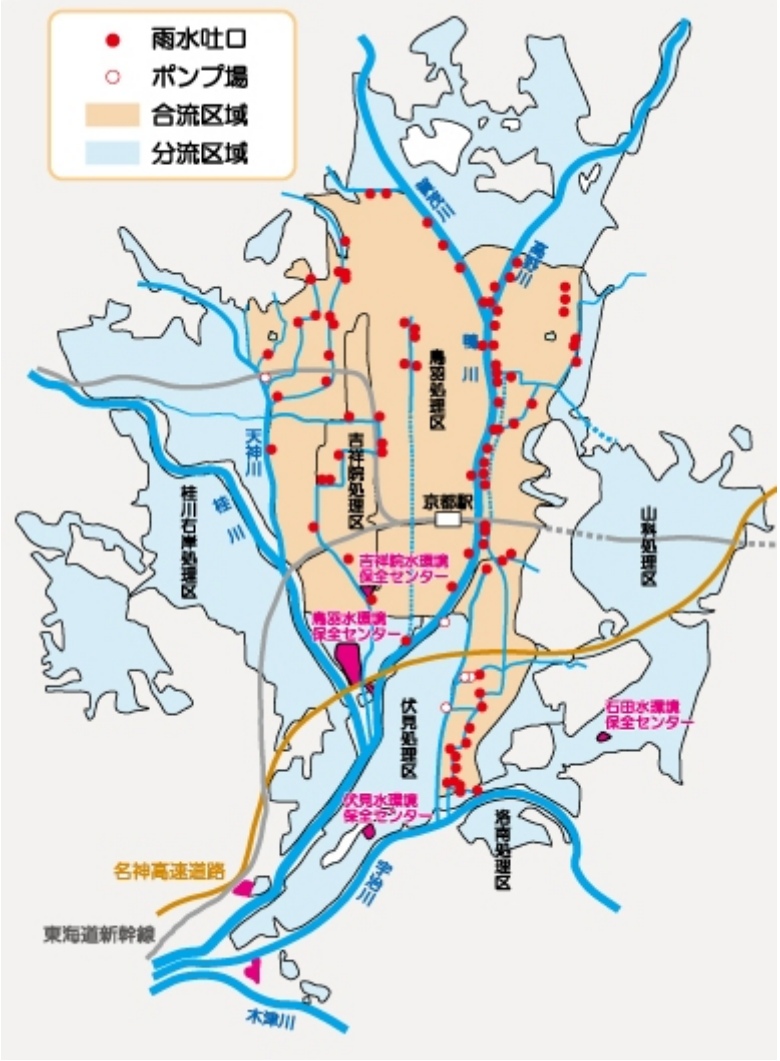

Figure 2-3 Map of sewerage drainage system in Kyoto (from Kyoto City Waterworks Bureau)

Table 2-1 Input data characteristics

Data type and station	Station	Period	Source	Data quality
Precipitation	Kyoto	1881-2014	JMA	Hourly, no data missing
Temperature	Kyoto	1881-2014	JMA	Hourly, no data missing
Wind speed	Kyoto	1943-2014	JMA	Daily, no data missing
Humidity	Kyoto	1961-2014	JMA	Daily, no data missing
Sunshine duration	Kyoto	1961-2014	JMA	Daily, no data missing
Precipitation	Hieizan	1963-2000	MLIT	Hourly, many data missing
Precipitation	Kumogahata	1942-2014	MLIT	Hourly from 1964 to 2009, others with daily records, many data missing
Precipitation	Hanasetouge	1976-2009	JMA	Hourly, many data missing
Precipitation	Hiei	2008-2014	MLIT	Hourly, some data missing
Precipitation	Hirokawara	1965-2014	MLIT	Hourly, many data missing
River discharge	Fukakusa	1962-2010	MLIT	Hourly from 1970 to 2010, others with daily records, data in 1988 missing
Water from Lake Biwa	-	1954-2014	KCWB	Monthly
Water intake to Waterworks	-	1954-2014	KCWB	Monthly,
Water usage	-	1954-2014	KCWB	Monthly
Water into urban sewerage system	-	1954-2014	KCWB	Monthly
Drainage area	-	1954-2014	KCWB	-
Land use	-	1976/1987/2006	MLIT	-
DEM, Soil type and River channel	-	-	MLIT	-

JMA: Japan Meteorological Agency; MLIT: Japan Ministry of Land, Infrastructure, Transport and Tourism; KCWB: Kyoto City Waterworks Bureau

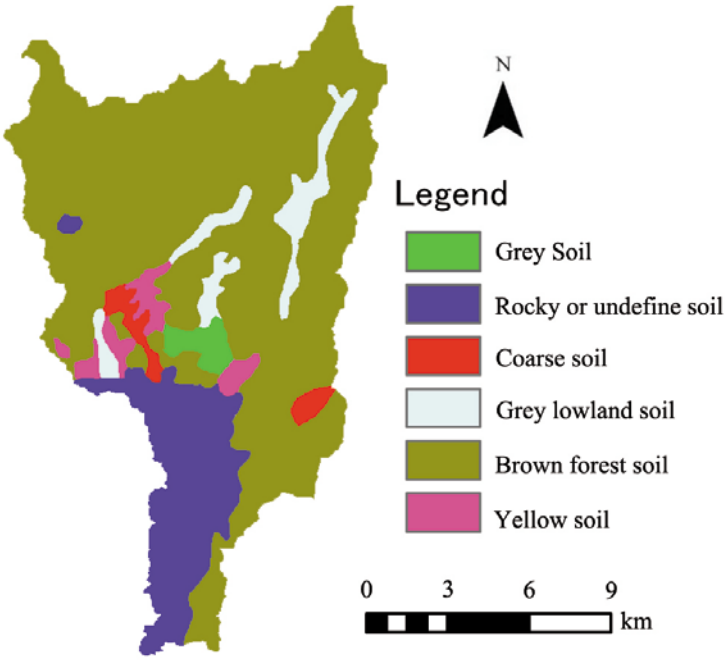

Figure 2-4 Soil type of KRB

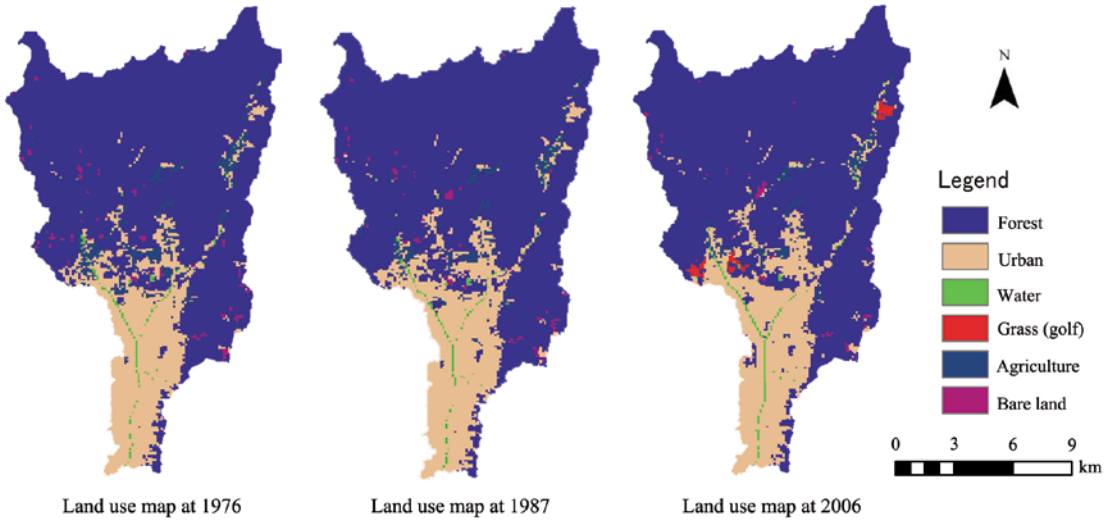

Figure 2-5 Land use types of the Kamo River basin

The water management related data obtained from Kyoto City Waterworks Bureau (KCWB) includes total water intake from Lake Biwa canal, water intake to all waterworks, water usage at the Kamo River basin, rainwater into urban sewerage system and drainage area. The drainage area of the sewerage system in Kyoto has

increased from 17.33 km^2 in 1962 to 82.99 km^2 in 2014.

The soil map of the Kamo River basin is presented in Figure 2-4. There are six types and the percentage distribution is: (1) Grey Soil (1.8 %), (2) Rocky or undefined Soil (14.8 %), (3) Coarse Soil (2.1%), (4) Grey Lowland Soil (5.4 %), (5) Brown Forest Soil (72.8 %), and (6) Yellow Soil (3.1 %).

The land use maps at 1976, 1987 and 2006 are used for land use impact assessment. The differences between the three maps are shown in Figure 2-5 and Table 2-2. From 1976 to 1987, about 2 km^2 of agriculture and bare land were converted into urban area. There were no changes in forest and water areas. From 1987 to 2006, about 1.7 km^2 of agriculture and bare land were converted into grass, water and urban areas. Overall, in the 30 years from 1976 to 2006, the city sprawled from 19.5% to 20.7% of total area. The decreased area of farmland was about 3 km^2. The changes of other types were less than 2 km^2. There were no obvious changes of land use from 1976 to 2006 in the Kamo River basin.

Table 2-2 Classification and areas of land use types in the Kamo River basin

ID	Name	Land use area (km^2)			Changed area from 1976 to 2006
		1976	1987	2006	(percentage of the basin, %)
1	Forest	133.9	133.9	133.9	0
2	Urban	35.0	37.0	37.1	1.1
3	Water	1.7	1.7	2	0.2
4	Grass (golf)	0	0	1.3	0.8
5	Agriculture	7.1	5.5	4.1	-1.7
6	Bare Land	1.5	1.1	0.8	-0.4

Chapter 3 Hydrological Model

3.1 Model description

The Hydrological Predictions for the Environment model (HYPE, Lindstrom et al., 2010; Strömqvist et al., 2012) was applied to investigate the effects of climate and land use change on the hydrology of the Kamo River basin. HYPE is a semi-distributed, dynamical hydrological and nutrient model forced with time series of precipitation and air temperature. The previous studies have shown the model performs well in simulating water flows in the landscape at the catchment scale in some different regions of the world in a range of climate conditions and resolutions. (Strömqvist et al., 2009; Arheimer et al., 2012; Jiang et al., 2013; Jomaa et al., 2013; Donnelly et al., 2014).

3.1.1 General structure

In HYPE model, a basin is divided into sub-basins, which are further divided into fractions based on landscape characteristics, for example, land use, soil type and elevation. These are called hydrological response units (HRUs) (Flügel, 1995). HYPE calculations are based on water balance in the soil profile for each HRU and the following functions are simulated (note that the list is not exhaustive): precipitation and snow pack, soil moisture and evapotranspiration, surface and soil runoff (Figure 3-1). The water outflows from all HRUs are converged and routed through rivers, lakes and reservoirs to downstream. There are three types of parameters linked to soil type, land use or global for the entire modelled domain of an application. The detailed calculation method of each model component can be found in the model manual (SMHI, 2014).

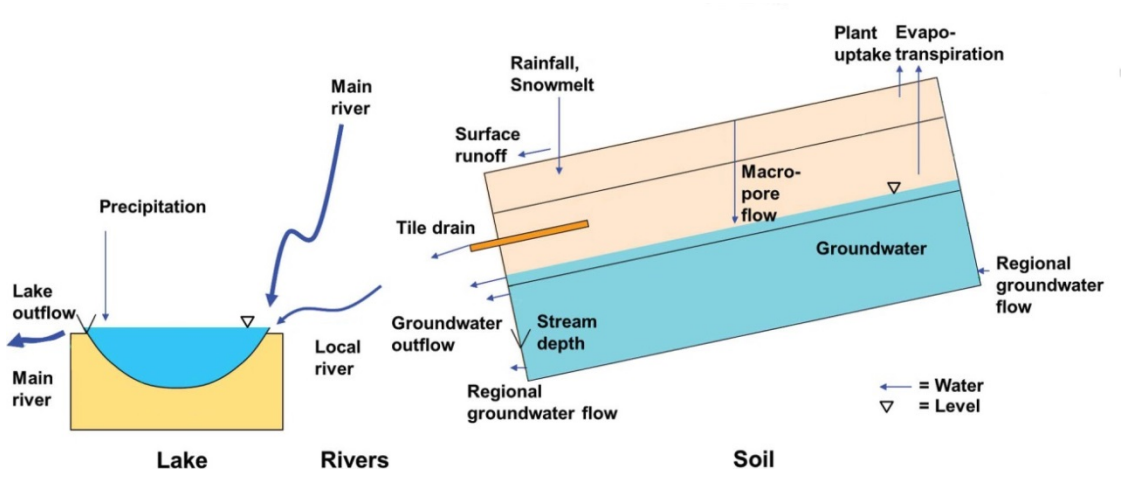

Figure 3-1 Schematic figure of one sub-basin of the HYPE model with one hydrological response unit (HRU, redrawn from Strömqvist et al., 2012)

3.1.2 Land routines

The model soil routine has (up to) three layers. The maximum water retention in the soil of i^{th} layer is determined by three parameters coupled to soil type, including wp (i) (wilting point), fc (i) (field capacity) and ep (i) (effective porosity). Water balance computations for each soil layer give total ground water table in the soil and soil moisture within each layer. Water table is regarded as a negative value from soil surface to bottom. Positive value indicates land is under water and the lowest soil layer is regarded as ground water table layer.

When water begins to fill pores, groundwater outflow begins from corresponding layers. The groundwater level is based on the fraction of pores that is filled in a layer and regional groundwater (Q_G) flow is defined as:

$$q_G = p_G * \left(W_{soil}(l) - wp(l) - fc(l)\right)$$

$$Q_G = \sum_n (q_G * S)$$

in which q_G is the regional groundwater outflow from a hydrological response unit; p_G is recession coefficient for groundwater flow; W_{soil} is the soil moisture; l is the lowest soil layer; S is the area of one

HRU; *n* is the number of HRUs in the sub-basin.

The surface runoff (Q_{SR}) is created when the potential infiltration is greater than infiltration capacity or ground water table has positive value that in the first soil layer reaches above the surface. It can be calculated as:

$$Q_{SR} = p_{SR} * (P - p_{TH}) \qquad if \;\; P > p_{TH}, W_{soil}(u) > wp(u) + fc(u) + ep(u)$$

in which p_{SR} is the recession coefficient for surface runoff; *P* is precipitation; p_{TH} is a soil type dependent parameter that flow threshold for surface runoff; *u* is the top soil.

3.1.3 Evapotranspiration

Potential evapotranspiration (*EPOT*) is calculated based on the temperature if there is no other observed data. When the air temperature (*temp*) is greater than a threshold (*ttmp*), evapotranspiration is assumed to occur. The equation is:

$$EPOT = cevp * (temp - ttmp) * epotcorr$$

in which *cevp* is a land-use based parameter; *epotcorr* is a seasonal factor to adjust the potential evapotranspiration in different seasons.

Evapotranspiration (*ET*) is assumed to occur from the two upper layers and is limited by the availability of water in the soil. When the soil moisture (W_{soil}) is greater than a certain threshold, evapotranspiration is potential. It can be defined as:

$$ET_i = \begin{cases} 0 & if\ \left(W_{soil} - wp(i)\right) \le 0 \\ EPOT * epotdist\ (i) & if\ \left(W_{soil}(i) - wp(i)\right) \ge lp * fc(i) \\ EPOT * epotdist\ (i) * \dfrac{W_{soil}(i) - wp(i)}{lp * fc(i)} & if\ 0 < \dfrac{W_{soil}(i) - wp(i)}{lp * fc(i)} < 1 \end{cases}$$

in which *i* is the soil layer; *epotdist (i)* is from a general parameter *epotdist* for evapotranspiration depth dependency; the general parameter of *lp* is coefficient for the soil water threshold that potential evapotranspiration occurs.

In addition, the model provides extra option that using some widely used potential evapotranspiration models for evapotranspiration simulation. For instance, we can use Penman-Monteith equation (Penman, 1948; Monteith, 1965), Hargreaves-Samani equation (Hargreaves and Samani, 1982), etc. instead of the original programs in the model.

3.1.4 River

There are two types of rivers (local streams and main rivers) in the model. The local rivers only receive local runoff from the sub-basin and lumped together into main rivers. According to the river length and a flood wave velocity, the river flow is delayed and damping in time. The river flow after delay and damping (Q_{RIV}) are defined as:

$$Q_D = (1 - t_1) * Q_I * t_2 + t_1 * Q_I * (t_2 + 1)$$

$$t_D = \frac{RL}{86400 p_R} = \frac{t_1 + t_2}{1 - p_D}$$

$$Q_{RIV} = \frac{a_D * V_R}{86400}$$

$$a_D = 1 - p_D * t_D + p_D * t_D * \exp(-\frac{1}{p_D * t_D})$$

in which Q_D is the river flow after delay; t_1 is remaining part of delay in translation; t_2 is the whole days of delay in translation; Q_I is total inflow to river; t_D is delay time in river through damping; *RL* is the river length; p_R is the river flow velocity; a_D is damping coefficient; p_D is part of delay time in river through damping and V_R is volume of river. The length of each local river

is the square root of the sub-basin area and the length of main rivers can be given as input.

3.1.5 Model calibration

The model is calibrated from the initial ranges of parameters values. The ranges are set manually based on hydrological knowledge and literature values. Based on a simple Monte Carlo simulation with random huge sets, the sample with the best performance is selected as a calibrated parameter set. The performance is evaluated by Nash-Sutcliff efficiency (NSE) and Pearson Correlation Coefficient (CC) between observations and simulations. The equations for CC and NSE are expressed as follows:

$$CC = \frac{\sum_{i=1}^{n}(O_i - \bar{O})(S_i - \bar{S})}{\sqrt{\sum_{i=1}^{n}(O_i - \bar{O})^2}\sqrt{\sum_{i=1}^{n}(S_i - \bar{S})^2}}$$

$$NSE = 1 - \frac{\sum_{i=1}^{n}(O_i - S_i)^2}{\sum_{i=1}^{n}(O_i - \bar{O})^2}$$

in which O_i and S_i are the observed and simulated data, respectively; n is the total number of data records; $\bar{O}$ and $\bar{S}$ are the mean observed and simulated data for the evaluation period.

NSE measures the efficiency of a model by relating the errors to the variance in the observations (Strömqvist et al., 2012). Larger NSE values indicate better model performance and a perfect fit corresponds to NSE =1.

3.2 Model setup

First, DEM, river channel map, land use and soil type data are processed in ArcGIS. The Kamo

River Basin is divided into 25 sub-basins (shown in Figure 2-1) using hydrological analysis tools. Hydrological response units are created by the combination of land use map and soil type map using the tool of raster calculation. Figure 3-2 shows the distribution of HRUs. There are 18 HRUs in the Kamo River basin at 2006, 16 HRUs at 1987 and 16 HRUs at 1976. Each HRU is named with double-digit. The first digit means land use type and the second digit means the soil type. In addition, precipitation of each sub-basin is taken from the nearest rainfall station.

After pre-processing in ArcGIS, the database is prepared into model input files including meteorological, geographical, hydrological information in each sub-basin. The model is calibrated from the initial ranges of parameters values. The ranges are set manually based on hydrological knowledge and literature values. After calibration, the model is validated and used for simulation.

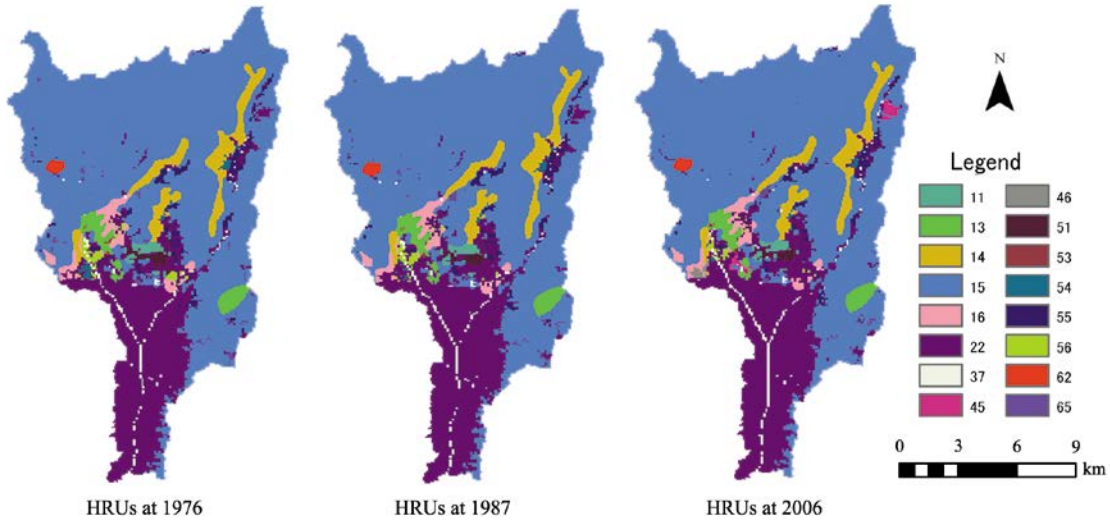

Figure 3-2 Hydrological response units (HRUs) at different periods in the Kamo River basin

Reference

Arheimer B, Dahne J and Donnelly C, 2012. Climate change impact on riverine nutrient load and land-based remedial measures of the Baltic sea action plan. *Ambio* 41, 600-612.

Donnelly C, Yang W and Dahne J, 2014. River discharge to the Baltic Sea in a future climate.

Climatic Change 122, 157-170.

Flugel W, 1995. Delineating hydrological response units by geographical information system analyses for regional hydrological modeling using PRMS/MMS in the drainagebasin of the River Brol, Germany. *Hydrological Processes*, 9, 423–436.

Hargreaves GH and Samani ZA, 1982. Estimating potential evapotranspiration. *Journal of the Irrigation and Drainage Division* 108, 225-230.

Jiang S, Jomaa S and Rode M, 2013. Identification and uncertainty analysis of a hydrological water quality model with varying input data information content. *Proceedings of the EGU General Assembly Conference Abstracts, 2013*, 7094.

StrÖmqvist J, Dahne J, Donnelly C, *et al.*, 2009. Using recently developed global data sets for hydrological predicitions. *IAHS Publ*, 121-127.

Jomaa S, Jiang S and Rode M, 2013. Effect of increased bioenergy crop production on hydrological response and nutrient emission in central Germany. *Proceedings of the EGU General Assembly Conference Abstracts, 2013*, 13645.

Lindstrom G, Pers C, Rosberg J, Stromqvist J and Arheimer B, 2010. Development and testing of the HYPE (Hydrological Predictions for the Environment) water quality model for different spatial scales. *Hydrology Research* 41, 295-319.

Monteith J, 1965. Evaporation and environment. *Proceedings of the Symp. Soc. Exp. Biol*, 205-233.

Penman HL, 1948. Natural evaporation from open water, bare soil and grass. *Proceedings of the Proceedings of the Royal Society of London A: Mathematical, Physical and Engineering Sciences*, The Royal Society, 120-145.

Strömqvist J, Arheimer B, Dahné J, Donnelly C and Lindström G, 2012. Water and nutrient predictions in ungauged basins: set-up and evaluation of a model at the national scale. *Hydrological Sciences Journal* 57, 229-247.

Swedish Meteorological and Hydrological Institue (2014). "User Manual: HYPE- Hydrological

Predictions for the Environment." http://hype.sourceforge.net/

Chapter 4 Assessment of Trends in Annual, Seasonal and Monthly Hydro-climatic Data

4.1 Introduction

Trend detection in hydro-meteorological variables on spatial and temporal scales has received a great deal of attention in recent decades (Burn and Hag Elnur, 2002; Turkes, 1996; Yue et al., 2003; St. George, 2007; Saidi et al., 2014) due to the attention given to global climate change. The monotonic changes in hydro-meteorological variables have great impacts on regional water resources applications, watershed management and hydraulic structure design (Crisci et al., 2002; Bae et al., 2008). It is crucial to detect whether there are monotonic trends in hydro-climatic variables and investigate the change per unit time.

Up to date, most studies focus on the changes in precipitation, temperature and streamflow. Burn and Hag Elnur (2002) analyzed the variations in the hydrological variables in 248 Canadian catchments using Mann-Kendall non-parametric test and concluded that spatial differences of trends in streamflow is related to the differences in meteorological variables while temporal differences in streamflow likely reflect non-uniform changes in precipitation and temperature. Partal and Kahya (2006) reported the trends in long-term annual and monthly precipitation in Turkey. Meanwhile, some studies paid attention to other metrological variables such as evapotranspiration,

relative humidity and wind speed. For instance, Singh et al. (2008) concluded that there were increasing trends in annual rainfall and relative humidity in most river basins in northwest and central India. Gocic and Trajkovic (2013) detected the annual and seasonal trends in temperature, relative humidity, actural vapor pressure, wind speed and precipitation from 1980 to 2010 in Serbia using Mann-Kendall and Sen's slope estimator.

In addition, observed high quality streamflow and evapotranspiration data are always not available in some basins. Simulated data by hydrological models are alternatives for trend analysis, which have been conducted in some literature (Bae et al., 2008; Hirabayashi et al., 2008). For instance, Bae et al. (2008) investigated the long-term trend of runoff in Korean river basins using model projected runoff data. Tao et al. (2011) estimated the changes in potential evapotranspiration which was calculated by the Penman-Monteith equation.

The changes in hydro-climatic variables have also been studied in Japan (Fujibe et al., 2005; Kanada et al., 2014). Yue and Hashino (2003) investigated long-term trends in annual, seasonal and monthly mean temperature from 1900 to 1996 over Japan. Oguchi and Fujibe (2012) estimated the spatial and temporal changes in precipitation from 1901 to 2009 over Japan. Also, Tachikawa et al., (2009) evaluated the changes of river discharge in the Mogami and Yoshino River basins under climate change by hydrological simulation. Although all of these studies detected the change characteristics of hydro-meteorological variables in Japan, climatic changes and induced streamflow changes always vary from basin to basin. It is necessary to conduct research on each basin with local historic data.

This study detects the trends in hydro-climatic variables in terms of precipitation, temperature, potential evapotranspiration and streamflow in the Kamo River basin.

Except potential evapotranspiration calculated by using the Penman-Monteith equation, others are from observed records (Table 2-1). The objectives of this study are to analyze and discuss the trends in hydro-climatic variables at different time scales and to quantify the change per unit time (deepness) and significance of trends using several statistical tests.

4.2 Methods

4.2.1 Homogeneity test

Homogeneity assessment of hydro-climatic data before test detection is important. Because observed long-term data series are easily affected by external factors such as movement of station location, application of certain practice, environment change and so on. It is necessary to detect and adjust the non-homogeneities. Metadata inspection and statistical tests are commonly used for homogeneity adjustment (Alexandersson, 1986; Peterson et al., 1998; Wijngaard et al., 2003). The popular statistical methods include standard normal homogeneity test, two-phase regression, multiple linear regression, t-test, Levene's test and rank order change point test (non-parametric test, Peterson et al., 1998).

In this study, the homogeneity tests are conducted in the software of SPSS using Levene's test (Levene, 1960; Brown and Forsythe, 1974). The family of Levene's test has three types. One is original or traditional Levene's test using group means, Secord is named Brown-Forsythe test using group medians and the last one is called Non-parametric Levene's test by performing traditional Levene's test on pooled ranked values. Here, the original and last types are used. Supposing that a potential changing point could be any date of the monitored data period, and breaking the data series (size

N) into *k* sub-groups, where N_i is the sample size of the i^{th} subgroup. The null hypothesis H_0 is that there are no significant differences between each two groups at the confidence level of 95%. The original Levene's test statistic *W* is defined as:

$$W = \frac{(N-k)}{(k-1)} \frac{\sum_{i=1}^{k} N_i (\bar{Z}_i - \bar{Z})^2}{\sum_{i=1}^{k} \sum_{j=1}^{N_i} (Z_{ij} - \bar{z}_i)^2} \qquad (4-1)$$

In the equation, $\bar{Z}_i$ is the mean of i^{th} group and $\bar{Z}$ is the overall mean of the Z_{ij}. Z_{ij} is calculated using following equation:

$$Z_{ij} = |y_{ij} - \bar{y}_i| \qquad (4-2)$$

In the Eq. (4-2), y_{ij} is the value of the measured variable for the j^{th} case from i^{th} group; $\bar{y}_i$ is the mean of i^{th} group. If *W* is more than the value of *F(0.05, k-1, N-k)*, the Levene's test rejects H_0. There are heterogeneities in the data series. *F(0.05, k-1, N-k)* is the upper critical value of the F-distribution at the significance level of 0.05 with *k-1* and *N-k* degrees of freedom.

4.2.2 Potential evapotranspiration

The potential evapotranspiration is calculated based on the equation of Penman-Monteith FAO 56 (Allen et al., 1998), which is the most commonly used method for potential evapotranspiration estimation. It can be defined as:

$$ET_0 = \left(0.408S(R_n - G) + \frac{900rW(e_s - e_a)}{T + 273}\right) \Big/ (S + r(1 + 0.24W)) \qquad (4-3)$$

in which

ET_0 is potential evapotranspiration, mm;

S is slope vapor pressure curve, kPa $°C^{-1}$;

Rn is net radiation, $MJm^{-2}day^{-1}$;

G is soil heat flux density, $MJm^{-2}day^{-1}$;

r is psychrometric constant, kPa $°C^{-1}$;

W is wind speed, ms^{-1};

e_s and e_a are saturation and actual vapour pressure, respectively, kPa;

T is daily air temperature, °C

4.2.3 Test for normality

The robustness of statistical methods is based on the distribution of test-data. Normality distribution is an underlying assumption of most parametric statistical procedures, such as analysis of variance, t-test and linear regression analysis (Shapiro and Wilk, 1965). Also, Olejnik and Algina (1987) reported that no test is robust and most powerful for all distributions. And non-parametric tests usually are more robust to non-normal distributions than parametric tests. Therefore, it is necessary to check the normality of hydro-climatic data before proceeding with any relevant statistical analysis. In general, there are three common ways to check the normality assumption (graphical methods, numerical methods and formal normality tests, Razali and Wah, 2011). In this study, the Shapiro-Wilk (SW) test (Shapiro and Wilk., 1965) is applied to check the normality of hydro-climatic data, which is regarded as the most powerful formal normality test (Keskin, 2006; Razali and Wah, 2011). The null hypothesis H_0 is that the sample data is normally distributed. And the SW test statistic *W* is described as:

$$W = \left(\sum_{i=1}^{n} a_i\, x_i\right)^2 \Big/ \sum_{i=1}^{n}(x_i - \bar{x})^2 \qquad (4-4)$$

in which

x_i is the i^{th} case in an ordered sample X;

n is the sample size of X;

$\bar{x}$ is the mean of the sample;

a_i is coefficient generated from the means, variances and covariance of a sample of size n with a normal distribution, which can be found in statistical tables (Pearson and Hartley, 1972).

The null hypothesis H_0 that the sample data is normally distributed will be rejected at the significance level of 0.05, if W is less than the critical value $W_{0.05}$.

4.2.4 Trend detection analysis

Trend analysis is conducted using the parametric linear regression t-test and non-parametric Mann-Kendall (MK) test. Linear regression t-test is applied to normal distributions with no data missing and MK test is used for non-normal distributions or the samples with missing data. The time series are aggregated in annual, seasonal and monthly time series to observe the changes between years and inter-years. In Japan, the spring season is considered as from March to May; the summer season is from June to August; the autumn season is from September to November and the winter season is from December to February.

(1) Linear regression t-test

This method is the most commonly used approach for trend detection and only

suitable for the sample with normal distribution (Gilbert, 1987; Hameed et al., 1997; Fadem, 2008). First, a linear regression model is supposed to fit the dependent variable *y* on independent variable time *x*.

$$Y = a + kx + \varepsilon \qquad (4-5)$$

in which *a* and *k* are the regression coefficients, ε is a random error with mean 0 and unknown variance σ^2. The coefficient of *k* is the slope of trend. A null hypothesis is the slope *k* is equal to 0 at the level of 0.05. The statistic *t* can be defined as:

$$t = k\sqrt{(n-2)\sum_{i=1}^{n}(x_i - \bar{x})^2} \Big/ \sqrt{\sum_{i=1}^{n}(y_i - \hat{y}_i)^2} \qquad (4-6)$$

in which

n is the sample size;

x_i is the i^{th} case in the independent variable time *x*;

y_i is the dependent hydro-climatic variable at time x_i;

$\hat{y}_i$ is the least-square estimator of y_i.

The statistic *t* has a T-distribution with *n-2* degrees of freedom under the null hypothesis H_0. If the value of t is large than the value of *T(0.05, n-2)*, H_0 is rejected and there is significant trend in the data. The change per unit time is the slope *k*.

(2) Mann-Kendall test

The MK test is a non-parametric statistical procedure used to test monotonic trends in time series data (Mann, 1945; Kendall, 1975). The null hypothesis H_0 is that the data

in a time-series y_i $\{y_i, i = 1, 2, \ldots, n\}$ are independent and randomness. The test statistic *S* is described as:

$$S = \sum_{i=1}^{n-1} \sum_{t=i+1}^{n} F(y_t - y_i) \qquad (4-7)$$

$$F(\emptyset) = \begin{cases} 1 & if\ \emptyset > 0 \\ 0 & if\ \emptyset = 0 \\ -1 & if\ \emptyset < 0 \end{cases} \qquad (4-8)$$

in which *y* is the hydro-climatic variable and $\emptyset = y_t - y_i$.

According to the research of Mann (1945), *S* has a normal distribution under H_0 with the mean and variance as follows:

$$E(S) = 0 \qquad (4-9)$$

$$Var(s) = {}^{[n(n-1)(2n+5) - \sum_m m(m-1)(2m+5)]}/_{18} \qquad (4-10)$$

in which *m* is extent of any give tie.

The standard variate *Z* is calculated by using the following equation:

$$Z = \begin{cases} \dfrac{S-1}{\sqrt{Var(S)}} & if\ S > 0 \\ 0 & if\ S = 0 \\ \dfrac{S+1}{\sqrt{Var(S)}} & if\ S < 0 \end{cases} \qquad (4-11)$$

Z is used to detect the significance of trend, if $|Z|$ is greater than $Z_{a/2}$, H_0 is rejected and there is significant monotonic trend. This procedure has been widely used in hydro-climatic analysis since there is no requirement on data distribution and missing values are allowed (Yu et al., 1993; Yue et al., 2002a, 2002b). However, MK test only gives increase or decrease trends indicated by the positive and negative values of *Z*. The magnitude of trend (change per unit time) has to be computed using other methods.

(3) Sen's Slope estimator

The non-parametric Sen's Slope procedure, developed by Sen (1968) and extended by Hirsch et al. (1982), is used to estimate the change per unit time in data. The slope *Q* is defined as:

$$Q = median\left[\left.(x_j - x_i)\right/(j - i)\right] \; for\ all\ i < j \qquad (4-12)$$

in which

x_j and x_i are the data values at time *j* and *i*, respectively;

j is the time after time *i*.

If the data has a significance monotonic trend under MK test, the slope *Q* is significance at the same level used in MK test. And the positive value of *Q* means the slope of the upward trend while negative value for downward trend. To date, many studies has applied Sen's Slope estimator in hydro-meteorological trend analysis (Partal and Kahya, 2006; Tabari and Talaee, 2011).

4.3 Results

4.3.1 Homogeneity test

As shown in Table 2-1, the precipitation time series at Hiei station are less than ten years (only seven years). The sample size is small for statistical significance of trend analysis. Also, the precipitation data at the station of Hanasetouge miss too many records. The monitoring at the station of Hieizan stoped since October in 2000. Therefore, for precipitation, only the data at other three stations (Kyoto, Kumogahata and Hirokawata) and basin average data are used for analysis.

The results of homogeneity adjustment in meteorological variables show that there are no non-homogeneities in the data at annual, seasonal and monthly scales. For streamflow, both of two tests found heterogeneities in the data from 1962 to2010. The observed data from 1978 to 1987 are outliers compared with the data in other period. Excluding the data from 1978 to 1987, the result of homogeneity test on the left data shows there are no heterogeneities at annual, seasonal and monthly scales. Table 4-1 shows the results of homogeneity test on all variables at annual scale.

Table 4-1 Results of homogeneity test on hydro-meteorological data at annual scale

	Homogeneity		Period
	Levene's test	Non-parametric Levene's test	
Precipitation at Kyoto station	Yes	Yes	1962-2014
Precipitation at Kumogahata station	Yes	Yes	1962-2014
Precipitation at Hirokawata station	Yes	Yes	1965-2014
Basin average precipitation	Yes	Yes	1962-2014
Air temperature	Yes	Yes	1962-2014
Maximum temperature	Yes	Yes	1962-2014
Minimum temperature	Yes	Yes	1962-2014
Potential evapotranspiration	Yes	Yes	1962-2014
Observed discharge	No	No	1962-2010

4.3.2 Trends in annual hydro-climatic data

In this study, the data time series for trend analysis are from 1962 to 2014, with some exceptions in case of missing data, e.g. precipitation at Hirokawata station and observed river discharge. The data series at the stations of Kumogahata, Hirokawata and Fukakusa are detected using MK test due to missing records in data series. The methods of trend test used on data series at other stations are based on the results of normality test. The distribution test results of annual data are shown in Table 4-2. It was found that at annual scale, precipitation, maximum and minimum temperature and potential evapotranspiration had normal distribution.

Table 4-2 Results of normality and trend tests in annual hydro-meteorological data

	Normality	Trend detection			
		Regression coefficient	p-value of t-test	Sen's Slope	p-value of MK test
Basin average precipitation	Y	4.231	0.128	-	-
Precipitation at Kyoto station	Y	-2.789	0.256	-	-
Precipitation at Kumogahata station	-	-	-	3.328	0.222
Precipitation at Hirokawata station	-	-	-	5.486	0.379
Air temperature	Y	0.027	0.000	-	-
Maximum temperature	Y	0.020	0.000	-	-
Minimum temperature	Y	0.034	0.000	-	-
Observed discharge at Fukakusa station	-	-	-	-0.092	0.002
Potential evapotranspiration	Y	1.279	0.000	-	-

Y means there is normality at the level p=0.05; N means there is non-normality. If p-value is less than 0.05, there is significant upward trend. The symbol of "-" means no test.

The results of trend test are shown in Table 4-2. Air, maximum and minimum temperature significantly increased from 1962 to 2014 at the statistical level of p=0.05. Also, potential evapotranspiration had same positive trend as temperature. Observed streamflow was found decreasing in this period. Figure 4-1 shows the time series of temperature variables with the significant linear regression trend lines. The minimum temperature had the maximum increase per year (about 0.034℃). The magnitudes of the slope in maximum and air temperature were 0.02℃ and 0.027℃, respectively. The time series of annual potential evapotranspiration is displayed in Figure 4-2 (a), which

significantly increased by 1.279 mm per year from 1962 to 2014. Figure 4-2 (b) indicates the annual mean discharge without the outliers of 1978-1987. The value of Sen's Slope is -0.092 m^3/s, which means observed streamflow decreased by 16.2 mm per year. For precipitation, there are no statistical significant trends at the level of p=0.05. And there is opposite linear regression coefficient between basin average precipitation and the data at Kyoto station. The slope of basin average precipitation is positive while the slope of precipitation at Kyoto station is negative.

Figure 4-3 shows the annual anomalies of basin average precipitation with respect to the mean value from 1981 to 2010. Positive anomaly values indicate the hydro-climatic variables were larger than the means from 1981 to 2010 while negative values mean smaller. There were one relatively consecutive lower rainfall period from 1962 to 1973 and one relative consecutive higher rainfall period from 1988 to 1993. The highest year on record occurred in 1993 and lowest year was 1963. The annual precipitation had strong fluctuation from 1974 to 2014.

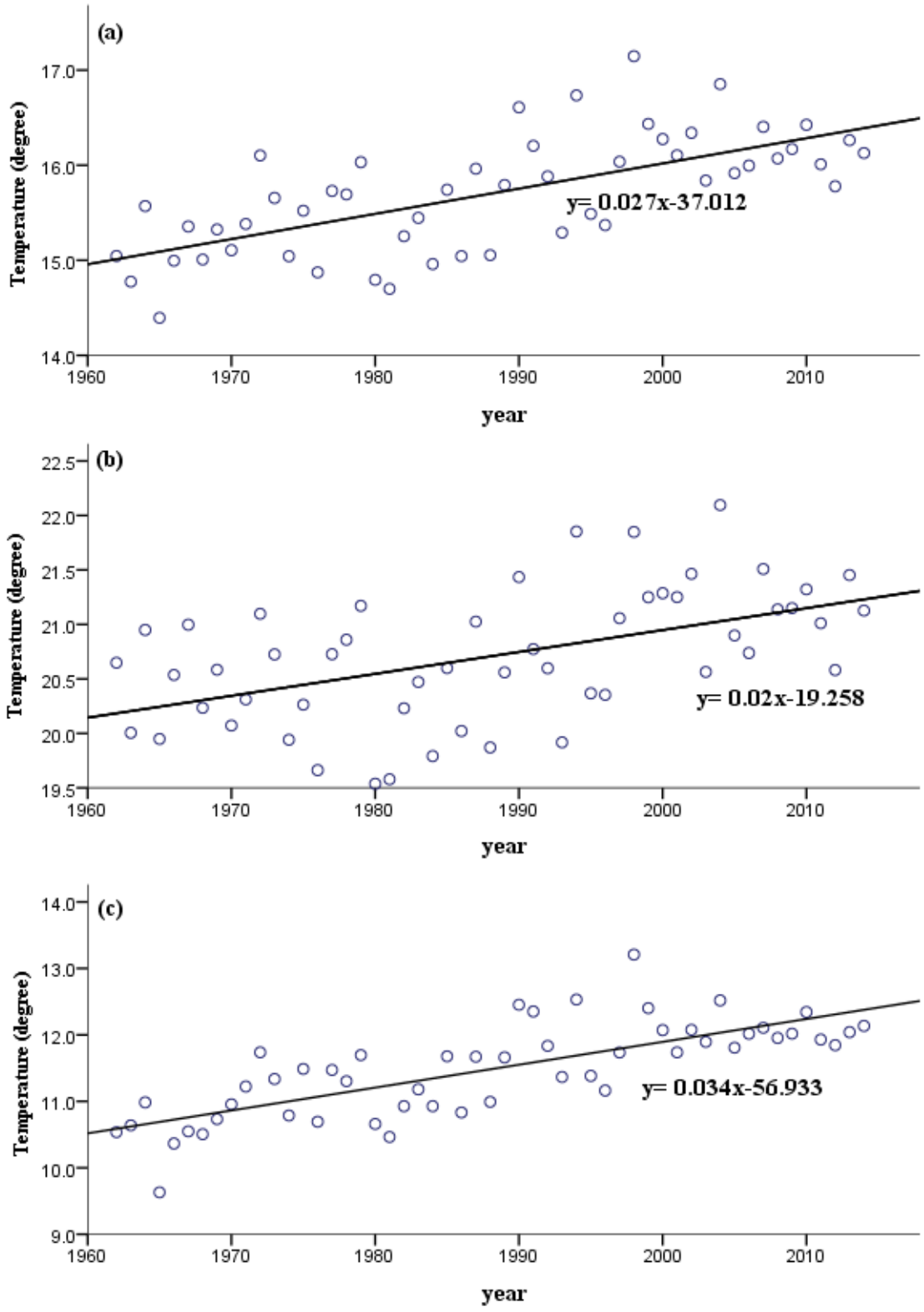

Figure 4-1 Time series of (a) air temperature, (b) maximum temperature and (c) minimum temperature in the Kamo River basin

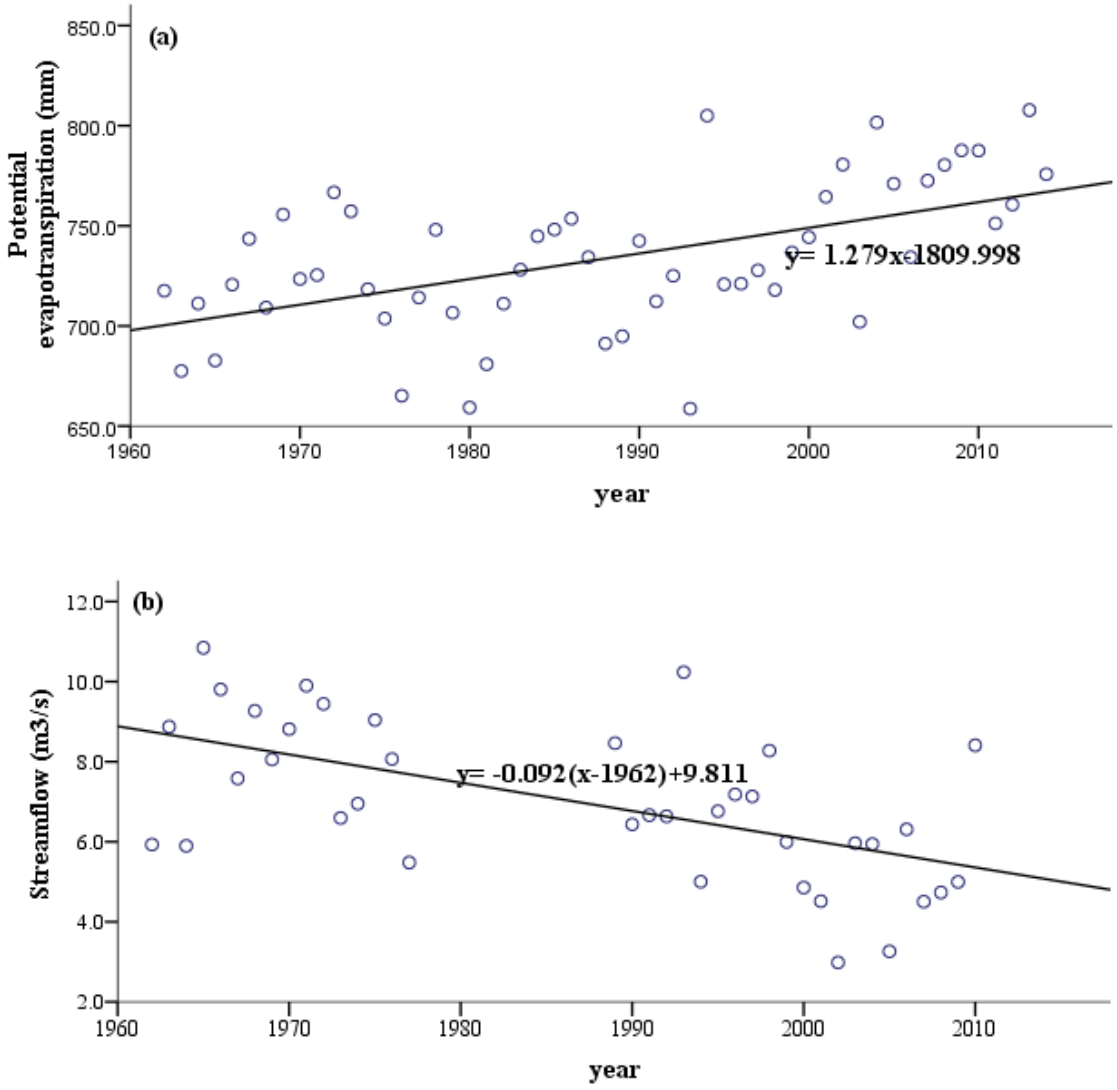

Figure 4-2 Time series of (a) potential evapotranspiration and (b) observed streamflow at Fukakusa station in the Kamo River bsain

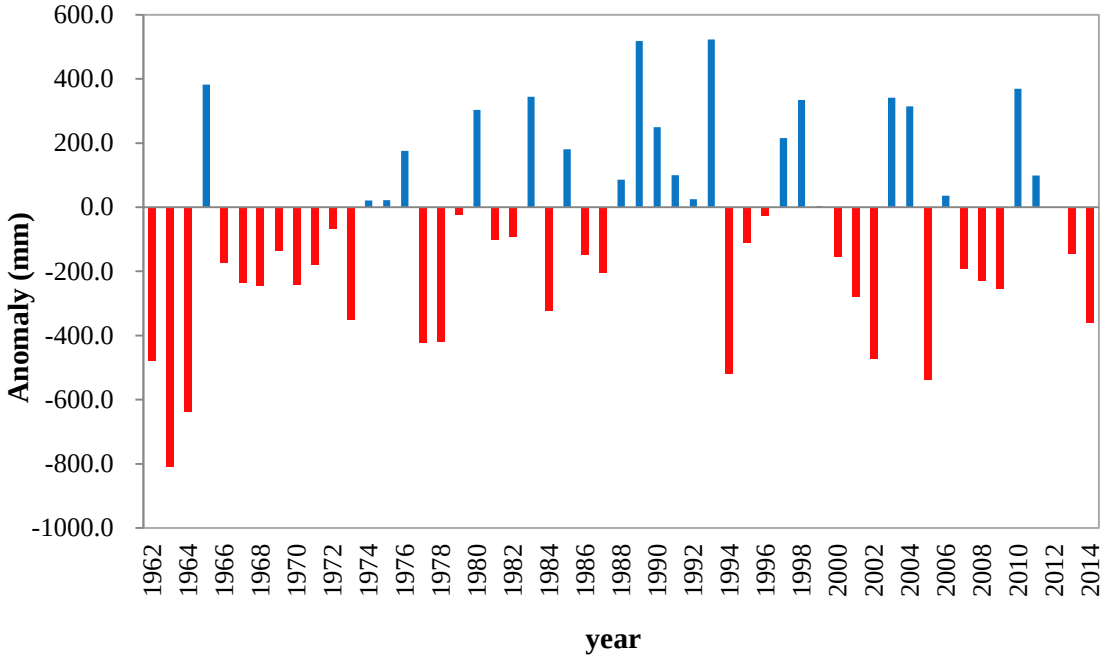

Figure 4-3 Time series of annual basin average precipitation anomalies in the Kamo River basin with respect to the average value from 1981 to 2010

The annual precipitation anomalies at Kyoto station, with respect to the average of 1981-2010, were analyzed and shown in Figure 4-4. Only the rainfall data from Kyoto station was selected for analysis was because there were highest quality and longest series data at this station. It was found that there was relatively higher precipitation from 1964 to 1972, which was contrary to the results of basin average precipitation. The differences are possibly induced by the elevation. Mountain terrain comprises about 70% of the surface in the Kamo River basin and the monitor locations of other stations are on the mountains with the elevation more than 200 m, while Kyoto station is located at plain with the elevation about 40m. The fluctuation also was strong from 1974 to 2014.

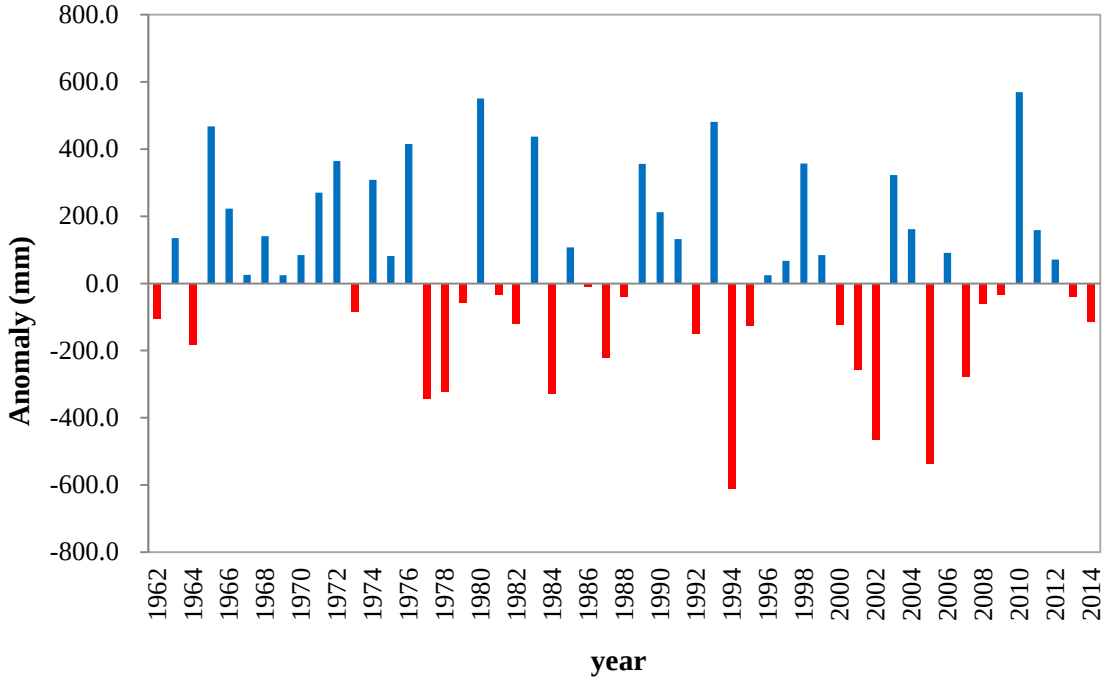

Figure 4-4 Time series of annual precipitation anomalies at Kyoto station in the Kamo River basin with respect to the average value from 1981 to 2010

4.3.3 Trends in seasonal hydro-climatic data

The normality test results of seasonal data are shown in Table 4-3 and this test was not taken on the data series with some records missing, the trend of which is taken by MK test. Temperature variables were normally distributed from 1962 to 2014. The summer precipitation was also normally distributed while the autumn precipitation had skew in distribution. Linear regression t-test is used to detect the trends in normal distributed data and MK test is used for non-normal distributions.

The magnitudes of trends and statistical significance level are shown in Table 4-4. If p-value is lower than 0.05, there is significant monotonic trend in the variable. For temperature variables, except winter maximum temperature had no statistical significant upward trend, all other temperature variables showed significant increasing trend. Among them, the magnitude of changes per year in minimum temperature was the

largest in every season. In addition, as shown in Figure 4-5, the trend slope of air temperature in autumn was obviously larger than that in other three seasons. The same phenomenon was also found in seasonal maximum and minimum temperature series. The autumn air, maximum and minimum temperature increased by 0.038℃, 0.028℃ and 0.049℃ per year, respectively. Potential evapotranspiration showed the same trend as air temperature, which significantly increased by 0.327 mm/year in spring, 0.383 mm/year in summer, 0.421 mm/year in autumn and 0.149 mm/year in winter. The time series of evapotranspiration with the significant linear trend lines are shown in Figure 4-6. Significant upward trends were found in winter basin average precipitation and the data at Kumogahata station. The slopes of other seasonal basin average precipitation are positive with p-value larger than 0.05. The slope magnitude of winter basin average precipitation is the largest. There was a shift to winter in the inter-year distribution of precipitation. Also, there is opposite linear regression coefficient between summer basin average precipitation and the data at Kyoto station. Summer basin rainfall seemed to increase while summer rainfall at Kyoto station seemed to decrease. And both of them have no significance. Observed streamflow had obviously decreasing trend in spring and summer (Figure 4-7). And summer had the highest reduction. The value of Sen's Slope of spring river discharge is -0.091 m^3/s, which means observed streamflow decreased by about 4.0 mm per year in spring. The summer river discharge decreased by about 6.8 mm (0.153 m^3/s) per year.

Table 4-3 Results of Normality in seasonal hydro-meteorological data

	Normality			
	Spring	Summer	Autumn	Winter
Basin average precipitation	N	Y	N	Y
Precipitation at Kyoto station	Y	Y	N	Y
Precipitation at Kumogahata station	-	Y	N	-
Precipitation at Hirokawata station	-	-	-	-
Air temperature	Y	Y	Y	Y
Maximum temperature	Y	Y	Y	Y
Minimum temperature	Y	Y	Y	Y
Observed discharge	-	-	-	-
Potential evapotranspiration	Y	Y	Y	Y

Y means there is normality at the level p=0.05; N means there is non-normality. The symbol of "-" means no test.

The yearly seasonal basin average precipitation anomalies (Figure 4-8), which were calculated by minus the mean value of 1981-2010, indicated that the anomalies of precipitation in winter had relatively smaller fluctuation and trend to change from negative to positive. From 1962 to 1988, winter had relative lower precipitation. The years with highest positive anomaly on record in spring, summer, autumn and winter were 1995, 1993, 2013 and 1989, respectively. While highest negative values occurred in 2013, 1963, 1963 and 1963, respectively.

Table 4-4 Results of trend detection in seasonal hydro-meteorological data

	Magnitude of slope and p-value							
	Spring	p-value	Summer	p-value	Autumn	p-value	Winter	p-value
Basin average precipitation	-0.016	0.992	0.008	0.996	1.787	0.142	1.989*	0.000
Precipitation at Kyoto station	-1.451	0.120	-2.746	0.077	0.38	0.795	0.797	0.091
Precipitation at Kumogahata station	0.199	0.881	-1.621	0.389	3.114*	0.021	3.125*	0.000
Precipitation at Hirokawata station	0.032	0.968	1.447	0.555	2.442	0.184	2.069	0.187
Air temperature	0.019*	0.004	0.027*	0.000	0.038*	0.000	0.021*	0.007
Maximum temperature	0.017*	0.024	0.024*	0.005	0.029*	0.000	0.009	0.246
Minimum temperature	0.023*	0.001	0.033*	0.000	0.049*	0.000	0.032*	0.000
Observed discharge	-0.091*	0.003	-0.153*	0.004	-0.065	0.059	-0.032	0.180
Potential evapotranspiration	0.327*	0.001	0.383*	0.023	0.421*	0.000	0.149	0.001

The symbol of "_" means the variable was detected by linear regression t-test. The symbol of "*" means there was significant monotonic trend at the level p=0.05.

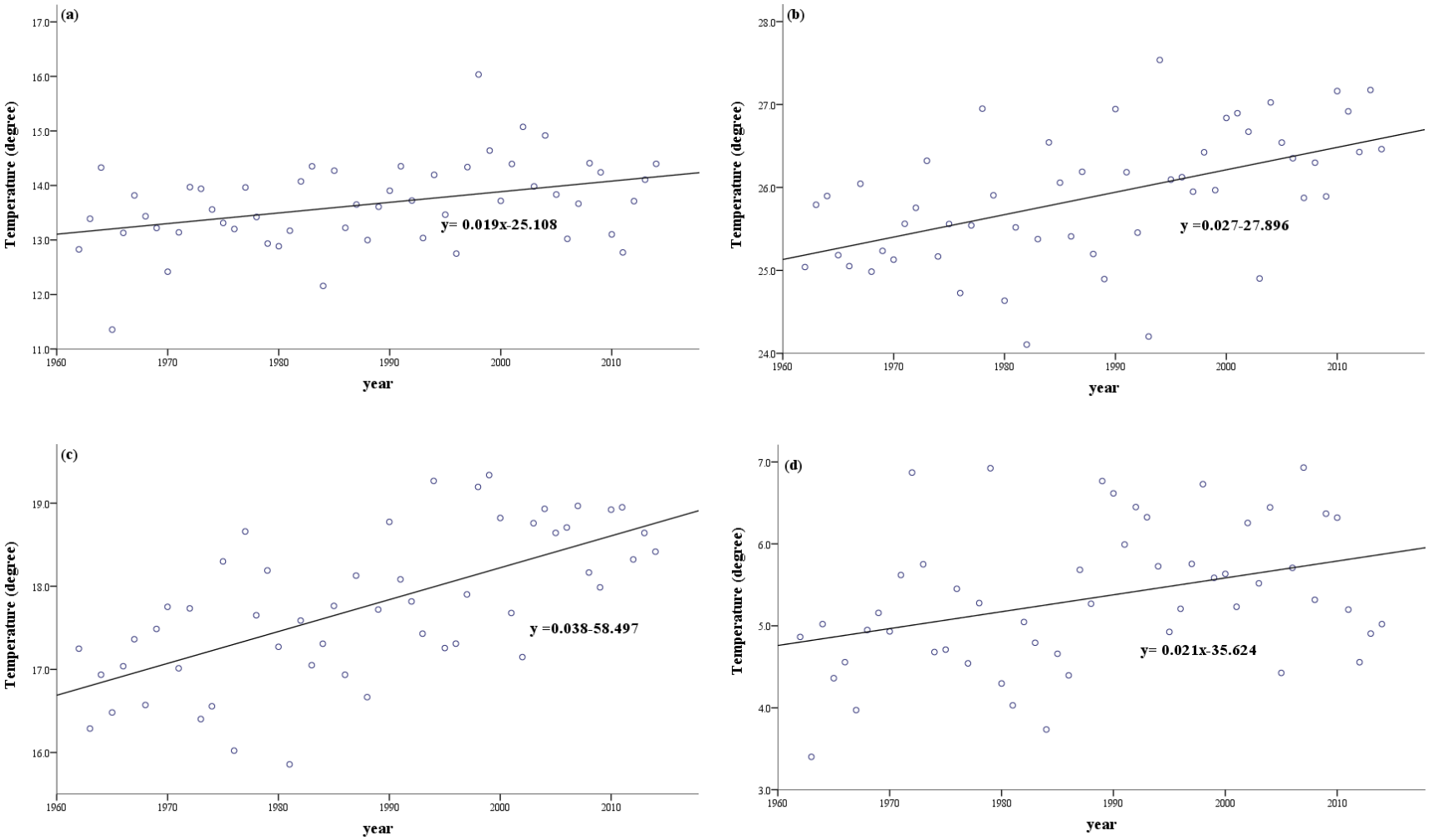

Figure 4-5 Time series of air temperature (a) spring, (b) summer, (c) autumn and (d) winter in the Kamo River basin

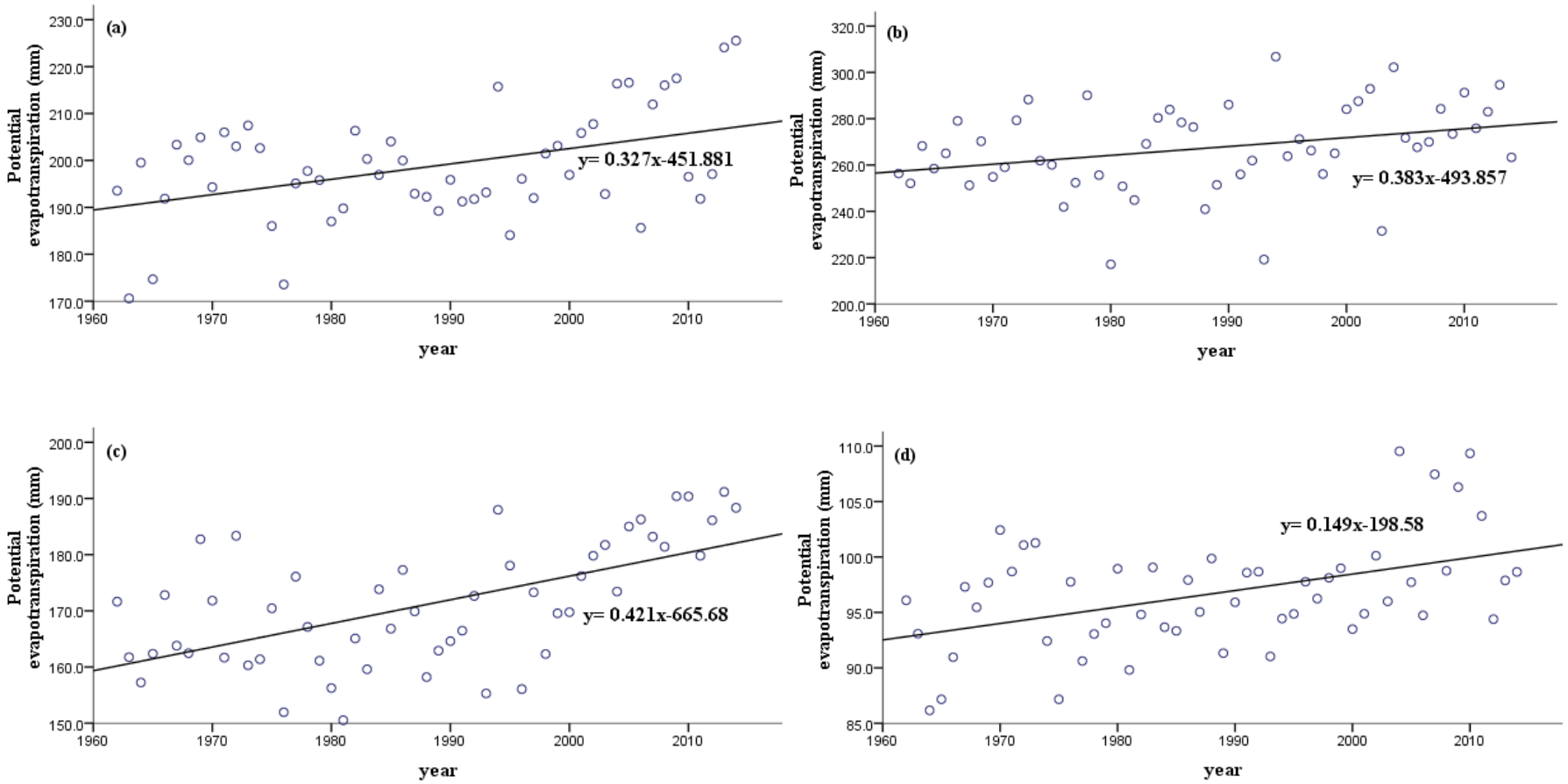

Figure 4-6 Time series of potential evapotranspiration (a) spring, (b) summer, (c) autumn and (d) winter in the Kamo River basin

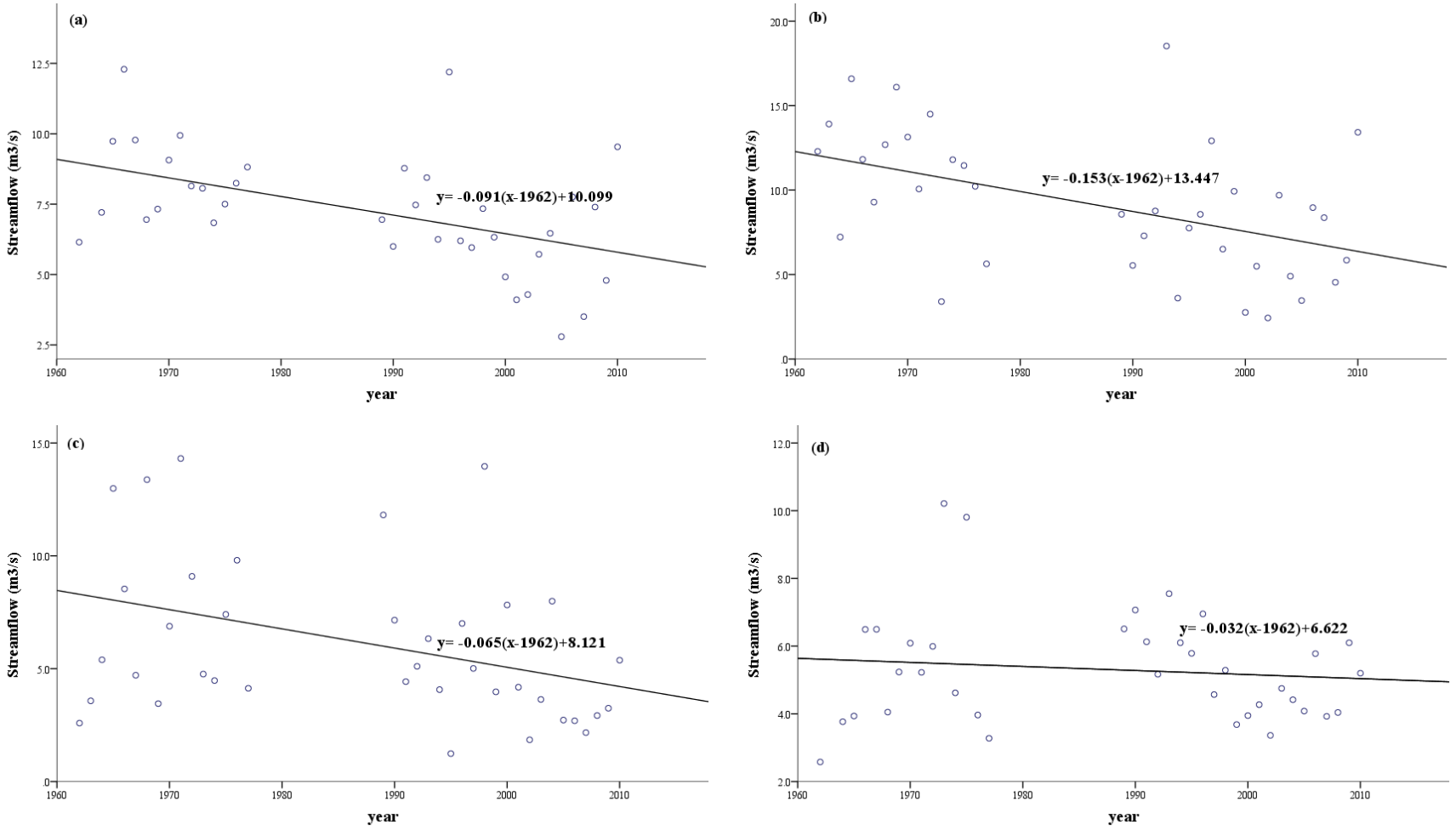

Figure 4-7 Time series of observed streamflow (a) spring, (b) summer, (c) autumn and (d) winter in the Kamo River basin (there is no statistical significance in the linear regression trend lines of autumn and winter data series at the 95% confidence level)

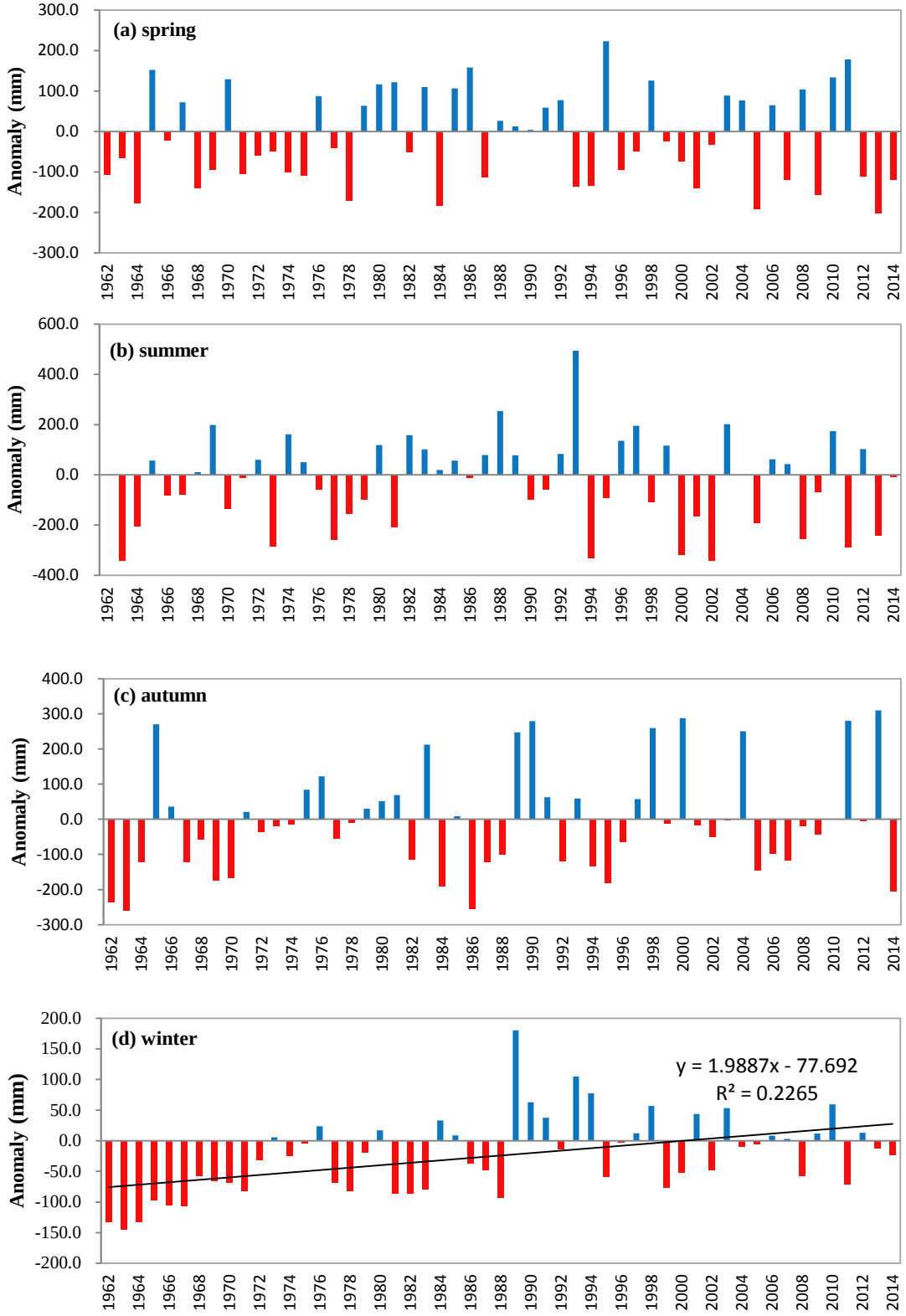

Figure 4-8 Time series of seasonal basin precipitation anomalies (a) spring, (b) summer, (c) autumn and (d) winter in the Kamo River basin with respect to the average value from 1981 to 2010

4.3.4 Trends in monthly hydro-climatic data

Table 4-5 shows the results of trend detection in monthly hydro-meteorological variables. It was found that October had the highest magnitude of significant increasing trend followed by February and December in basin average precipitation. Minimum temperature had the largest magnitude of slope in all months except April followed by air temperature and maximum temperature. September had largest increase in air temperature. Potential Evapotranspiration rose significantly in the months February-April and September-December. The top slope was in September due to the large increase of temperature. For observed discharge, significant decrease was observed in April-July and November. In addition, the precipitation, potential evapotranspiration and river discharge in millimeters are presented in Figure 4-11. These variables are uneven distributed inter-year. Most water concentrated in the period from April to October. Observed discharge was larger than precipitation in January and February due to the effects of human activities.

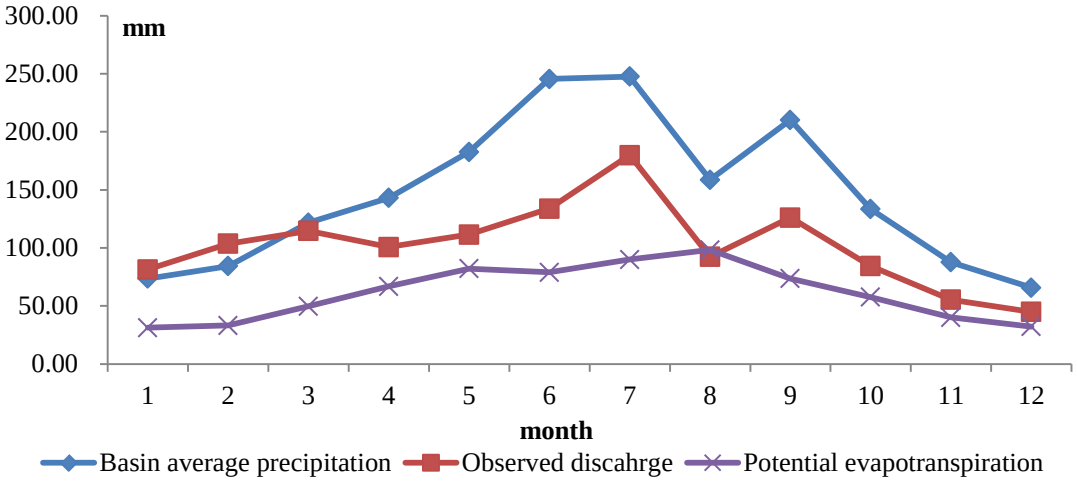

Figure 4-9 Average monthly hydro-climatic variables from 1962 to 2014 in millimeter in the Kamo River basin

Table 4-5 Results of trend detection in monthly hydro-meteorological data

	Magnitude of Sen's slope											
	Jan.	Feb.	Mar.	Apr.	May	Jun.	Jul.	Aug.	Sep.	Oct.	Nov.	Dec.
Basin average precipitation	0.159	1.068*	0.586	-0.812	0.508	-0.625	-0.214	0.298	0.44	1.126*	0.108	0.858*
Precipitation at Kyoto station	-0.152	0.439	0.072	-1.505*	-0.038	-1.79*	-1.136	-0.228	-0.184	0.612	0	0.505*
Precipitation at Kumogahata station	0.5	1.611*	0.456	-0.89	0.65	-0.381	-1.08	0.124	1.268	1.452	0.25	1.101*
Precipitation at Hirokawata station	1.935*	0.695	0.235	0.087	1.045	-0.605	0.172	1.268	1.256	1.969	0.159	1.083
Air temperature	0.02	0.029*	0.035*	0.006	0.017*	0.035*	0.024*	0.024*	0.039*	0.047*	0.029*	0.014
Maximum temperature	0.009	0.022	0.031*	0.009	0.012	0.032*	0.022	0.021	0.038*	0.036*	0.014	-0.003
Minimum temperature	0.031*	0.035*	0.04*	0.003	0.025*	0.04*	0.028*	0.031*	0.043*	0.059*	0.044*	0.031*
Observed discharge	0.008	-0.036	-0.01	-0.138*	-0.117*	-0.185*	-0.171*	-0.055	-0.076	-0.043	-0.05*	-0.027
Potential evapotranspiration	0.032	0.064*	0.091*	0.146*	0.09	0.152*	0.107	0.124	0.234*	0.131*	0.056*	0.053*

The symbol of "*" means there was significant monotonic trend at the level p=0.05. The symbol of "_" means the variable was detected by linear regression t-test.

4.4 Discussion

4.4.1 Annual scale

Although the statistical significant monotonic trend was not detected in precipitation in the Kamo River basin, the fluctuation became more frequent and intense since 1970s. Thus, the risk of alternate drought and flood probably increase, which will increase the difficulties of water resources management. Meanwhile, the characteristics of changes in precipitation were different at different gauged stations. For instance, the data from Kyoto station indicated there was relative higher precipitation from 1964 to 1972, which was contrary to basin average precipitation. This is not induced by data biases according to homogeneity test results. The probable reason is the difference of changes in water vapor flux on different terrains. Precipitation changes are less regular and heterogeneity in different regions (IPCC, 2013). Also, Oguchi and Fujibe (2012) concluded that features of precipitation changes in Japan have regional differences. In addition, upward trend was observed in air, maximum and minimum temperature, which is consistent with the findings of some studies (Yue and Hashino, 2003; Fujibe, 2015).

Observed discharge has decreased significantly by discarding the outliers. The changes of patterns and trends in streamflow are different from the changes of basin average precipitation. Precipitation showed an insignificant upward trend from 1962 to 2014 and the relatively drier period in precipitation was from 1964 to 1973. Herein, the changes in river discharge probability caused by the increase of evapotranspiration and effects of human activities. How human activities affect the streamflow and the contribution rate of driving factors to the changes of river discharge will be discussed in next Chapter.

4.4.2 Seasonal and monthly scales

With regard to winter, it is highlight that our findings on precipitation are inconsistent with the findings of some previous studies in Japan. In this study, winter precipitation was observed increasing at all stations (one with significance, two without significance) and the computed basin average basin precipitation also increased with statistical significance. However, the weakening of the winter monsoon over Japan, which can be regarded as the distribution of winter precipitation over Japan, was reported by some studies (Nakamura et al., 2002; Hirano and Matsumoto, 2011). Oguchi and Fujibe (2012) found that total precipitation and the number of days in winter with precipitation more than 1 mm slightly decreased on the Sea of Japan coast of Honshu. This is probably caused by the differences of study scale and terrain, because KRB is a small basin with 70% mountain terrain. All these previous studies conducted their analysis at large national or global scale.

In addition, we found that there are similarities in patterns and trends between potential evapotranspiration and air temperature. The changes in potential evapotranspiration are related to changes in temperature. In addition, October had largest increase in temperature, while the top rising in potential evapotranspiration occurred in September. This is due to the difference in precipitation. The precipitation in September was quite larger than in October (Figure 4-11). Precipitation allows identification of water availability for evapotranspiration (Beskow et al., 2012).

4.4.4 Limitations

One problem in our study is that we did not consider and remove the serial correlation in the data before trend test, which can complicate the identification of

trends (von Storch and Navarra, 1999). Another problem is that the statistical significant level was fixed to be set as p=0.05, which has great impacts on significant trend results. In this study, if the statistical significance level was set as p=0.1, seasonal monotonic trends would be detected in precipitation at Kyoto station and some monthly variables. Duan (2014) proved that the stations with significant monotonic trends in precipitation at the level of p=0.1 were much larger than that at the level of p=0.05 over Japan.

4.5 Conclusion

In this chapter, parametric linear regression t-test and non-parametric Mann-Kendall test were applied to detect monotonic trends in the data series of hydro-meteorological variables from 1962 to 2014 in the Kamo River basin, which had been pre-processed with homogeneity and normality tests. In addition, the change per year (magnitude of slope) was quantified by using linear regression coefficient or Sen's slope estimator based on their distributions and records integrity. The conclusions are summarized as follows:

(1) The fluctuation in precipitation is frequent and intense since 1970s. Basin average precipitation has increased by 4.2 mm per year without statistical significance. And a significant upward trend was observed in winter, actually in February and December. In addition, the change in precipitation at a location is likely to be not in correspondence with regional average precipitation variations. Compared with the data at other gauged stations and basin average precipitation, the precipitation at Kyoto station indicated different changes.

(2) River discharge has significantly decreased 16.2 mm per year, which is not induced by precipitation changes and probably caused by the increase of

evapotranspiration and the effects of human activities. Significant decrease was detected in annual, seasonal and monthly observed streamflow, while no similar changes were observed in precipitation.

(3) Air, maximum and minimum temperature increased obviously at annual, seasonal and monthly scales. The magnitude of rising slope in minimum temperature was largest at annual, seasonal and monthly scales. In addition, autumn has the highest upward in temperature. Actually, October and September had the maximum and second increase during a year.

(4) The similarities in patterns and trends in potential evapotranspiration and temperature at different time scales imply that the changes in potential evapotranspiration are related to changes in temperature.

Reference

Alexandersson H, 1986. A homogeneity test applied to precipitation data. *Journal of climatology* 6, 661-675.

Allen RG, Pereira LS, Raes D and Smith M, 1998. Crop evapotranspiration-Guidelines for computing crop water requirements-FAO Irrigation and drainage paper 56. *FAO, Rome* 300 (9), D05109.

Bae DH, Jung IW and Chang H, 2008. Long‐term trend of precipitation and runoff in Korean river basins. *Hydrological Processes* 22, 2644-2656.

Beskow S, Norton LD and Mello CR, 2012. Hydrological Prediction in a Tropical Watershed Dominated by Oxisols Using a Distributed Hydrological Model. *Water Resources Management 27,* 341-363.

Brown MB and Forsythe AB, 1974. Robust tests for the equality of variances. *Journal*

of the American Statistical Association 69, 364-367.

Burn DH and Elnur MaH, 2002. Detection of hydrologic trends and variability. *Journal of Hydrology 255*, 107-122.

Crisci A, Gozzini B, Meneguzzo F, Pagliara S and Maracchi G, 2002. Extreme rainfall in a changing climate: regional analysis and hydrological implications in Tuscany. *Hydrological Processes* 16, 1261-1274.

Fadem B, 2008. High-Yield Behavioral Science (High-Yield Series). Hagerstwon, MD: Lippincott Williams & Wilkins. ISBN 0-7817-8258-9.

Fujibe F, 2015. Relationship between Interannual Variations of Extreme Hourly Precipitation and Air/Sea-Surface Temperature in Japan. *Sola* 11, 5-9.

Fujibe F, Yamazaki N, Katsuyama M and Kobayashi K, 2005. The increasing trend of intense precipitation in Japan based on four-hourly data for a hundred years. *Sola* 1, 41-44.

Gilbert RO, 1987. Statistical methods for environmental pollution monitoring. John Wiley & Sons.

Gocic M and Trajkovic S, 2013. Analysis of changes in meteorological variables using Mann-Kendall and Sen's slope estimator statistical tests in Serbia. *Global and Planetary Change* 100, 172-182.

Hameed T, Mariño MA, Devries JJ and Tracy JC, 1997. Method for trend detection in climatological variables. *Journal of Hydrologic Engineering* 2, 154-160.

Hirabayashi Y, Kanae S, Emori S, Oki T and Kimoto M, 2008. Global projections of changing risks of floods and droughts in a changing climate. *Hydrological Sciences Journal* 53, 754-772.

Hirano J and Matsumoto J, 2011. Secular and seasonal variations of winter monsoon weather patterns in Japan since the early 20th century. *International Journal of*

Climatology 31, 2330-2337.

Levene, H, 1960. In Contributions to Probability and Statistics: Essays in Honor of Harold Hotelling, I. Olkin et al. eds., Stanford University Press, 278-292.

Kanada S, Tsuguti H, Kato T and Fujibe F, 2014. Diurnal variation of precipitation around western Japan during the warm season. *Sola* 10, 72-77.

Kendall MG, 1975. Rank Correlation Methods. London, UK: Griffin.

Keskin S, 2006. Comparison of several univariate normality tests regarding type I error rate and power of the test in simulation based small samples. *Journal of Applied Science Research* 2, 296-300.

Longobardi A and Villani P, 2010. Trend analysis of annual and seasonal rainfall time series in the Mediterranean area. *International Journal of Climatology* 30, 1538-1546.

Mann HB, 1945. Nonparametric tests against trend. *Econometrica: Journal of the Econometric Society*, 245-259.

Nakamura H, Izumi T and Sampe T, 2002. Interannual and decadal modulations recently observed in the Pacific storm track activity and East Asian winter monsoon. *Journal of Climate* 15, 1855-1874.

Oguchi S and Fujibe M, 2012. Seasonal and regional features of long-term precipitation changes in Japan. *Papers in Meteorology and Geophysics* 63, 21-30.

Olejnik SF and Algina J, 1987. Type I error rates and power estimates of selected parametric and nonparametric tests of scale. *Journal of Educational and Behavioral Statistics* 12, 45-61.

Partal T and Kahya E, 2006. Trend analysis in Turkish precipitation data. *Hydrological Processes* 20, 2011-2026.

Pearson E and Hartley H, 1972. Biometrika Tablesfor Statisticians, Vol. 2. In.:

Cambridge, UK: Cambridge University Press.

Peterson TC, Easterling DR, Karl TR, et al., 1998. Homogeneity adjustments of in situ atmospheric climate data: a review. *International Journal of Climatology* 18, 1493-1517.

Razali N and Wah Y, 2011. Power comparisons of shapiro-wilk, kolmogorov-smirnov, lilliefors and anderson-darling tests. *Journal of Statistical Modeling and Analytics* 2, 21-33.

Sen PK, 1968. Estimates of the regression coefficient based on Kendall's tau. *Journal of the American Statistical Association* 63, 1379-1389.

Shapiro SS and Wilk MB, 1965. An analysis of variance test for normality (complete samples). *Biometrika*, 591-611.

Siegel S and Castellan N, 1988. Nonparametric Statistics for the Beha6ioral Sciences. New York: McGraw-Hill.

Singh P, Kumar V, Thomas T and Arora M, 2008. Changes in rainfall and relative humidity in river basins in northwest and central India. *Hydrological Processes* 22, 2982-2892.

St. George S, 2007. Streamflow in the Winnipeg River basin, Canada: Trends, extremes and climate linkages. *Journal of Hydrology* 332, 396-411.

Tabari H and Talaee PH, 2011. Temporal variability of precipitation over Iran: 1966–2005. *Journal of Hydrology* 396, 313-320.

Tachikawa Y, Takino S, Ichikawa Y and Shiiba M, 2009. Study on the Impact of Climate Change on River Flow Regime in the Mogami and Yoshino River Basins, . *J. Japan Soc. of Civil Eng.* 53, 475-480. [In Japanese]

Tao H, Gemmer M, Bai Y, Su B and Mao W, 2011. Trends of streamflow in the Tarim River Basin during the past 50years: Human impact or climate change? *Journal of*

Hydrology 400, 1-9.

Turkes M, 1996. Spatial and temporal analysis of annual rainfall variations in Turkey. *International Journal of Climatology* 16, 1057-1076.

Von Storch H and Navarra A, 1999. Analysis of climate variability: applications of statistical techniques. Springer Science & Business Media.

Wijngaard J, Klein Tank A and Können G, 2003. Homogeneity of 20th century European daily temperature and precipitation series. *International Journal of Climatology* 23, 679-692.

Yu YS, Zou SM and Whittemore D, 1993. Nonparametric Trend Analysis of Water-Quality Data of Rivers in Kansas. *Journal of Hydrology* 150, 61-80.

Yue S and Hashino M, 2003. Temperature trends in Japan: 1900–1996. *Theoretical and Applied Climatology* 75, 15-27.

Yue S, Pilon P and Cavadias G, 2002a. Power of the Mann–Kendall and Spearman's rho tests for detecting monotonic trends in hydrological series. *Journal of Hydrology* 259, 254-271.

Yue S, Pilon P, Phinney B and Cavadias G, 2002b. The influence of autocorrelation on the ability to detect trend in hydrological series. *Hydrological Processes* 16, 1807-1829.

Yue S, Pilon P and Phinney B, 2003. Canadian streamflow trend detection: impacts of serial and cross-correlation. *Hydrological Sciences Journal* 48, 51-63.

Chapter 5 Impact Assessment of Human Activities and Climate Change on Runoff Variations

5.1 Introduction

Understanding hydrological processes, especially in the context of climate change, land use change and the current water management is necessary for sustainable water resources management. In pre-chapter, the trend changes in hydro-climatic variables were detected and found that the changes in river discharge cannot be explained by the changes in meteorological variables. Human activities play important role in streamflow variations. It is necessary to assess the dominant reason for river discharge decreasing and evaluate the contribution rate of each driving factor.

Hydrological dynamics are complex processes affected by various factors like climatic change, land use change and water management (Cuo et al., 2013; Cornelissen et al., 2013; Öztürk et al., 2013; Arheimer et al., 2012; Chu et al., 2012; Zhang et al., 2012A; Zhang et al., 2012B; Delpla et al., 2009). Hu et al. (2015) investigated that surface water resources were more sensitive to climate fluctuation than human activities in the middle reaches of the Yellow River. Cuo et al. (2013) found that the upper Yellow River Basin hydrological regimes had undergone changes over the past decades as reflected by a decrease in wet and warm season stream flow, and annual stream flow due to climate change and human activity. Öztürk et al. (2013) showed the water budget

was more sensitive to variations in precipitation and conversion between forest and agricultural lands but was less sensitive to the type of forest stands in the Bartin spring watershed, Turkey. Zeng et al. (2014) found that climate change played a dominant role followed by human activities in annual streamflow in the Zhang River basin, China. Abundant studies have also been conducted in Japan on the impact of climate change and human activities (Sayama et al., 2008). Fan and Shibata (2015) evaluated the impacts of land use and climate change on the water cycle in the Teshio River Basin, northern Japan. Yoshimura and Koike (2015) evaluated dam volume reallocation under climate change in the Kono River basin. Satoh et al. (2015) reported that effective water management could mitigate natural variability of drought and alleviate the increasing rate of the drought days due to global climate change. However, the studies on the integrated impact of climate change and water management are still limited. In addition, the responses to climate change are high regional-dependence. In the Kamo River basin, to date, there has been limited research on discharge variation. Luo et al. (2014) took a palaeoflood simulation in the Kamo River basin and found that lower discharge and earlier peak discharge time were exhibited under historical land use. It is necessary to further investigate to what degree water discharge has been altered under climate change, land use change and water management.

Many methods have been used to quantify hydrological variations to all kinds of driving factors in river basins (Swank and Crossley, 1988; Sayama and McDonnell, 2009; Singh and Gosain, 2011; Beskow et al., 2012; Dixon and Earls, 2012; Dechmi et al., 2012; Koch et al., 2013). Swank and Crossley (1988) studied hydrological responses of deforestation and forestation from an early age using comparative tests method. Dixon and Earls (2012) examined the effects of land use change on a stream flow with a hydrological model. Hao et al. (2008) reports the variations of surface runoff under

climate change and human activities in the Tarim River Basin by trend analysis of meteorological, socioeconomic and hydrological data. Among them, hydrological simulation is the most widely used method and modelling can be regarded as an objective and repeatable method with which to interpolate and extrapolate knowledge in time and space between observations (Strömqvist et al., 2012). Also, the modelled data can be widely used by water authorities where measured data are not available for expert judgments.

This study, aims to investigate the dominant reasons for the streamflow reduction of the Kamo River and to estimate the relative contributions of precipitation, evapotranspiration and water management to the changes of streamflow by applying rigorously calibrated and validated HYPE model (described in Chapter 3) over the Kamo River basin.

5.2 Water balance analysis

To separate the effects of water management from natural variabilities, we first estimate “natural discharge” by excluding the impact of water management from observed discharge at Fukakusa station. For the Kamo River basin, the water input includes precipitation and water from Lake Biwa. The water output contains evapotranspiration, river discharge at Fukakusa station, water into all water supply systems taking from Lake Biwa, water through Kamo River Cancal into the Uji River and rainwater by sewerage drainage system to the downstream of Fukakusa station. Thus, the water balance equation is as follows:

$$Q_O = Q_N + V_B - V_S - V_C - V_R \qquad (5-1)$$

in which

Q_O is the observed discharge at Fukakusa station;

Q_N is the natural river discharge;

V_B is the water from Lake Biwa;

V_S is water into purification plants taking from Lake Biwa;

V_C is the water through Kamo River Cancal into Uji River;

V_R is rainwater by sewerage drainage system to the downstream.

Since the volume of rainwater directly flowing into sewage (V_R) is not recorded, we estimate V_R as total water into sewage system (V_{DK}) minus water use in the basin (V_{SK}) by assuming all the water use flows into the sewage system. The natural discharge (Q_N) at Fukakusa station can be calculated as follows:

$$Q_N = Q_O - (V_B - V_S - V_C - V_{DK} + V_{SK}) \qquad (5-2)$$

Figure 5-1 displays the annual observed streamflow, water from Lake Biwa and basin average precipitation. It was found that the observed streamflow shows unrealistic high values from 1978 to 1987. Especially, in 1984 the value of observed streamflow is more than the sum of precipitation and water from Lake Biwa. Thus, only the natural discharge in the period from 1989 to 2010 is estimated using Equation (5-2) due to higher reliability in the recent record. The annual value of ($V_B - V_S - V_C - V_{DK} + V_{SK}$) is equally divided into each day to estimate the daily natural discharge. In addition, since there is no record of the volume of water flows through Kamo River Canal to the Uji River (V_C), the value of natural discharge (Q_N) is estimated on the assumption that all the water from Biwa Lake (V_B) is used by water treatment plant (V_S) and flows through

Kamo River Canal (V_C). The reasonability of this assumption will be tested by water balance equation (5-1) using simulated evapotranspiration values. The results of estimated daily natural discharge (Q_N) from 1989 to 2010 are used for model calibration and validation as presented in Figure 5-2.

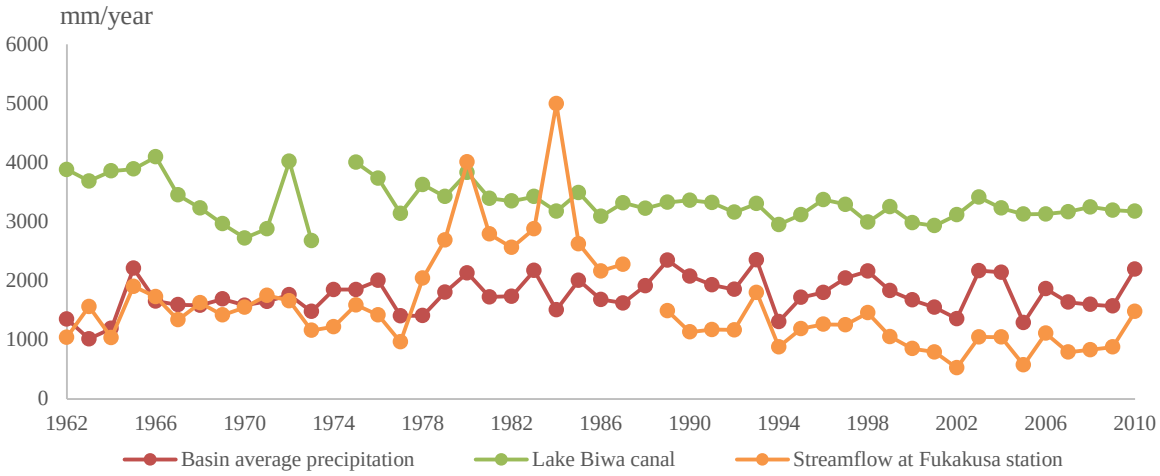

Figure 5-1 Annual statistics of observed data from 1962 to 2010

5.3 Hydrological simulation

5.3.1 Model calibration and validation

The estimated natural discharge from 1989 to 2010 at Fukakusa station is used to calibrate and validate the model. The warm-up period is from 1989 to 1990 and the calibration period is from 2001 to 2010 while validation period is from 1991 to 2000. The HYPE model is calibrated using the land use at 2006. Nine parameters for land use and soil types and other ten general parameters were calibrated. Each parameter was assigned with minimum, maximum and tolerance values before calibration. The characteristic and optimal value of each parameter after the daily calibration is shown in Table 5-1. Because the land use or soil dependent parameters might have different

values for different land use or soil types, Table 5-1 only shows the range of these parameters. If the value for each land use or soil type is same, only one value is shown in Table 5-1. Each general parameter has only one value. The resulting parameters were kept constant for the validation step.

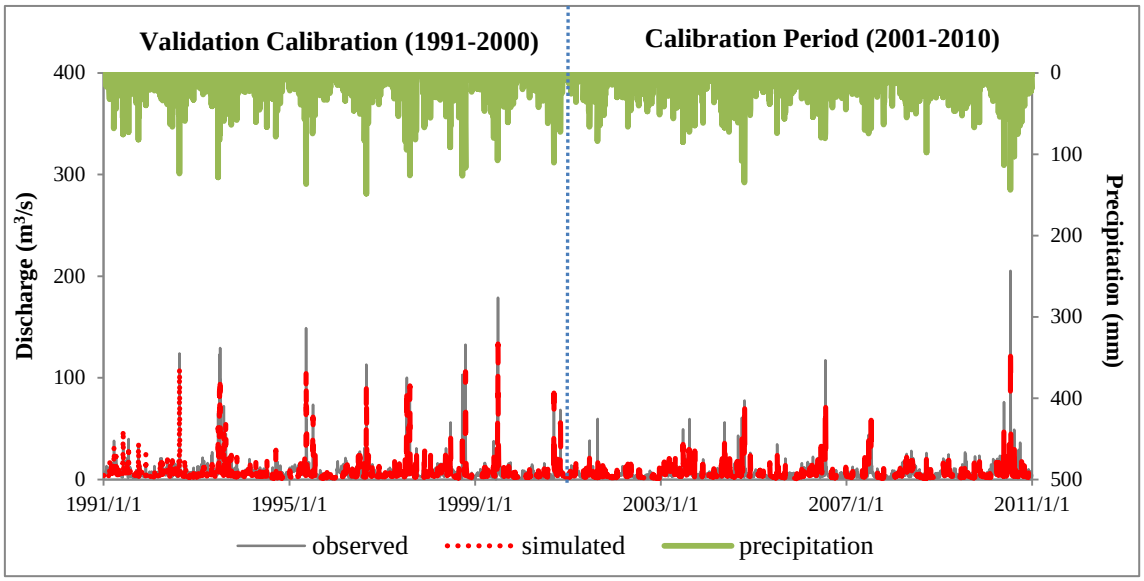

Figure 5-2 Comparison of simulated and natural daily streamflow at KRB outlet

Figure 5-2 displays the simulated and natural daily streamflow for both the calibration and validation periods. Simulations during the calibration and validation periods captured the natural evolution well for daily time scales. Generally, the natural peak flow was higher than the modelled peak flow. Deficiency in HYPE simulations was mismatched peak flows for some days during high flow. The values of NSE for calibration and validation periods were 0.82 and 0.79, respectively. The criteria for model performance vary in different studies. Moriasi et al. (2007) proposed the model performance can be evaluated as satisfactory if NSE $>$ 0.5. Donnelly et al. (2014) used the standard of NSE $>$ 0.4 as acceptable model results. In this study, we considered NSE $>$ 0.6 as the criterion of satisfied model results. Thus, the HYPE model has well performance over the Kamo River basin. In addition, the Pearson correlation

coefficients (CC) of calibration and validation periods are 0.91 and 0.9, respectively, shown in Figure 5-3. The regression lines have a slope close to 1, thus there is a good correlation between daily simulated streamflow and natural streamflow.

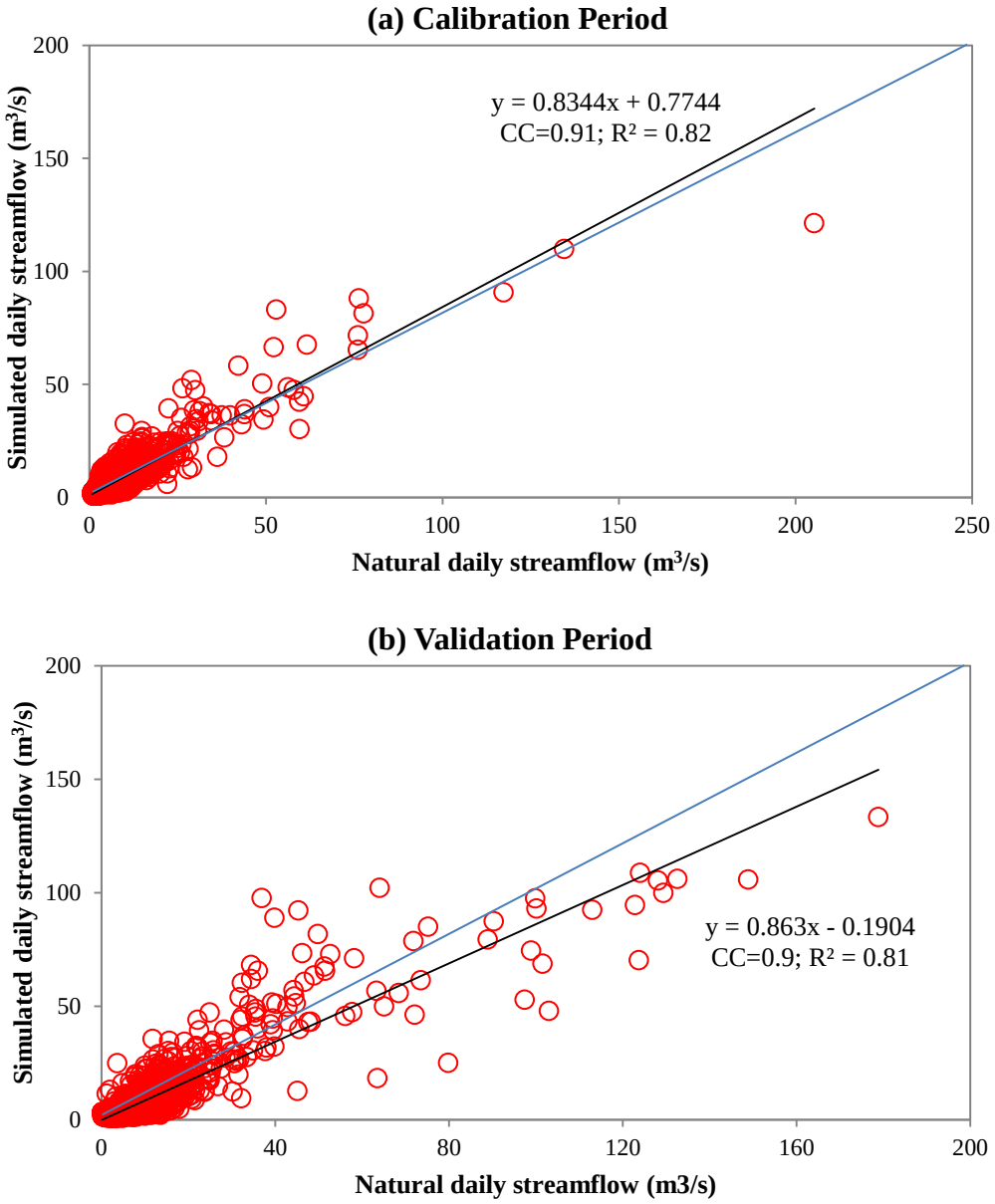

Figure 5-3 Correlation between daily simulated and natural streamflow in (a) calibration and (b) validation periods

Table 5-1 Parameter for model calibration and final results

ID	Parameter	Description	Value	Type
1	wcwp	Wilting point as a fraction	0.11-0.5	Soil dependent
2	wcfc	Field capacity as a fraction	0.15-0.49	Soil dependent
3	wcep	Effective porosity as a fraction	0.11-0.46	Soil dependent
4	cevp	potential evapotranspiration coefficient (mm/degree/d)	0.14-0.27	Land use dependent
5	cevpam	Amplitude of sinus function for potential evapotranspiration	0.49	General
6	cevpph	Phase of sinus function for potential evapotranspiration (days)	62	General
7	epotdist	Coefficient for potential evapotranspiration's depth dependency	8.47	General
8	lp	Limit for potential evapotranspiration	0.95	General
9	rrcs1	Recession coefficient for uppermost soil layer	0.05-0.49	Soil dependent
10	rrcs3	Recession coefficient for slope	0.0005	General
11	mactrinf	Threshold for macro-pore flow (mm/times-step)	2.56-14.95	Soil dependent
12	mactrsm	Threshold soil water for macro-pore flow and surface runoff	0.45-0.84	Soil dependent
13	srrate	Fraction of surface runoff	0.08-0.17	Soil dependent
14	srrcs	Recession coefficient for surface runoff	0.13-0.28	Land use dependent
15	gldepi	Depth for all local water bodies (m)	2.48	General
16	rivvel	Celerity of flood in watercourse (m/s)	1.62	General
17	damp	Fraction of delay in the watercourse	0.14	General
18	gratp	Discharge curve for local water bodies	18.77	General
19	gratk	Discharge curve for local water bodies	5.87	General

5.3.2 Simulated natural discharge

To separate the impacts of climate and land use changes, we divided the climatic data series from 1962 to 2010 into three periods. The climatic data at each period was coupled with a land use map at this period for model simulation. The simulated streamflow from each period is regarded as "natural streamflow" (Q_N) under the impact of climate and land use change. In addition, climatic data from 1962 to 2010 was coupled with land use at 2006 for model simulation and the results are named as "climatic streamflow" (Q_C). The differences between Q_N and Q_C are the effects of land use change.

Table 5-2 Coupling of climatic data and land use for the simulation of natural and climatic streamflow from 1962 to 2010

	Climatic data series	The year of land use map
Modeled natural streamflow (Q_N)	1962-1979	1976
	1980-1995	1987
	1996-2010	2006
Modeled climatic streamflow (Q_C)	1962-2010	2006

As shown in Table 2-1, three land use maps at 1976, 1987 and 2006 were collected. The period of 1962-2010 were divided into three periods of 1962-1979, 1980-1995 and 1996-2010. The division principles are the weights of equal three periods and the media year between the periods of two land use maps. The combination of land use maps and simulation periods are shown in Table 5-2. Q_N in the period of 1962-1979 was simulated using land use data at 1976 and that in the period of 1980-1995 was simulated using land use data at 1987. In the period of 1996-2010 Q_N was modeled using land use data at 2006. The simulated results of Q_N and Q_C are used for contribution analysis of each

factor to the changes of streamflow and trend analysis of long-term average conditions.

5.4 Contribution analysis

5.4.1 Methods

For the Kamo River basin, the changes of river discharge are induced by climatic variability, land use change and water management. By assuming their impacts are independent each other, the following relationship is derived:

$$\Delta Q_O = \Delta Q_C + \Delta Q_L + \Delta Q_w \qquad (5-3)$$

in which

$\triangle Q_O$ is the total change in river discharge;

$\triangle Q_C$ is the change caused by precipitation and temperature;

$\triangle Q_L$ is the change caused by land use change;

$\triangle Q_w$ is the change caused by water management.

$\triangle Q_O$ can be estimated from observed records and $\triangle Q_C$ can be estimated from simulated climatic streamflow. Thus, if $\triangle Q_L$ or $\triangle Q_W$ is known, the contribution ratio of each impact factor is known. In this study, $\triangle Q_L$ is quantified using following equation.

$$\Delta Q_L = \Delta Q_N - \Delta Q_C \qquad (5-4)$$

In the equation, $\triangle Q_N$ is the change in natural discharge, which can be estimated from simulated natural streamflow. As mentioned above, the observed streamflow shows unrealistic high values from 1978 to 1987, thus the first 15 years (1962-1976)

and last 15 years (1996-2010) of the period 1962-2010 are selected to estimate the variations in hydro-climatic variables.

5.4.2 Results

Table 5-3 and Figure 5-4 shows the annual average water balance components in millimeter for the periods of 1962-1976 and 1996-2010. We decided to plot on different directions according to in (+) or out (-) for water balance in the Kamo River basin. It was found that the annual average basin rainfall, evapotranspiration and natural streamflow in the period 1996-2010 were about 161.4 mm, 31.8 mm and 32.3 mm more than that of the period 1962-1976. Land use change contributed positive 3.6 mm to the increase of natural streamflow. The effects of land use change are slight. In addition, climate variability resulted in a slight increase in natural streamflow (28.7 mm) due to the increase of precipitation. However, there was a decrease of 470.1 mm in observed annual discharge from the period 1962-1976 to the period 1996-2010. The primarily reasons are the variations in the water intake from Lake Biwa canal to the Kamo River and the increase of drainage areas of sewer system. It was found that the drainage area of the sewage system increased by 65.7 km^2 from 1962 to 2010. Water from Lake Biwa (V_B) of the period 1996-2010 was about 115.1 mm less than that of the period 1962-1976 whereas water into watertakes (V_S) increased about 304.6 mm. Though water through Kamo River Canal into the Uji River (V_C) reduced about 80.4 mm, the water flowing from Lake Biwa canal to the Kamo River ($V_B - V_S - V_C$) had a reduction of about 339.3 mm. Meanwhile, rainwater by sewerage system to the downstream (V_R) increased by 163.2 mm due to the increase of drainage area of sewerage system. In a total, there was a decrease of 502.5 mm in annual average discharge due to water management. The contribution radios of climate variability, land use change and water

management to the discharge reduction from the period 1962-1987 to the period 1989 to 2010 are about -6.1 %, -0.8 % and 106.9 % (Table 5-4).

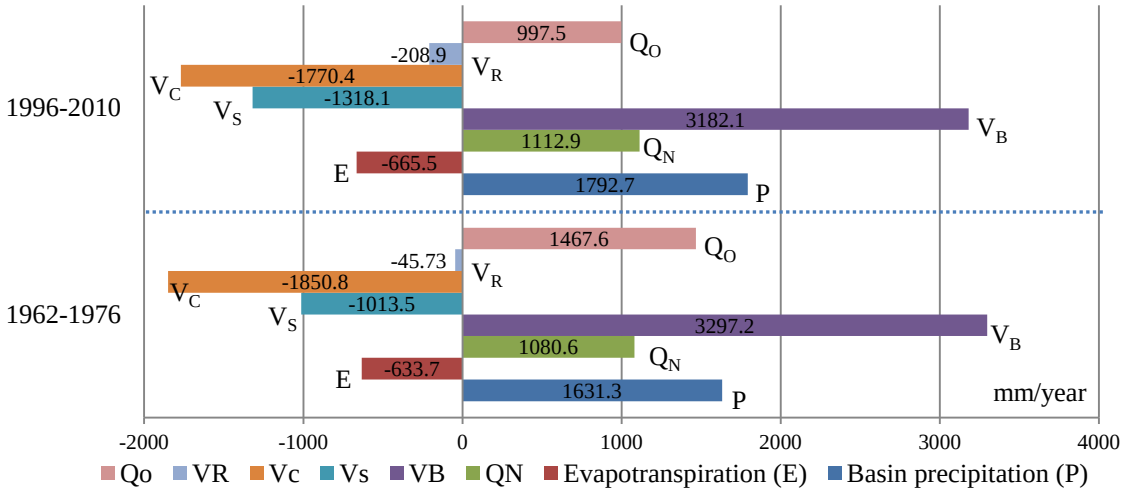

Figure 5-4 Annual average water balance components in the Kamo River Basin for the periods 1962-1976 and 1996-2010 (Minus value represents water going out from the basin)

Table 5-3 Water balance components in the KRB for the periods 1962-1976 and 1996-2010

Unit: mm	1962-1976	1996-2010	Change
Basin precipitation (*P*)	1631.3	1792.7	161.4
Evapotranspiration (*E*)	633.7	665.5	31.8
Natural discharge (Q_N)	1080.6	1112.9	32.3
Water from Lake Biwa (V_B)	3297.2	3182.1	-115.1
water into watertakes (V_S)	1013.5	1318.1	304.6
Water through Kamo River Cancal into the Uji River (V_C)	1850.8	1770.4	-80.4
Rainwater through sewerage system to the downstream (V_R)	45.7	208.9	163.2
Observed discharge (Q_O)	1467.6	997.5	470.1

Table 5-4 Contribution radios of different factors to river discharge change

	Variations (mm/year)	Contribution to discharge reduction (%)
Total change ($\triangle Q_O$)	-470.2	100
Change by climate variability ($\triangle Q_C$)	28.7	-6.1
Change by land use change ($\triangle Q_L$)	3.6	-0.8
Change by water management ($\triangle Q_W$)	-502.5	106.9
Change by Lake Biwa canal	-339.3	72.2
Change by sewage drainage system	-163.2	34.7

The variations of the average seasonal water balance components were presented with a unified unit millimeter in Figure 5-5 and Figure5-6 for the periods of 1962-1976 and 1996-2010. It was found that from the period 1962-1976 to the period 1996-2010 (below if not mention, all increases and decreases are from period 1962-1976 to period 1996-2010) the average seasonal precipitation increased about 19.3 mm, 9.2 mm, 64.1 mm, and 68.2 mm in spring (from March to May), summer (from June to August), autumn (from September to November) and winter (from December to February), respectively. The increases in precipitation concentrated in autumn and winter. Except summer season, natural discharge (Q_N) of all other seasons had increased and there was an obvious rising in winter natural discharge (about 50 mm). Summer natural discharge showed a reduction of about 31.6 mm. However, the value of basin average precipitation minus evapotranspiration (*P-E*) increased in all seasons. Thus, the changes of *P-E* in summer cannot explain the variations in natural discharge. The water flowing from Lake Biwa canal to the Kamo River ($V_B - V_S - V_C$) had a reduction of about 74.2 mm, 117.3 mm, 71.8 mm, and 40.3 mm in spring, summer, autumn and winter, respectively. While rainwater by sewerage system to the downstream (V_R) increased by

46.3 mm, 48.2 mm, 43 mm and 35.3 mm, respectively.

Table 5-5 Contribution radios of monthly variables to river discharge change

	Basin Precipitation (mm/month)			Evapotranspiration (mm/month)		
	1962-1976	1996-2010	changes	1962-1976	1996-2010	changes
1	66.3	80.9	14.6	26.3	29.1	2.9
2	66.9	88.2	21.4	29.3	32.3	3.0
3	95.8	126.0	30.3	44.8	49.4	4.6
4	165.9	126.1	-39.8	60.6	62.0	1.5
5	163.2	192.7	29.5	73.4	74.1	0.7
6	241.6	244.5	2.9	68.4	71.8	3.4
7	248.4	235.6	-12.7	78.2	80.6	2.4
8	145.8	164.8	19.0	77.0	79.1	2.0
9	196.4	196.8	0.5	62.4	66.1	3.8
10	120.3	163.9	43.5	49.3	53.6	4.3
11	74.8	94.9	20.1	35.9	36.3	0.4
12	46.1	78.2	32.2	28.1	30.9	2.9

After the investigation of changes in annual and seasonal hydro-climatic variables, the variations at monthly scale were analyzed. Figure 5-7 shows the contribution radios of climate variability, land use change and water management to discharge variations from the period 1962-1987 to the period 1989 to 2010 in different months. Negative value represents a decreasing impact of the factor to discharge. The impact of land use change was small, less than 3 % in each month. Water management practices resulted in a decrease in streamflow over 12 months. The contributions of climate variability were different in different months. During the months from April to July and September, streamflow showed decreasing under the effects of climate variability while in other months increasing. The primarily reason is likely to be the effects of increase in evapotranspiration diminished the effect of increase in precipitation. Especially, in April

and July the monthly precipitation decreased (Table 5-5).

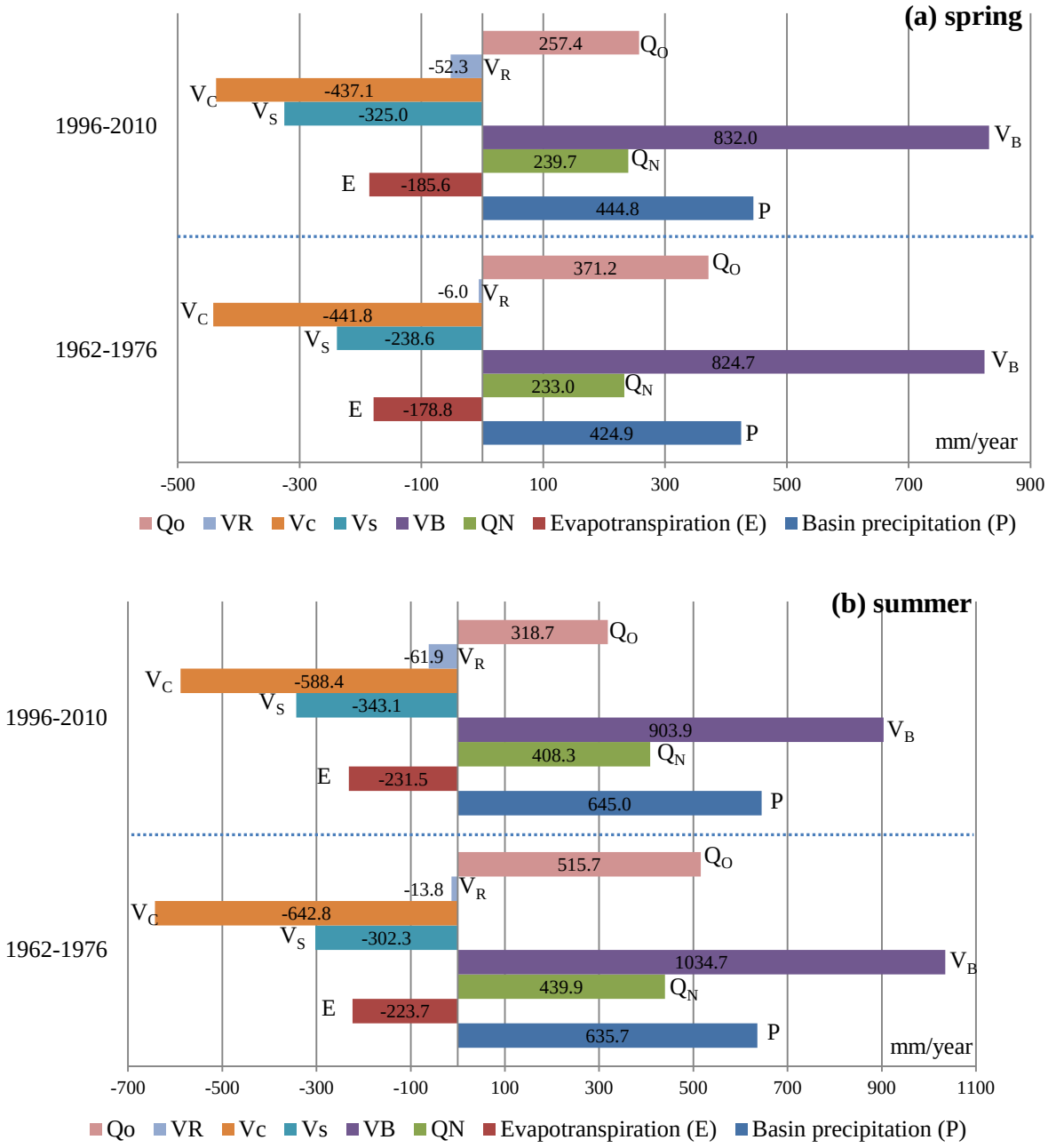

Figure 5-5 Seasonal average water balance components for the periods 1962-1976 and 1996-2010 (Minus value represents water going out from the basin) (a) spring (b) summer

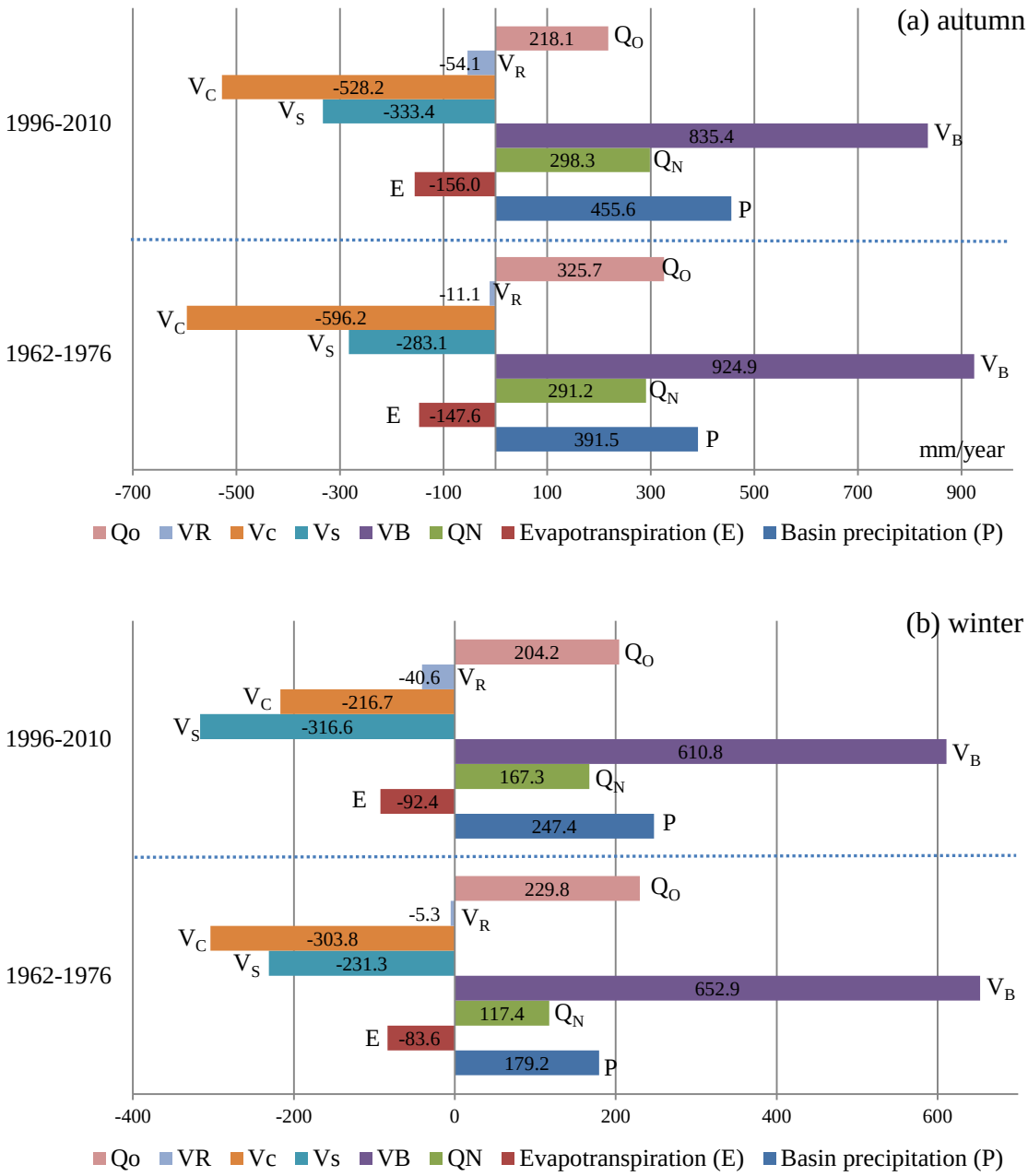

Figure 5-6 Seasonal average water balance components for the periods 1962-1976 and 1996-2010 (Minus value represents water going out from the basin) (a) autumn (b) winter

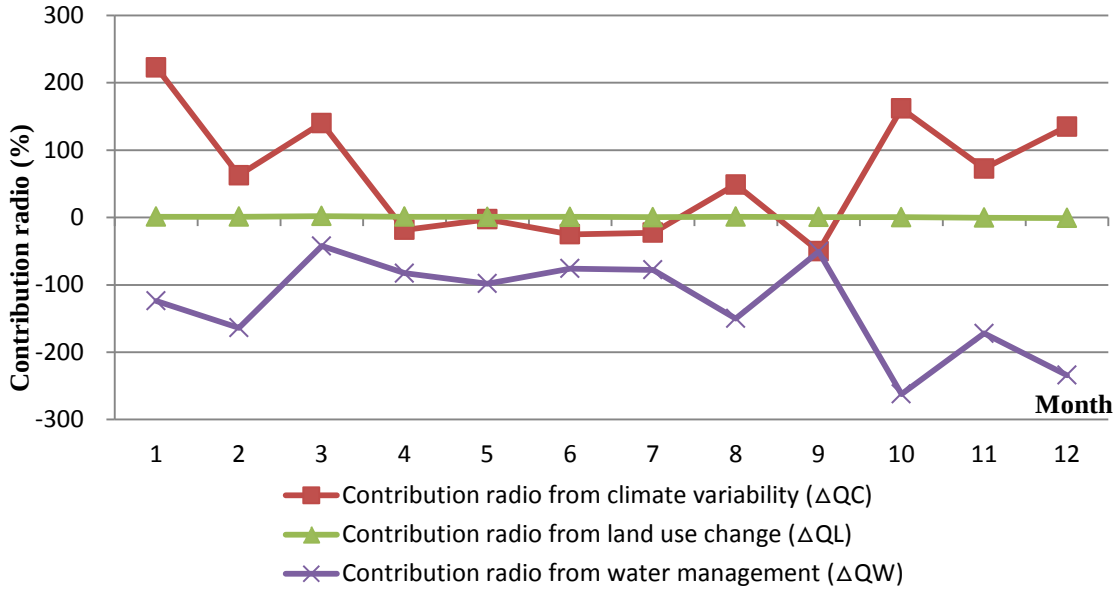

Figure 5-7 Contribution radio of different factors to streamflow in the Kamo River basin for the periods 1962-1976 and 1996-2010 (Minus value represents water going out from the basin)

5.5 Discussion

Climatic variability resulted in a slight increase in annual average streamflow from the period 1962-1976 to the period 1996-2010. However, at the seasonal scale or monthly scale, negative effects of climatic variability on natural streamflow were observed in summer or some months. Especially, in May, the value of basin average precipitation minus evapotranspiration (*P*-*E*) increased by 28.8 mm while natural streamflow decreased by 1.6 mm in streamflow. Thus, the changes in (*P*-*E*) cannot be used to directly explain the changes in streamflow. The primarily reason is that streamflow is the integrated consequence of climatic variables and catchment characteristics. The elasticity of streamflow changes with respect to the changes of precipitation and evapotranspiration are different. In some conditions, streamflow was more sensitive to precipitation than to evapotranspiration, which is contrary in some other conditions. Similar results have been reported in some studies. Hirabayashi et al.

(2008) concluded that variations in floods and droughts cannot be interpreted by changes in precipitation, evapotranspiration or differences between precipitation and evapotranspiration in some conditions. Zheng et al. (2009) reported that streamflow is more sensitive to precipitation than to potential evapotranspiration in the headwaters of the Yellow River basin. A 10% change in precipitation will result in a 21% change in streamflow while a 10% change in potential evapotranspiration will lead a 10.4% change in streamflow.

In addition, the impact of land use change on streamflow was small in this study period. This is due to the slight changes in land use from 1976 to 2006 (Table 2-2). The rapid urbanization in Japan was in 1960s and from the late of 1970s, Japanese urbanization has become slowly. In this research, we did not collect the data of land use before 1970s, the effects of land use change was not significant. However, many studies have proved the impact of land use change on hydrological cycle (Braud et al., 2013). Luo et al. (2014) reported that the increases of forest and paddy fields resulted in a delay and reduction of the peak discharge in the Kamo River basin. Suriya and Mudgal (2012) reported the flooded area and the water depth increased due to urbanization at the same amount of rainfall and different land use conditions.

Meanwhile, there are some uncertainties in this study. First, although the model has well performance in the Kamo River basin according to the calibration and validation results, uncertainties are associated with model dynamics and parameter values. Second, the natural discharge (1989-2010) used for model calibration and validation was calculated based on the assumption that all the water from Biwa Lake (V_B) is either used by water treatment plant (V_S) or flows through Kamo River Canal (V_C). The test results showed that there was less than 100 mm per year flows from Biwa Lake canal to Kamo River in the period from 1989 to 2010, which was less than 3% of the total water per

year from Lake Biwa canal. There is bias in this assumption although the bias is not large and the assumption is reasonable.

5.6 Conclusion

In this chapter, the methods of water balance analysis, hydrologic simulation and statistical analysis have been applied to investigate the dominant reasons for the streamflow changes and quantify the contribution ratio of each factor. The results of calibration and validation show that HYPE model has high performance in the Kamo River basin.

It was estimated that for the period 1962-2010, the effects of increase in annual precipitation diminished the effects of increase in annual evapotranspiration. Climate variability resulted in a slight increase in streamflow. However, the impacts of climate variables on streamflow at seasonal scale are different. Excluding natural discharge of summer season showing a reduction due to climate variability, those of all other seasons increased because of the increase of precipitation. The effects of increase in summer seasonal evapotranspiration diminished the effects of increase in summer seasonal precipitation. At the monthly scale, the effects of precipitation and temperature are various in different months. From April to July and September, natural streamflow showed decreasing due to climate variability while in other months increasing. The impacts of land use change are small in the study period.

Water management practices resulted in a decrease in annual, seasonal and monthly streamflow. And at the annual and seasonal scales, water management played a more important role than climate variability in streamflow change. There was a decrease of 502.5 mm in annual average river discharge from the period 1962-1976 to the period

1996-2010 due to the impact of water management. At monthly scale, except for January and March, water management played a more important role in other months. There are two primary reasons for streamflow decreasing. One is because of the reduction of intake from Lake Biwa canal to Kamo River, while the other is the increase of drainage areas of the sewage system in Kyoto city. At the annual scale, about 72.2% of the reduction in streamflow was caused by change in Lake Biwa canal and 34.7% was induced by sewage system.

Reference

Arheimer B, Dahne J and Donnelly C, 2012. Climate change impact on riverine nutrient load and land-based remedial measures of the Baltic sea action plan. *Ambio* 41, 600-612.

Beskow S, Norton LD and Mello CR, 2012. Hydrological Prediction in a Tropical Watershed Dominated by Oxisols Using a Distributed Hydrological Model. *Water Resources Management* 27, 341-363.

Braud I, Breil P, Thollet F, *et al.*, 2013. Evidence of the impact of urbanization on the hydrological regime of a medium-sized periurban catchment in France. *Journal of Hydrology* 485, 5-23.

Chu JG, Zhang C, Wang YL, Zhou HC and Shoemaker CA, 2012. A watershed rainfall data recovery approach with application to distributed hydrological models. *Hydrological Processes* 26, 1937-1948.

Cornelissen T, Diekkrüger B and Giertz S, 2013. A comparison of hydrological models for assessing the impact of land use and climate change on discharge in a tropical catchment. *Journal of Hydrology* 498, 221-236.

Cuo L, Zhang Y, Gao Y, Hao Z and Cairang L, 2013. The impacts of climate change and land cover/use transition on the hydrology in the upper Yellow River Basin, China. *Journal of Hydrology* 502, 37-52.

Dechmi F, Burguete J and Skhiri A, 2012. SWAT application in intensive irrigation systems: Model modification, calibration and validation. *Journal of Hydrology* 470, 227-238.

Delpla I, Jung AV, Baures E, Clement M and Thomas O, 2009. Impacts of climate change on surface water quality in relation to drinking water production. *Environ Int* 35, 1225-1233.

Dixon B and Earls J, 2012. Effects of urbanization on streamflow using SWAT with real and simulated meteorological data. *Applied Geography* 35, 174-190.

Donnelly C, Yang W and Dahne J, 2014. River discharge to the Baltic Sea in a future climate. *Climatic Change* 122, 157-170.

Fan M and Shibata H, 2015. Simulation of watershed hydrology and stream water quality under land use and climate change scenarios in Teshio River watershed, northern Japan. *Ecological Indicators* 50, 79-89.

Hao XM, Chen YN, Xu CC and Li WH, 2008. Impacts of climate change and human activities on the surface runoff in the Tarim River basin over the last fifty years. *Water Resources Management* 22, 1159-1171.

Hirabayashi Y, Kanae S, Emori S, Oki T and Kimoto M, 2008. Global projections of changing risks of floods and droughts in a changing climate. *Hydrological Sciences Journal* 53, 754-772.

Hu Z, Wang L, Wang Z, Hong Y and Zheng H, 2015. Quantitative assessment of climate and human impacts on surface water resources in a typical semi‐arid watershed in the middle reaches of the Yellow River from 1985 to 2006. *International Journal*

of Climatology 35, 97-113.

Koch S, Bauwe A and Lennartz B, 2013. Application of the SWAT Model for a Tile-Drained Lowland Catchment in North-Eastern Germany on Subbasin Scale. *Water Resources Management* 27, 791-805.

Luo P, Takara K, Apip, He B and Nover D, 2014. Palaeoflood simulation of the Kamo River basin using a grid-cell distributed rainfall run-off model. *Journal of Flood Risk Management* 7, 182-192.

Moriasi D, Arnold J, Van Liew M, Bingner R, Harmel R and Veith T, 2007. Model evaluation guidelines for systematic quantification of accuracy in watershed simulations. *Trans. Asabe* 50, 885-900.

Öztürk M, Copty NK and Saysel AK, 2013. Modeling the impact of land use change on the hydrology of a rural watershed. *Journal of Hydrology* 497, 97-109.

Satoh Y, Yoshimura K, Kim H, and Oki T, 2015. Study on Impact of the Water Resources Management on Projected Future Change of Drought. *J. Japan Soc. of Civil Eng.* 59, I_391-396. [In Japanese]

Sayama T and Mcdonnell JJ, 2009. A new time‐space accounting scheme to predict stream water residence time and hydrograph source components at the watershed scale. *Water Resources Research* 45, W07401.

Sayama T, Tachikawa Y, Takara K, Masuda A and Suzuki T, 2008. Evaluating the impact of climate change on flood disasters and dam reservoir operation in the Yodo river basin. *Journal of Japan Society of Hydrology and Water Resources* 21, 296-313. [In Japanese]

Singh A and Gosain AK, 2011. Climate-change impact assessment using GIS-based hydrological modelling. *Water International* 36, 386-397.

Strömqvist J, Arheimer B, Dahné J, Donnelly C and Lindström G, 2012. Water and

nutrient predictions in ungauged basins: set-up and evaluation of a model at the national scale. *Hydrological Sciences Journal* 57, 229-247.

Suriya S and Mudgal BV, 2012. Impact of urbanization on flooding: The Thirusoolam sub watershed – A case study. *Journal of Hydrology* 412-413, 210-219.

Swank WT and Crossley DA, 1988. Forest hydrology and ecology at Coweta. New York, Springer.

Yoshimura K and Koike T, 2015. Dam Volume Reallocation between Flood Control and Water Use as an Adapting Policy under Climate Change in Kino River Basin. *J. Japan Soc. of Civil Eng.* 59, I_385-390. [In Japanese]

Zeng SD, Xia J and Du H, 2014. Separating the effects of climate change and human activities on runoff over different time scales in the Zhang River basin. *Stochastic Environmental Research and Risk Assessment* 28, 401-413.

Zhang MF, Wei XH, Sun PS and Liu SR, 2012a. The effect of forest harvesting and climatic variability on runoff in a large watershed: The case study in the Upper Minjiang River of Yangtze River basin. *Journal of Hydrology* 464, 1-11.

Zhang YY, Zhang SF, Zhai XY and Xia J, 2012b. Runoff variation and its response to climate change in the Three Rivers Source Region. *Journal of Geographical Sciences* 22, 781-794.

Zheng H, Zhang L, Zhu R, Liu C, Sato Y and Fukushima Y, 2009. Responses of streamflow to climate and land surface change in the headwaters of the Yellow River Basin. *Water Resources Research* 45, W00A19.

Chapter 6 Impact Assessment of Climate Change on Hydrological Extremes

6.1 Introduction

Extreme events and their changes are of particular important for society and ecosystems due to their potentially severe impacts as emphasized in the Special Report on Extreme Events (SREX) of IPCC (Field, 2012). For instance, floods and droughts can evidently cause tremendous damage to human society, e.g. economic losses and environmental health, even human life (Lehner et al., 2006; Zhou et al., 2002). Unfortunately, the frequency and intensity of heavy precipitation events over land will likely increase in the near term as mentioned in IPCC AR5. The increase of extreme events brings large challenge for existing disaster defense structures, which have demonstrated their downslides in some extreme events like 2011 Tohoku tsunami and Thailand floods. It is of scientific and practical merit to understand characteristics of weather and hydrological extremes associated with global warming for effective disaster risk management (Zhang et al., 2011a).

Many studies have addressed the changes of meteor-hydrological extremes over the world (Retchless et al., 2014; Duan et al., 2015). Mann and Gleick (2015) analyzed California drought in the early 21st century and reported that it is likely that the droughts in California will be more severe due to climate change. Hirabayashi et al. (2013) found an increase in flood frequency in lower-latitude countries and a decrease

in certain areas of the world in a warmer future climate. Coumou and Rahmstorf (2012) reviewed the extremes from 2000 to 2011 and argued that the human influence on climate contributed to the increasing of recent extreme weather events. Also, some literatures have addressed the changes of hydro-climatic extremes across Japan (Ohba et al., 2015). Most notably, Fujibe et al. (2005, 2006) argued that the extreme daily precipitation, extreme four-hourly and hourly precipitation have increased over Japan in the past century. In addition, Takeshita (2010) evaluated the changes of precipitation in Miyazaki. Kanae et al. (2004) discussed the changes of hourly heavy precipitation at Tokyo from 1890 to 1999. However, due to the substantial spatial variability of climate, the responses to climate change are high regional-dependence (Parr and Wang, 2015). The critical peak flows of floods are often determined by small to meso-scale processes and require to be analyzed in basin-specific approaches, focusing on single watershed (Lehner et al., 2006). It is necessary to conduct research on each basin with local historical data. Due to Baiu front and typhoon, the Kamo River basin has been vulnerable to floods and suffered from some disastrous floods in the history (Uemura, 2011). The previous sections found river discharge had been decreasing under the impact of water management, which posed a potential threat for the ecosystem and natural amenities. However, what are the variations in extreme events? Does the existing water management adapt to the variations? Up to present, few studies have been conducted on the extremes in the Kamo River basin. Thus, it is of significance to address behaviors of hydro-meteorological extremes in this basin.

The most common approach of hydrological extreme assessments is to analyze the variability of extreme precipitation events from past using observed data and projected precipitation based on different warming scenarios by GCMs (Retchless et al., 2014; Zolina et al., 2014). For example, Krishnamurthy et al. (2009) illustrated that extremes

of rainfall over many parts of India trended to significantly increase using gridded daily rainfall from 1951 to 2003. Dai et al. (2004) estimated the Palmer drought severity index for the USA based on temperature and gauged precipitation. In order to better understand weather extremes variations, the concept of “extreme indices” has been used, which are more generally defined for daily temperature and precipitation characteristics such as the hottest or coldest day of a year, heavy precipitation events, and dry spells (Zhang et al., 2011b). Moreover, a total of 27 indices for weather extremes have been proposed by the Expert Team on Climate Change Detection and Indices (ETCCDI) to describe and assess climate extremes (Alexander et al., 2006). In addition, some studies have started to estimate hydrological extreme events in terms of river discharge (Tachikawa et al., 2011), because any type of flood and drought is likely to show a concurrent augment or reduction in streamflow. Milly et al. (2002) reported an increasing trend of great floods risk over the northern high latitudes using annual maximum monthly-mean river discharge. Hirabayashi et al. (2013) evaluated the global flood risk using annual maximum daily discharge data. In the study of Zhang et al. (2011a), the characteristics of 7-day high and low flows were taken to analyze the changes of extreme events in the Pearl River Basin. In this study, both the changes of extreme river discharge and precipitation are analyzed to estimate hydrological extremes variations in KRB. The changes of extreme river flow are used to represent the variability of floods and droughts. The relationships between the changes of extreme river discharge and precipitation are contribution to understand the variations of floods and droughts at large.

The objectives of this analysis are to 1) to develop hydro-climatic indices for extreme analysis; 2) to estimate the changes of extreme hydro-climatic events which are defined by extreme indices; and 3) to present the relationships between the changes in

extreme precipitation and streamflow.

6.2 Index definition

Extreme indices find multiple applications in hydro-metrological research and related fields due to their robustness and fairly straightforward calculation and interpretation (Sillmann et al., 2013a and 2013b). Also, there are many types of conceivable extremes, e.g. different entities, time periods or parameters (Coumou and Rahmstorf, 2012). In this study, a series of indices in terms of precipitation, temperature and river discharge are used to evaluate the changes of magnitude and frequency of hydro-meteorological extreme events and investigate the relations between meteorological variables and streamflow. For all extreme indices, the analysis commonly starts by selecting either annual maximum/minimum or all events that exceed a certain threshold, independent of their time lag (partial duration series) (Katz, 2006). Herein, the indices in this study are defined with reoccurrence times of a year.

(1) River discharge indices

The discharge indices are divided in to two types, flood indices and drought indices. Flood indices are referred to as annual maximum series, including annual hourly peak flow, daily peak flow and 5-days maximum flow (Table 6-1). In Japan, due to monsoon climate, persistent heavy rainfall in several days frequently occurs during the Baiu Season. SX5day is a useful index to represent the potential damage of persistent heavy rain. Drought indices are referred to as annual minimum series (annual minimum 7-days streamflow, SN7day) and partial duration series under threshold data (Table 6-1). The general option of the threshold level is of high significance. Marginal differences can decide between termination and continued growth of a drought event (Lehner et al.,

2006). In this study, the constant threshold was applied as the tenth percentile of daily discharge data from 1981-2010. The index (CDS) was defined by the longest consecutive days in a year that daily discharge was lower than the reference threshold. If a drought spell starts in a year and ends in next year, the accumulated drought days are reported for the year that the spell starts.

(2) Precipitation indices

ETCCDI has attempted to facilitate the analysis of weather extremes by defining a set of climate indices which provide a comprehensive overview of precipitation statics focusing particularly on extremes aspects (Klein et al., 2009; Sillmann et al., 2013a). A full descriptive list of the indices can be obtained from the website (http:// cccma.seos.uvic.ca/ETCCDMI/list_27_indices.html). In this study, five precipitation indices are used and three of them are referred from ETCCDMI (shown in Table 6-1). The indices of RX1day and RX5day represent annual maximum daily and 5-days precipitation. The CDD index is the longest consecutive days in a year that daily precipitation less than 1 mm (Alexander et al., 2006). If a dry spell starts in a year and ends in next year, the accumulated dry days are reported for the year that the spell starts. In addition, the indices of the annual maximum hourly precipitation (RX1hour) and the times that hourly precipitation is more than 10mm (R10mm) in a year are also used.

(3) Temperature indices

Five temperature extreme indices are referred from ETCCDMI and shown in Table 6-1. The indices of TXx and TXn are the maximum and minimum daily maximum temperature in a year. While the indices of TNx and TNn are the maximum and minimum daily minimum temperature in a year. HT index represents the number of days that daily maximum are more than 30 °C in a year.

Table 6-1 Definitions of extreme indices used in this study

	ID	Indicator name	Definitions	Units
River discharge Indices	CDS	Consecutive low flow days	Annual maximum number of consecutive days with daily streamflow $<10^{th}$ percentile of the ones in the 1981-2010 period	days
	SN7day	Min 7-day flow	Lowest average streamflow in consecutive 7 days	m^3/s
	SX1hour	Max 1-hour flow	Peak hourly streamflow	m^3/s
	SX1day	Max 1-day flow	Highest daily streamflow	m^3/s
	SX5day	Max 5-day flow	Highest average streamflow in consecutive 5 days	m^3/s
Precipitation Indices	CDD	Consecutive dry days	Annual maximum number of consecutive days with daily precipitation＜1mm	days
	RX1hour	Max 1-hour precipitation	Maximum 1-hour precipitation	mm
	R10mm	Heavy precipitation days	Number of times where hourly precipitation >10mm in a year	times
	RX1day	Max 1-day precipitation	Maximum 1-day precipitation	mm
	RX5day	Max 5-day precipitation	Maximum consecutive 5-day precipitation	mm
Temperature indices	TXx	Max Tmax	Maximum daily maximum temperature	℃
	TNx	Max Tmin	Maximum daily minimum temperature	℃
	TXn	Min Tmax	Minimum daily maximum temperature	℃
	TNn	Min Tmin	Minimum daily minimum temperature	℃
	HT	Hot days	Number of days where daily maximum temperature >30℃ in a year	days

Note: all indices are defined with reoccurrence times of a year

6.3 Frequency analysis

6.3.1 Distribution function and return period

Extreme events are stochastic and frequency analysis is a good choice to quantify extreme events (Yevjevich, 1972). Probability distribution can interpret past records of hydro-meteorological events in terms of future probabilities of occurrence, which is useful for engineering design of hydraulic structures. Also, extreme change can be represented as the changes of the probability of occurrence of extremes at certain magnitude from past to current or future. Probability distribution could be represented as the probability density function (PDF) or the cumulative distribution function (CDF). CDF of a random variable X $F_X(x)$ is the probability P of the event that the value of X is no more than x, described as Eq. (6-1). Hereafter $F_X(x)$ is replaced by a simpler expression $F(x)$. PDF of a random variable X is related to CDF, as shown in Eq. (6-2).

$$F_X(x) = P[X \leq x] \tag{6-1}$$

$$F(x) = \int_{-\infty}^{x} f(t)dt \tag{6-2}$$

For an extreme hydrological event with specific value W, there is a relationship:

$$T = \frac{1}{1 - P[X \leq W]} \tag{6-3}$$

In the equation, T is the return period (year) of X=W, and W is often called as T-year event. Note that if the extreme indices are not defined with reoccurrence times of a year, T has to be multiplied by a parameter in the Eq. (6-3) (Takara, 2009). According

to Eq. (6-3), the T-year event *W* can be obtained by using the following equation:

$$W = F^{-1}\left(1 - \frac{1}{T}\right) \qquad (6-4)$$

Now, the frequency of extreme index is related to return period. The extreme changes can be quantified in magnitude by the changes of T-year event *W* or frequency by the changes of return period with the same value of *W*.

6.3.2 Probability distributions

Takara and Stedinger (1994) recommended several important families of probability distributions for modeling extreme events, including the normal, log-normal, extreme-value type I (Gumbel) and type II, and Pearson type III (Gamma) distributions. Takara and Tosa (1999) further reported that the family of the extreme-value distribution was most popularly applied in the frequency analysis of extreme events. In this study, the distributions of log-normal 3p, generalized extreme-value (GEV) and Gamma are used and the final best distribution function is determined by goodness of fit test.

A random variable *X* is log-normal when its logarithm, log(*X*), is normal. The CDF of the log-normal distribution with three parameters (LN3) is in a form of standard normal distribution function Φ:

$$F(x) = \Phi\left(\frac{\ln(x-a) - b}{\sigma}\right) \qquad (6-5)$$

In the Eq. (6-5), σ, a, b are the scale, lower boundary, and location parameters,

respectively.

The CDFs of Gumbel and GEV distributions are:

$$F(x) = \begin{cases} \exp\left[-exp\left(-\dfrac{x-b}{\sigma}\right)\right] & k = 0 \\ \exp\left[-\left(1-k\dfrac{x-b}{\sigma}\right)^{\frac{1}{k}}\right] & k \neq 0 \end{cases} \qquad (6-6)$$

In the Eq. (6-6), k, σ, and b are the shape, scale and location parameters, respectively. When k=0, it is the cumulative function of Gumbel distribution. Whereas $k \neq 0$, it is the cumulative function of GEV distribution.

The Gamma distribution is a generalization of the exponential distribution. Its CDF is defined as following:

$$F(x) = \frac{\Gamma\left(k, \dfrac{x-a}{\sigma}\right)}{\Gamma(k)} \qquad (6-7)$$

In the Eq. (6-7), σ, a, k are the scale, lower boundary, and shape parameters, respectively. And $\Gamma(k)$ is the gamma function, $\Gamma(k,x)$ is the "incomplete gamma function".

$$\Gamma(k) = \int_0^\infty t^{k-1}e^{-t}dt \qquad (6-8)$$

$$\Gamma(k,x) = \int_0^x t^{k-1}e^{-t}dt \qquad (6-9)$$

6.3.3 Parameter estimation methods

Estimation of parameters of distribution functions is to fit a probability function to a set of data. Some methods have been developed and the most common methods for extremes analysis are method of moments, Least square fitting method, Graphical method, Maximum likelihood method and L-moments method (Yevjevich, 1972; Hosking and Wallis, 2005； Alias, 2014). It is different to definitely say which method is the best for a certain model and dataset (Takara, 2009). Each method has different accuracy and limitations. The selection depends on the type of probability distribution functions. Takara and Stedinger (1994) summarized Monte Carlo studies to compare and evaluate various fitting methods for the LN3, Gumbel, GEV and Gamma distributions. The results concluded that the method of maximum likelihood gave more accurate quantile for LN3 and Gamma distributions. The method of L-moments (or probability-weighted moments) is most appropriate for Gumbel and GEV distributions. Alias (2014) reported method of moments, least square fitting method and graphical method are more suitable for distributions with less than three parameters and easily calculated than maximum likelihood and L-moments methods. The detailed information of various parameter estimate methods can be found in Yevjevich (1972), Murshudov et al. (1997) and Hosking and Wallis (2005). In this study, the maximum likelihood method and L-moments method are used for parameter estimation.

6.3.4 Goodness of Fit Tests

The criterion of standard least-square (SLSC) is one of the simplest and most commonly used methods for goodness of fit test (Alias, 2014). Besides SLSC, Takara and Takasao (1988) used three other criteria to evaluate goodness of fit of each

distribution, including COR (correlation coefficient), MLL (maximum log-likelihood) and AIC (Akaike's information criterion). They found that SLSC, COR and MLL gave good rankings to the distributions with three parameters like LN3 and Gamma, while AIC was appropriate for the distribution with two parameters. Stephens (1986) introduced a modified Anderson-Darling (AD) criterion to validate the probability distribution models. Also there are some studies using Kolmogorov-Smirnov (KS) criterion (Conover, 1980). In addition, Castillo et al., (2005) suggested that graphical displays, e.g. Quantile-Quantile (Q-Q) plots and Probability-Probability (P-P) plots, are simple and useful methods for distribution model validation. In this study, the criteria of SLSC, COR, AD and KS are used for goodness of fit test. And the graphical displays are used as reference to suppose the test statistics from vision.

(1) Standard least-square test (Takara, 2009)

The SLSC is one of the simplest methods for evaluating linearity of the data. The calculation equation is as follows:

$$SLSC = \frac{\sqrt{\sigma_{min}^2}}{\left|S_{1-p}^* - S_p^*\right|} \qquad (6-10)$$

$$\sigma^2 = \frac{1}{N}\sum_{i=1}^{N}(S_i - r_i)^2 \qquad (6-11)$$

Here S_p^* is a particular value of the reduced variate S_i corresponding to the non-exceedance probability p, σ_{min}^2 is obtained by minimizing σ^2, N is the number of sample size (observations). S_i is obtained using the transformation function $g(x)$ described as:

$$S_i = g(y_i) \quad (6-12)$$

$$r_i = g\left(F^{-1}(p_i)\right) \quad (6-13)$$

in which y_i is the sorted of the variable x from least to largest, r_i is the standard variate for empirical data, p_i is the non-exceedance probability assigned to y_i and it can be calculated using a plotting position formula.

$$p_i = \frac{i-a}{N+1-2a} \quad (6-14)$$

In the Eq. (6-14), a is a constant based on probability distributions. The use of Hazen's formula (a=0.5) is recommended by Takasao et al. (1986). They compared six formulae, including the Weibull (a=0), Adamowski (a=0.25), Bolm (a=0.375), Cunnane (a=0.4), Gringorten (a=0.44) and Hazen, and found that the formula of Hazen gave relatively better results. The smaller the SLSC is, the better the fitting of the distribution is. Takasao et al. (1986) considered SLSC<0.03 as a good fit for precipitation extremes analysis. Tanaka and Takara (1999) concluded that SLSC<0.04 is acceptable for streamflow extremes frequency analysis in Japan.

(2) Correlation coefficient test

The criterion of correlation coefficient between y_i and r_i is defined as follows:

$$COR = \sum_{i=1}^{N}(y_i-\bar{y})(r_i-\bar{r}) \Big/ \sqrt{\sum_{i=1}^{N}(y_i-\bar{y})^2 \sum_{i=1}^{N}(r_i-\bar{r})^2} \quad (6-15)$$

In the Eq. (6-15), $\bar{y}$ and $\bar{r}$ are the means of y and r. Values of COR closer to unity indicates better fits (Takara and Takasao, 1988).

(3) Kolmogorov-Smirnov test

The KS test is used to test if a sample of data came from a hypothesized continuous distribution in which the theoretical distribution function of the test distribution is compared with the empirical distribution function of the time series data (Conover, 1980). The statistic *D* is defined as:

$$D = sup|Fn(x) - S(x)| \qquad (6-16)$$

In the Eq. (6-16), *Fn(x)* is the empirical cumulative distribution function of the random sample X; $S(x)$ is the theoretical cumulative distribution function. The smaller value of *D* is, the better the fitting of the distribution is.

(4) Anderson-Darling test

The AD test is an alternative to the KS test and it gives more weight to tails compared with the KS test. Supposing the sample X ($x_1<x_2<\ldots<x_n$) comes from an expected distribution with the cumulative function *S(x)*, the statistic *A* is defined as:

$$A^2 = -n - \sum_{i=1}^{n} \frac{2i-1}{n}\left[lnS(x_i) + ln\left(1 - S(x_{n+1-i})\right)\right] \qquad (6-17)$$

In the Eq. (6-17), x_i is the i^{th} case in the sample X; *n* is the number of the sample. The smaller value is, the better the fitting of the distribution is.

6.3.5 Study period

As shown in Chapter 2 (Table 2-1), the lengths of hydro-meteorological observed data series at different stations are various, especially for hourly data. It is difficult to quantify the changes of frequency and magnitude of extreme events between two periods at all stations. Herein, the data series of temperature, basin average rainfall and HYPE-simulated hourly streamflow are used to evaluate the extreme events changes. The total period is from 1962 to 2014, which is then equally divided into two periods (1962-1988 and 1989-2014). The first period of 27 years is used as reference and the latter period of 26 years is used to examine changes from the reference.

6.3 Results

6.3.1 Goodness of fit

Before considering frequency analysis, homogeneity test is conducted on the data series of extreme indices and no heterogeneities are found. Then, the data series are fitted for three probability distributions (LN3, GEV and Gamma 3p) and goodness of fit is tested using four criteria (SLSC, COR, KS and AD). According to the recommendation (SLSC<0.04) by Tanaka and Takara (1999) and with the accuracy in our study of three numbers after decimal point (0.000), SLSC<0.045 is considered as a good fit for extremes analysis. The other three criteria are less likely to reject the good fit, and are successfully used to compare the goodness of fit of different fitted distributions. If the results of distribution fitting tests are the same in one period, the better result in the other period is adopted. When results in both periods between different distributions are similar, the results of other criteria are referenced. If the better

result in two periods is different, the results of other criteria are also used.

Table 6-2 shows the test results of good fit of different distributions to extreme river discharge indices. It was found that the ranking of distributions from the KS and AD tests are similar and different from the results under SLSC and COR tests. The GEV and LN3 distributions show better rankings in the criteria of SLSC, KS and AD, while the Gamma and GEV distributions show better rankings under COR. In addition, the SLSC values of all fitted distributions in the data series of SN7day and SX1hour from 1962 to 1988 and SX5day from 1989 to 2014 are more than 0.045. In general, for the indices of CDS, SN7day and SX5day, the good fit distribution is GEV. For SX1day index, LN3 has best ranking under SLSC but the results are almost same as the ones of GEV. And KS and AD show the best fit distribution is GEV. Thus, the SX1day data series is also fitted to the GEV. For the SX1hour, because the results of different criteria vary, the Q-Q plots are used to be compared. Figure 6-1 indicate that LN3 has better fit to SX1hour, especially in the period 1962-1988. The best fit of distribution to each index is summarized in Table 6-5. The Q-Q plots of selected distribution for each index are shown in Figure 6-3 and 6-4.

Table 6-2 Results of goodness of fit tests for river discharge extreme indices

		CDS		SN7day		SX1hour		SX1day		SX5day	
		P1	P2	P1	P2	P1	P2	P1	P2	P1	P2
SL	LN3	0.066	0.068	0.071	0.036	0.059	0.046	0.034	0.044	0.033	0.055
SC	GEV	0.023	0.038	0.052	0.036	0.047	0.030	0.034	0.045	0.032	0.048
	Gamma	0.033	0.086	0.083	0.037	0.066	0.038	0.036	0.044	0.033	0.057
CO	LN3	0.933	0.962	0.893	0.982	0.900	0.948	0.978	0.974	0.981	0.959
R	GEV	0.992	0.974	0.962	0.983	0.949	0.979	0.972	0.975	0.980	0.971
	Gamma	0.988	0.976	0.893	0.982	0.951	0.986	0.982	0.973	0.984	0.956
KS	LN3	0.138	0.305	0.179	0.126	0.111	0.121	0.114	0.172	0.088	0.152
	GEV	0.086	0.145	0.137	0.110	0.160	0.134	0.105	0.149	0.091	0.109
	Gamma	0.121	0.293	0.179	0.124	0.161	0.122	0.126	0.181	0.117	0.154
AD	LN3	4.58	11.17	0.953	0.436	0.404	0.348	0.264	0.695	0.247	0.804
	GEV	0.209	0.817	0.774	0.370	0.734	0.568	0.249	0.535	0.230	0.514
	Gamma	3.890	10.75	0.816	0.427	4.964	1.241	0.332	0.744	0.322	0.801

P1: 1962-1988; P2: 1989-2014; the symbol of "_" means the best ranking under each criterion.

Table 6-3 displays the goodness of fit test results of different distributions to extreme precipitation indices. For RX1hour, LN3 and GEV seem to have good fit. It is difficult to determine the best distribution according the four test criteria, the Q-Q plots of LN3 and GEV are compared and LN3 looks better fit (shown in Figure 6-2). In addition, for the index of RX1day no good fit distribution is tested by SLSC in the period 1989-2014. For other precipitation extreme indices, GEV is the best fit distribution.

Table 6-3 Results of goodness of fit tests for precipitation extreme indices

		CDD		RX1hour		R10mm		RX1day		RX5day	
		P1	P2	P1	P2	P1	P2	P1	P2	P1	P2
SL	LN3	0.041	0.043	0.023	0.020	0.030	0.021	0.037	0.056	0.023	0.046
SC	GEV	0.033	0.039	0.025	0.019	0.030	0.021	0.036	0.054	0.025	0.042
	Gamma	0.044	0.048	0.023	0.020	0.030	0.022	0.039	0.057	0.028	0.048
CO	LN3	0.978	0.971	0.993	0.994	0.988	0.993	0.981	0.957	0.990	0.979
R	GEV	0.984	0.978	0.992	0.994	0.987	0.993	0.977	0.965	0.992	0.979
	Gamma	0.976	0.966	0.993	0.994	0.988	0.993	0.980	0.954	0.989	0.979
KS	LN3	0.111	0.149	0.105	0.084	0.090	0.101	0.161	0.203	0.116	0.115
	GEV	0.119	0.139	0.117	0.093	0.104	0.094	0.132	0.159	0.106	0.083
	Gamma	0.112	0.132	0.111	0.094	0.092	0.104	0.165	0.210	0.110	0.120
AD	LN3	0.369	0.442	0.230	0.195	0.251	0.233	0.475	1.080	0.212	0.569
	GEV	0.383	0.378	0.224	0.183	0.233	0.212	0.412	0.687	0.186	0.309
	Gamma	0.391	0.447	0.237	0.202	0.251	0.239	0.507	1.086	0.214	0.611

P1: 1962-1988; P2: 1989-2014; the symbol of "_" means the best ranking under each criterion.

Table 6-4 shows the goodness of fit test results of different distributions to extreme temperature indices. For the indices of TXx, TXn, TNn and HT, most criteria indicate the best ranking is the GEV distribution. For the TNx index, in the period 1989-2014, the best fit distribution is GEV. However, it is rejected by SLSC in the period 1962-1988. Thus, the TNx data series are fitted for the LN3 distribution. The final selection for all indices and validation of the selected distributions by the Q-Q plots are shown in Table 6-5 and Figure 6-3, 6-4.

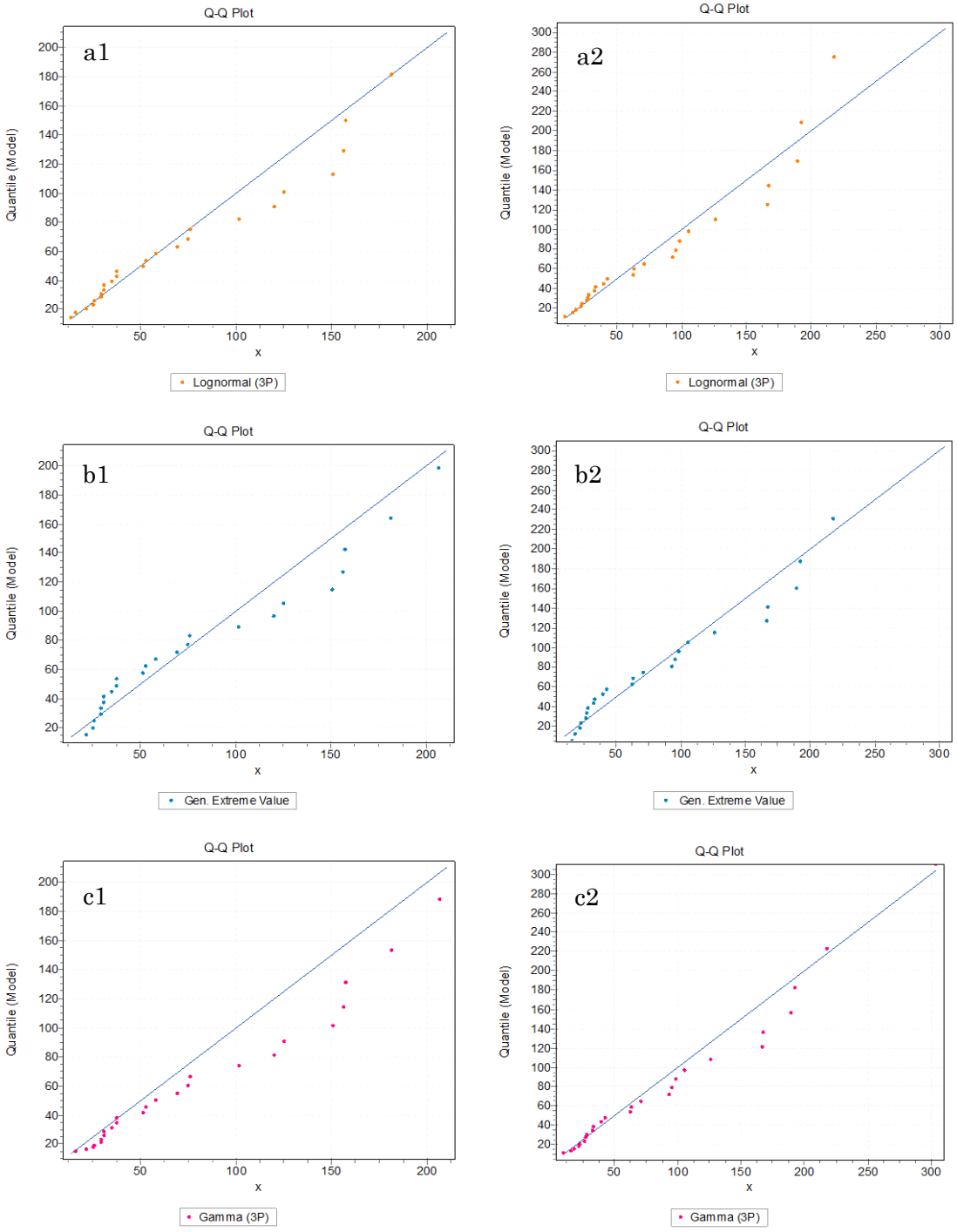

Figure 6-1 Quantile-Quantile (Q-Q) plots of SX1hour with different distributions in the period 1962-1988 and 1989-2014: a1) LN3 in the period 1962-1988; a2) LN3 in the period 1989-2014; b1) GEV in the period 1962-1988; b2) GEV in the period 1989-2014; c1) Gamma in the period 1962-1988; c2) Gamma in the period 1989-2014.

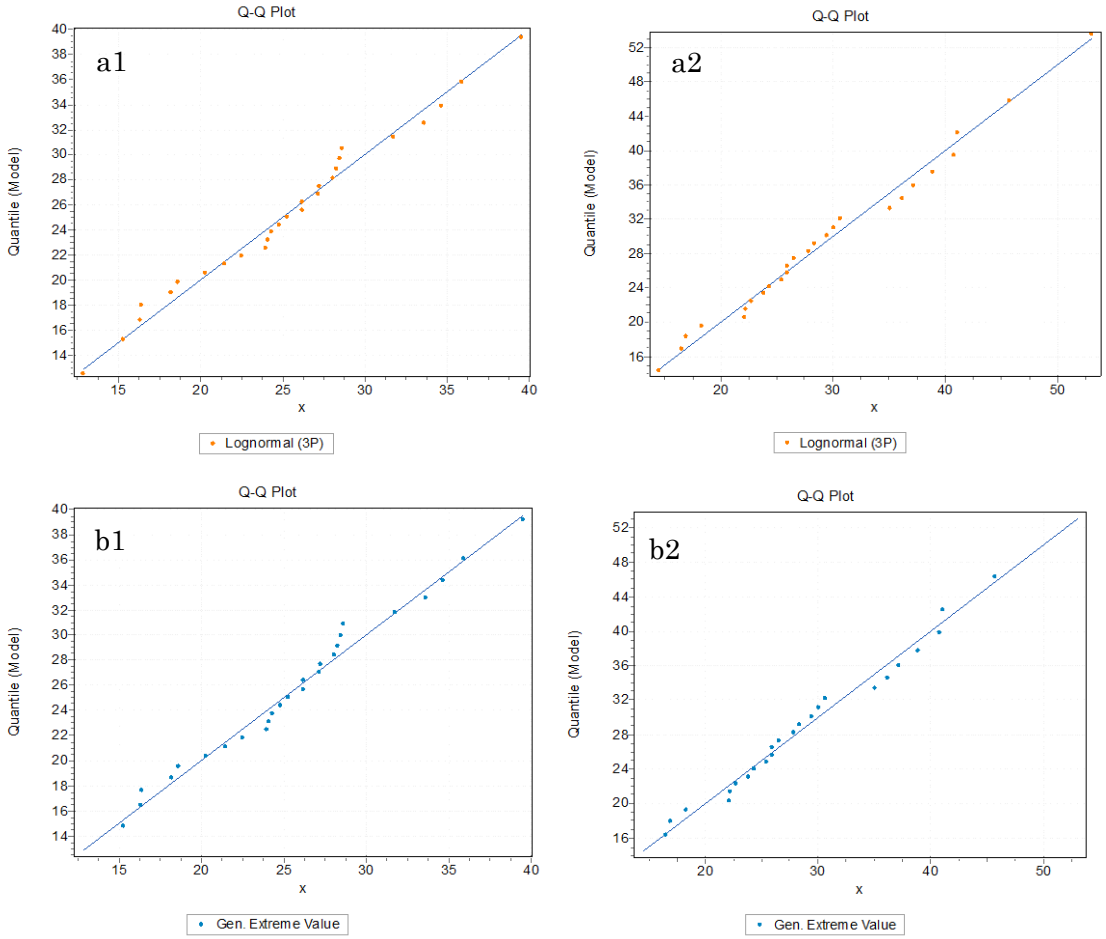

Figure 6-2 Quantile-Quantile (Q-Q) plots of RX1hour with different distributions in the period 1962-1988 and 1989-2014: a1) LN3 in the period 1962-1988; a2) LN3 in the period 1989-2014; b1) GEV in the period 1962-1988; b2) GEV in the period 1989-2014

Table 6-4 Results of goodness of fit tests for temperature extreme indices

		TXx		TNx		TXn		TNn		HT	
		P1	P2	P1	P2	P1	P2	P1	P2	P1	P2
SL	LN3	0.038	0.027	0.044	0.034	0.022	0.020	0.037	0.048	0.037	0.056
SC	GEV	0.029	0.027	0.051	0.025	0.022	0.020	0.029	0.036	0.036	0.036
	Gamma	0.039	0.027	0.045	0.035	0.022	0.024	0.038	0.050	0.037	0.057
CO	LN3	0.981	0.991	0.973	0.985	0.993	0.993	0.982	0.968	0.982	0.957
R	GEV	0.990	0.990	0.969	0.992	0.994	0.993	0.990	0.984	0.984	0.984
	Gamma	0.979	0.990	0.973	0.983	0.993	0.992	0.980	0.966	0.981	0.954
KS	LN3	0.092	0.137	0.137	0.113	0.067	0.094	0.145	0.137	0.103	0.129
	GEV	0.078	0.110	0.124	0.083	0.075	0.099	0.128	0.099	0.100	0.087
	Gamma	0.096	0.138	0.136	0.125	0.067	0.116	0.159	0.150	0.099	0.134
AD	LN3	0.311	0.289	0.413	0.313	0.160	0.221	0.411	0.554	0.410	0.458
	GEV	3.962	0.259	0.455	0.201	0.159	0.190	0.353	0.347	0.319	0.222
	Gamma	0.341	0.292	0.417	0.369	0.161	0.270	0.468	0.590	0.431	0.542

P1: 1962-1988; P2: 1989-2014; the symbol of "_" means the best ranking under each criterion.

Table 6-5 Probability distributions fitted to extreme indices for frequency analysis

	Distribution		Distribution		Distribution
CDS	GEV	CDD	GEV	TXx	GEV
SN7day	GEV	RX1hour	LN3	TNx	LN3
SX1hour	LN3	RX10mm	GEV	TXn	GEV
SX1day	GEV	RX1day	GEV	TNn	GEV
SX5day	GEV	RX5day	GEV	HT	GEV

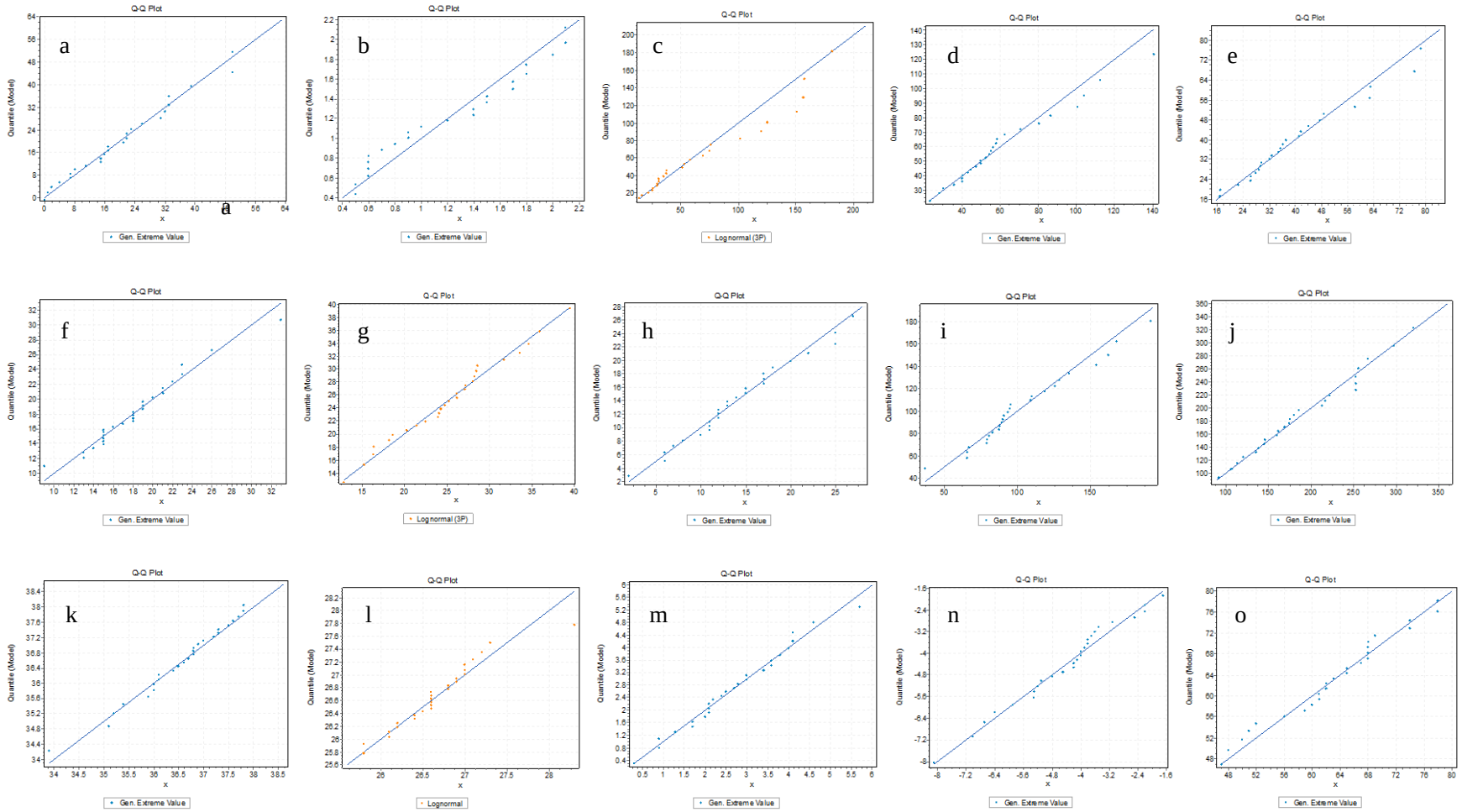

Figure 6-3 Quantile-Quantile (Q-Q) plots of extreme indices fitted for optimal distribution in the period 1962-1988: a) CDS, b) SN7day, c) SX1hour, d) SX1day, e) SX5day, f) CDD, g) RX1hour, h) R10mm, i) RX1day, j) RX5day, k) TXx, l) TNx, m) TXn, n) TNn, o) HT.

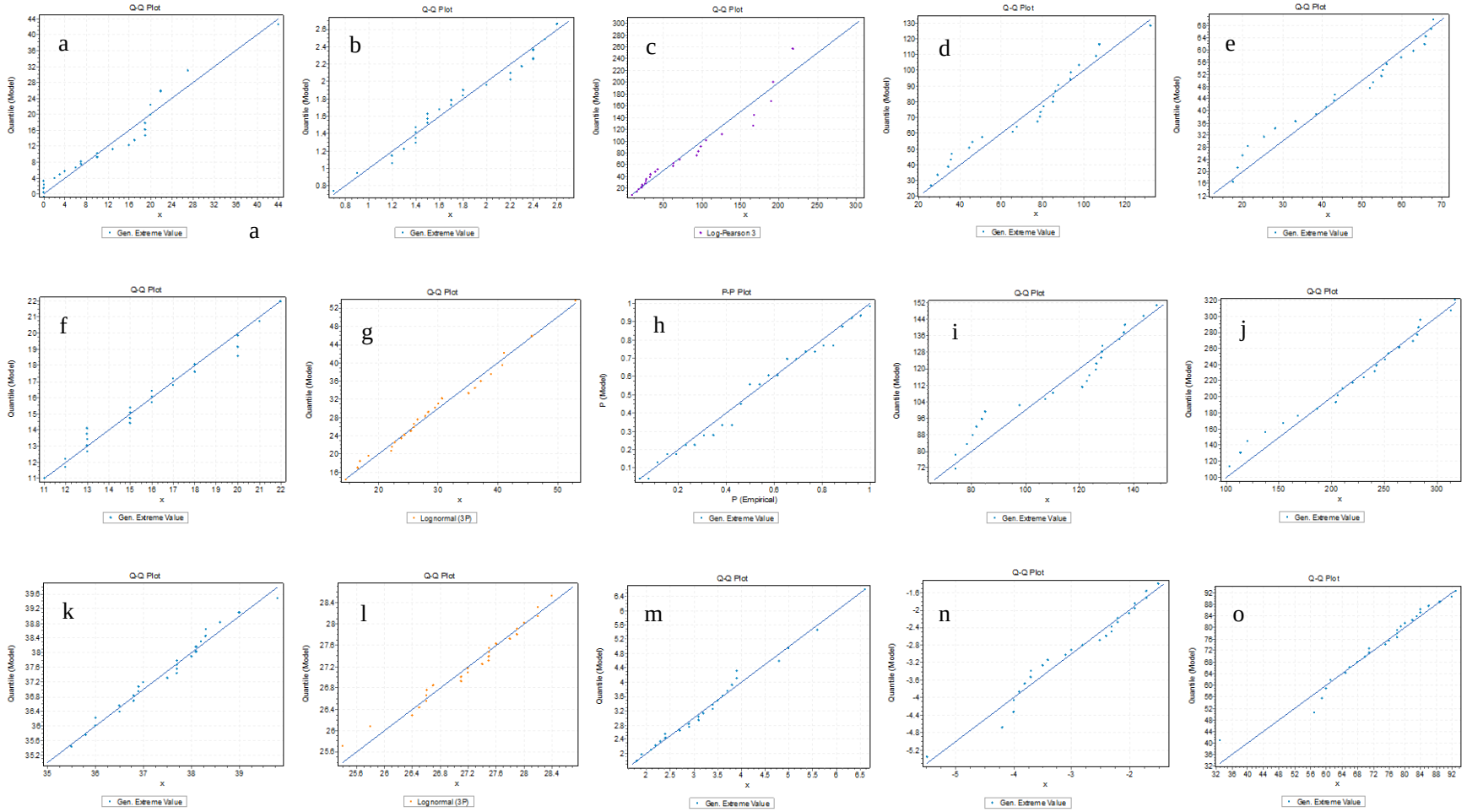

Figure 6-4 Quantile-Quantile (Q-Q) plots of extreme indices fitted for optimal distribution in the period 1989-2014: a) CDS, b) SN7day, c) SX1hour, d) SX1day, e) SX5day, f) CDD, g) RX1hour, h) R10mm, i) RX1day, j) RX5day, k) TXx, l) TNx, m) TXn, n) TNn, o) HT.

6.3.2 Frequency distribution changes in river discharge extremes

In this study, the changes in the return period of 100-year events from the period 1962-1988 (P1) to the period 1989-2014 (P2) are illustrated (hereafter referred to as"P1 or P2 100-year event"). The recurrence of 100-year event is chosen because the design standard of flood control in the Kamo River basin is 100-year. In addition, the differences between the magnitudes of P1 100-year event and P2 100-year event are presented.

Figure 6-5 shows the changes in the return period of river discharge indices and magnitude of 100-year event by the inverse cumulative distribution functions. For the dry condition index of CDS, the magnitude of 100-year event decreased by 34% from P1 to P2 and the return period of P1 100-year event shifted to 800-year in P2. For flood indices, SX1hour presents different changes from SX1day and SX5day. It increased by 23% in the magnitude of 100-year event and the return period of P1 100-year event reduced to 60-year. Whereas SX1day and SX5day decreased by 14% and 13% in the magnitude of 100-year event and the return periods of P1 100-year event of SX1day and SX5day moved to 550-year and 560-year, respectively. However, the means of SX1day and SX5day (2-year event) in the period 1989-2014 are larger than the means in the period 1962-1988.

In addition, the probability distribution function of SN7day is shown in Figure 6-6 instead of the inverse cumulative distribution. This is because SN7day is an index for extreme minimum event and cumulative distribution function cannot be used to evaluate extreme minimum values. It was found that the occurrence of extreme low 7-day streamflow was notably reduced in the period 1989-2014 and the magnitude of SN7day had also increased in the period 1989-2014.

6.3.3 Frequency distribution changes in precipitation extremes

Figure 6-7 and 6-8 shows the changes of extreme precipitation indices in return period and the magnitude of 100-year event by the inverse cumulative distribution functions. For the dry condition index of CDD, the magnitude of 100-year event decreased by 22% from P1 to P2 and the return period of P1 100-year event extended to more than 1000-year in P2. For wet condition indices, RX1hour and R10mm increased by 41% and 27% in the magnitude of 100-year event and the return period of P1 100-year event of RX1hour and R10mm reduced to 10-year and 25-year, respectively. There is a notable increase in the occurrence and magnitude of extreme hourly precipitation. Whereas RX1day and RX5day decreased by 18% and 9% in the magnitude of 100-year event and the return periods of P1 100-year event of RX1day and RX5day moved to more than 1000-year and 350-year, respectively. However, the means of RX1day and RX5day (2-year event) in the period 1989-2014 are larger than the means in the period 1962-1988. There is an increase in the average condition of annual daily and 5-day maximum precipitation, and there is a notable decrease in the magnitude of extreme daily and 5-day precipitation. In addition, the changes in extreme river discharge are related to the changes in extreme precipitation. There are similarities in the changes of magnitude and return period between the indices of extreme precipitation and river discharge, for example CDS and CDD, SX1day and RX1day, etc.

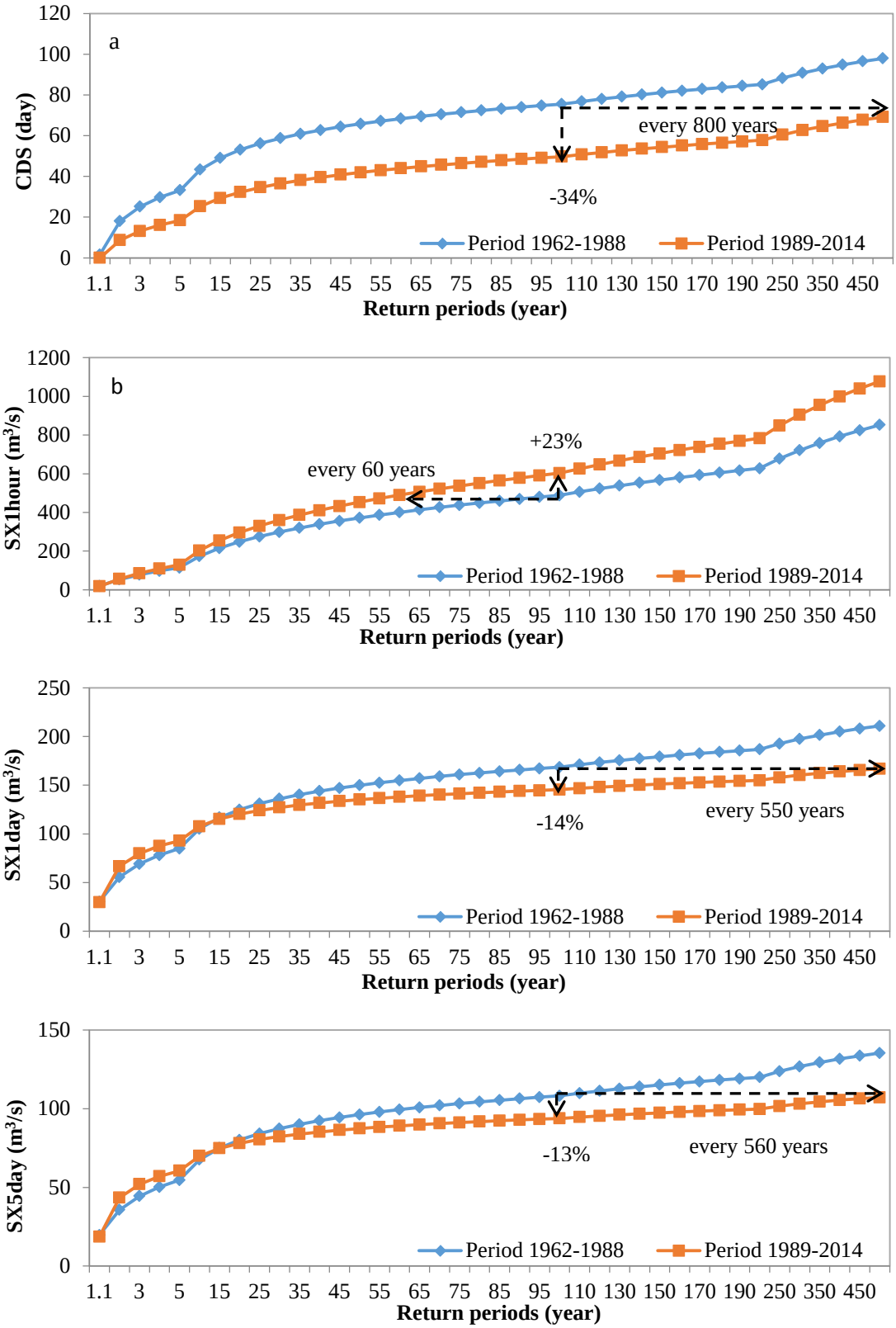

Figure 6-5 Annual inverse cumulative distribution functions of river discharge indices: a) CDS, b) SX1hour, c) SX1day, d) SX5day

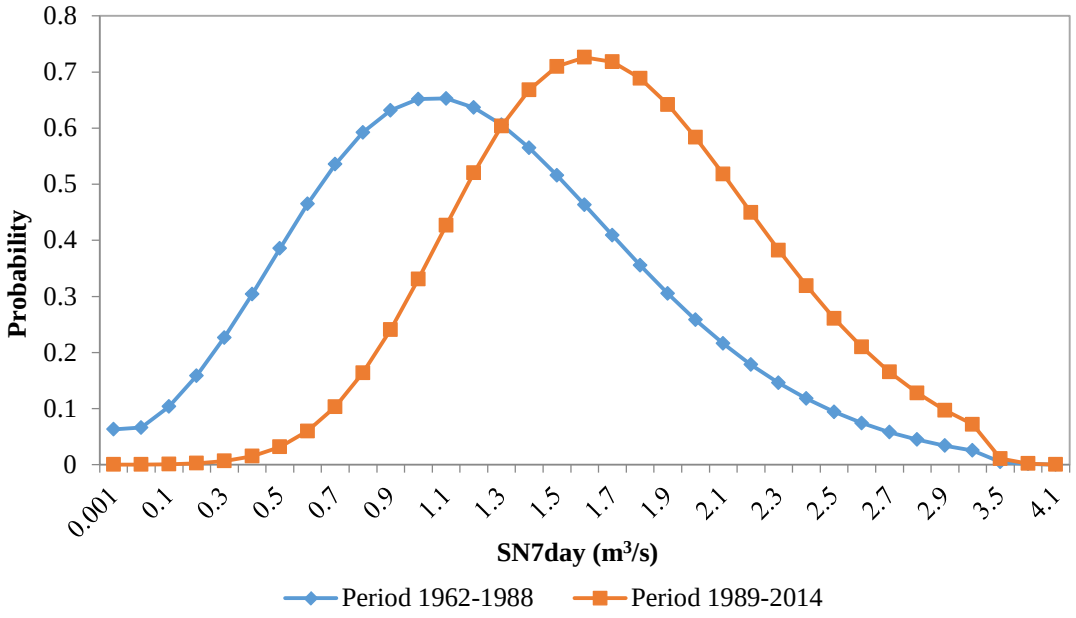

Figure 6-6 Annual probability distribution functions of SN7day index

6.3.4 Frequency distribution changes in temperature extremes

Figure 6-9 shows the changes of extreme temperature indices in return period and magnitude of 100-year events by the inverse cumulative distribution functions. For the maximum daily maximum and minimum temperature (TXx and TNx), the magnitude of 100-year event increased 3% and 4% from P1 to P2 and the return period of P1 100-year event shifted to 5-year and 7-year in P2. Although the changes in magnitude are not obvious, the changes in return period are notable. The hot days index (HT) increased by 12% in the magnitude of 100-year event and the return period of P1 100-year event reduced to 4-year. Thus, there are notable increases in extreme temperature indices over 1962-2014.

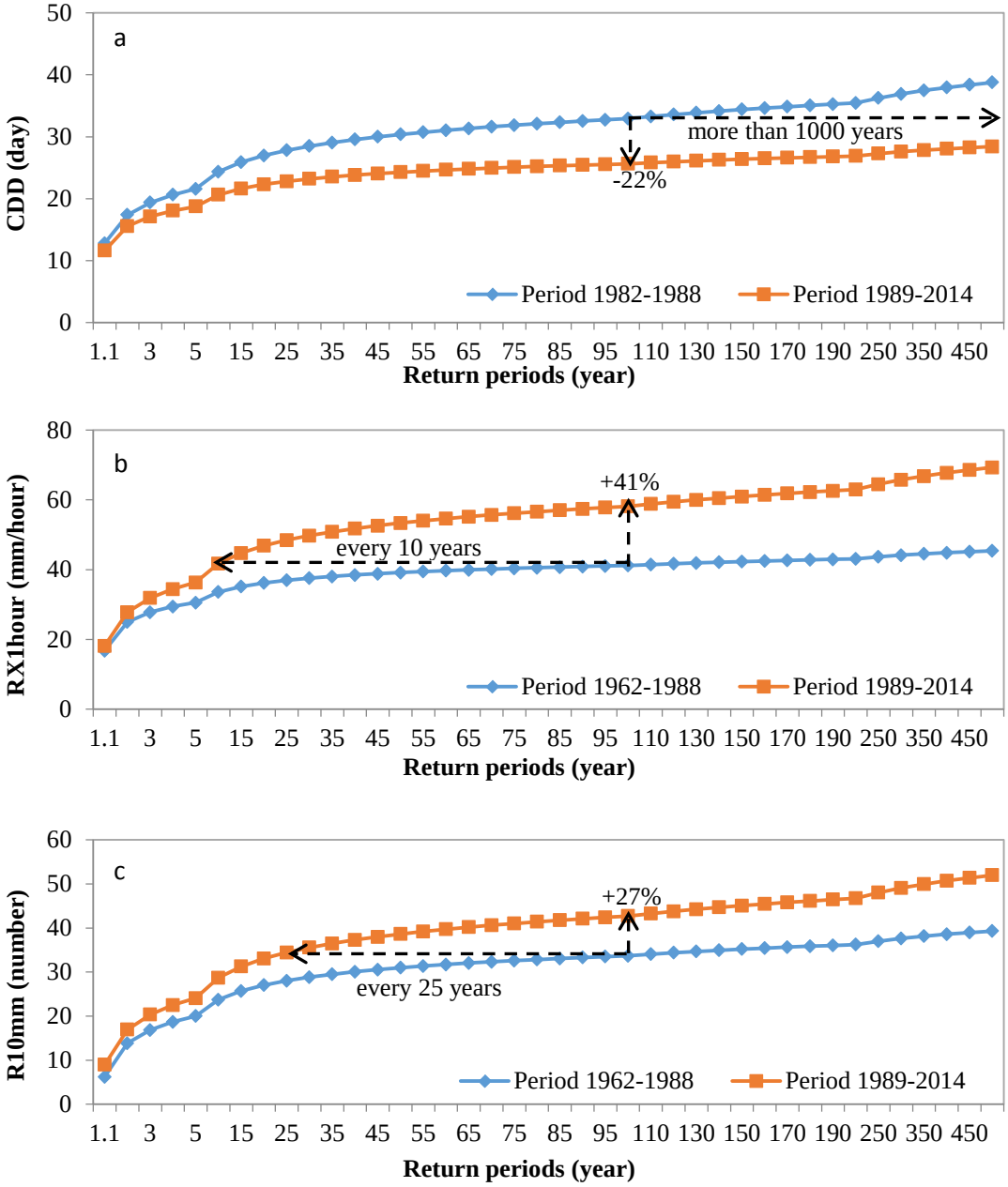

Figure 6-7 Annual inverse cumulative distribution functions of extreme precipitation indices: a) CDD, b) RX1hour, c) R10mm

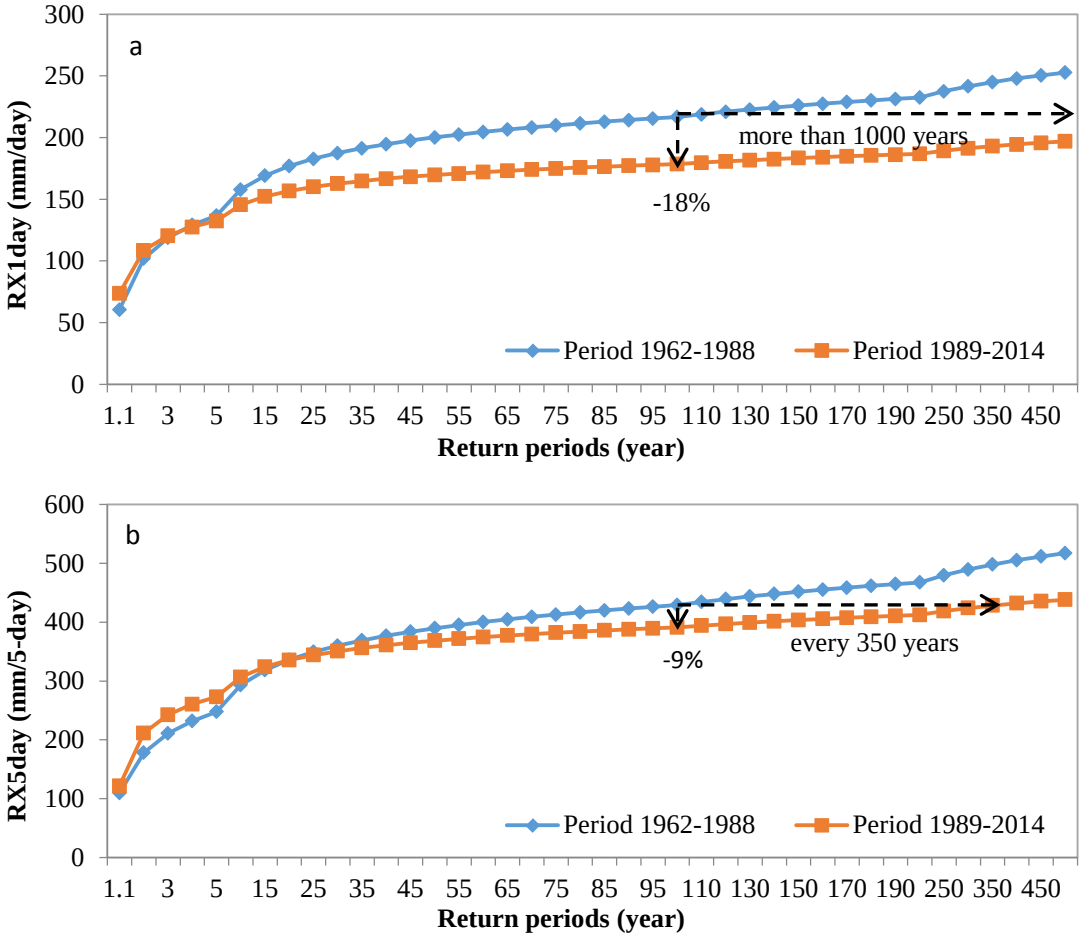

Figure 6-8 Annual inverse cumulative distribution functions of extreme precipitation indices: a) RX1day and b) RX5day

In addition, the probability distribution functions of TXn and TNn are shown in Figure 6-10 instead of the inverse cumulative distribution. This is because TXn and TNn are indices for extreme minimum events and cumulative distribution function cannot be used to evaluate extreme minimum values. It was found that the occurrence of extreme low daily maximum and minimum temperature were notably reduced in the period 1989-2014 and the magnitude of TXn and TNn had also increased in the period 1989-2014. There is notable warming in extreme temperature indices over 1962-2014.

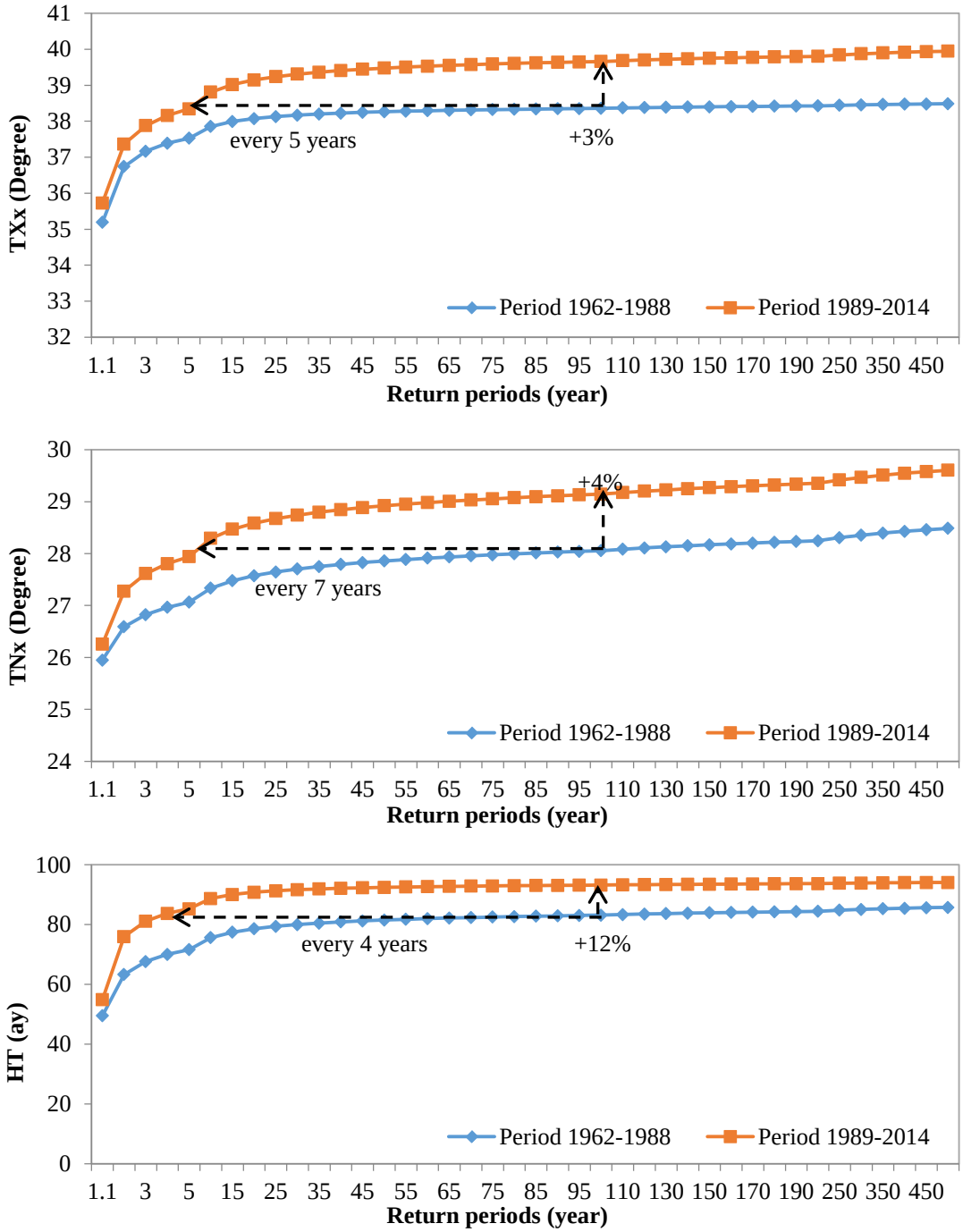

Figure 6-9 Annual inverse cumulative distribution functions of extreme temperature indices: a) TXx, b) TNx, c) HT

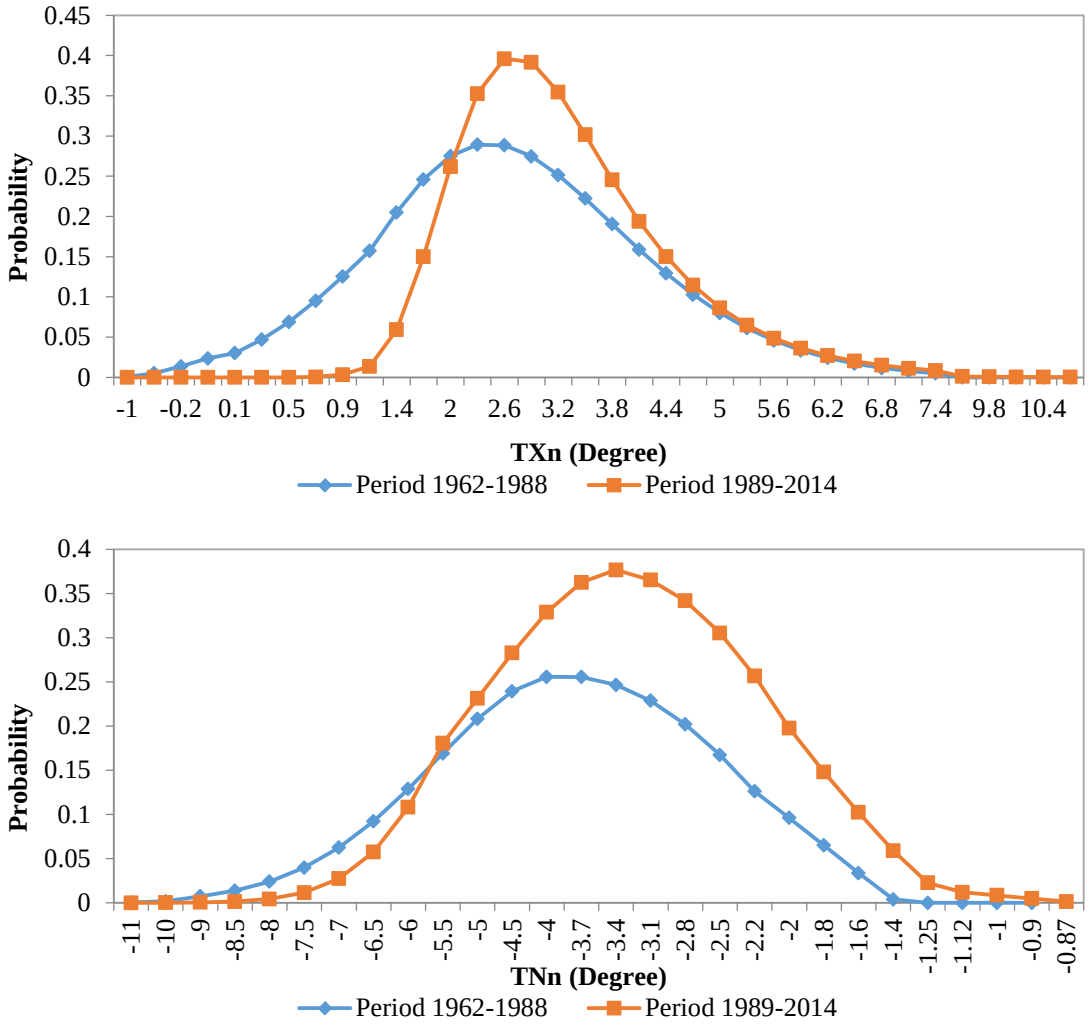

Figure 6-10 Annual probability distribution functions of TXn and TNn

6.4 Discussion

6.4.1 Implication of recent changes in climate extremes

The extreme temperature has obviously increased over 1962-2014 in the Kamo River basin. Similar findings are concluded in many regions of Japan. Most notably, the 2014 report of climate change monitoring by Japan Meteorological Agency (2015) showed that the occurrence of extreme high temperature increased and the occurrence of extreme low temperature decreased from 1901 to 2014.

Another finding is that there is an increase in the average condition of annual daily and 5-day maximum precipitation (2-year events), while there is a notable decrease in the magnitude of 100-year daily and 5-day maximum precipitation from P1 to P2. Thus, the results of extreme analysis would be different if the criterion of return period is changes. And there results agree with the previous findings in Chapter 4 that there is insignificant increase in annual precipitation, which has frequent fluctuation.

In addition, 100-year RX1hour and R10mm increased, whereas 100-year RX1day and RX5day decreased. The difference changes between extreme daily and hourly precipitation are probably caused by the effects of topography. Allamano et al (2009) found there was negative correlation between extreme precipitation and elevation. There is a feature that hourly precipitation is correlated mainly to the northward terrain slope, while daily precipitation is highly related to the eastward terrain slope (Miyajima and Fujibe, 2011).

Moreover, the changes in extreme hourly precipitation agree with the findings by other studies in different regions. Fujibe et al., (2005) concluded that hourly precipitation intensity had increased from 1898 to 2003 over Japan. Kanae et al., (2004) reported that hourly heavy precipitation at Tokyo in the 1990s was strong and frequent from 1890 to 1999. However, the changes in extreme daily precipitation are different from the findings of some studies. Fujibe et al. (2006) found that extreme daily precipitation had increased from 1901 to 2004 over Japan, while RX1day in the Kamo River basin decreased according to our study. Oguchi and Fujibe (2012) presented that the consecutive dry days (CDD) increased from 1901 to 2009 over Japan, while CDD decreased in the Kamo River basin. The probable reasons will be discussed in the next section 6.4.2.

6.4.2 Implication of changes in flood and drought

The changes in flood are highly related to the changes in heavy precipitation in the Kamo River basin. There are similarities in the changes of magnitude and return period between the indices of extreme precipitation and river discharge, for example CDS and CDD, SX1day and RX1day, etc.

The increase of SX1hour indicates that flood probability has increased over 1962-2014. This agrees with the findings by Miyajima and Fujibe (2011) over Japan. In addition, Tachikawa et al. (2011) also found that there was an increase in annual maximum hourly discharge over south regions of Kinki, Japan.

The decrease of the occurrence of extreme SN7day and CDS indicate that drought probability has decreased over 1962-2014. However, some studies have reported that there is an increase in no rainy days and low streamflow over Japan (Fujibe et al., 2006; Oguchi and Fujibe, 2012). For instance, Tachikawa et al., (2011) presented that there was a decrease in the daily low streamflow. The different findings in this study in KRB are likely to be caused by the spatial variability of climate. Duan et al. (2015) found spatial differences in the trends of precipitation extremes were obvious in Japan and the extreme change in Hokkaido was different from that in other regions. Another probability is due to the study period chosen. The results of trend detection and frequency analysis are of high relevance with time period. If it is extended or changed to different time periods, a different conclusion might be drawn (Bae et al., 2008).

6.4.3 Water resource management

The decrease in drought frequency and the increase in 2-year SX1day and SX5day are positive information for the decreasing streamflow. However, due to the requirement

of the Kamo river ecosystem (i.e. freshwater habitat) and natural amenities, the future policies of water management could be inclination to increase the water in the Kamo River by the indicator of the decrease in extreme SX1day and SX5day. In addition, the extreme hourly precipitation and peak flow became heavier and more frequent in the last 50 years. It clearly poses a challenge for the flood management. Also, the variation of extreme daily and 5-day floods represent a significant difference to patters across most other regions of Japan (Tachikawa et al., 2011; Duan et al., 2015). Apparently, hydrological responses to climate change are different from place to place at different scales. Scientific knowledge about the variations of hydrological cycle is thus clearly the first step in sustainable water management, and the present study thus makes a significant contribution in this direction.

6.4.4 Limitations

The extreme changes in river discharge were estimated using simulated values, which could be affected by uncertainties, associated with model dynamics and parameter values, although a well performance of HYPE has been proved in Chapter 5.

Also, the results of frequency analysis are of high relevance with time period. If it is extended or changed to different time periods, a different conclusion might be drawn (Bae et al., 2008). The sample size of each period is less than 30 years, the changes between these two periods may be induced by regular climatic activities instead of climate change. It is necessary to extend the periods in future study. Moreover, goodness of fit of probability distribution functions is important in frequency analysis. In this study, the SLSC test results show that the selected distribution function has relatively low fit for some indices in one period but good in the other period. This is probably due to the small sample size (less than 30) and it would bring biases in the

magnitude of changes in extreme indices. However, the facts of increase or decrease in frequency of extreme event are not affected. In the future, the other distributions and test methods will be tried.

In addition, there is no investigation on whether the statistically estimated extremes in discharge represented actual floods and droughts. Especially, for low flow, the duration period is decided by the magnitude of the threshold level. With a low level the likelihood for a high number of consecutive days being divided into several small consecutive dry days increases. In contrast, a high level might lead to a higher number of consecutive days. It is merit to evaluate whether the threshold level reflected historical disastrous drought or not.

Finally, seasonal and monthly changes of extremes in hydro-climatic variables patterns are of practical importance for water recourse management. The topic of how floods and droughts shift inter a year will be concerned in the future.

6.5 Conclusion

In this chapter, the variations of hydro-climatic extremes are evaluated by frequency analysis using a series of extreme indices of precipitation, temperature and river discharge. Three commonly used probability distribution functions for extremes analysis (LN3, GEV and Gamma) are applied and four criteria are used for goodness of fit test. The changes of extreme indices are quantified in magnitudes by the changes of 100-year event from P1 to P2 and in frequency by the changes of return period of P1 100-year event in P2 using inverse cumulative distribution functions. In addition, extreme low value events (SN7day, TXn and TNn) are estimated by the changes in occurrence of probability using probability density functions.

It was found that the changes in extreme streamflow in the Kamo River basin are highly correlated with the changes in extreme precipitation indicated by the similarities in the changes of magnitude and return period between the indices of extreme precipitation and river discharge.

In addition, the occurrence of drought has decreased and the occurrence of flood has increased over 1962-2014 according to the reduction in CDD and CDS and increase in RX1hour, R10mm and SX1hour. It was observed that the magnitude of 100-year events of RX1hour and SX1hour increased by 41% and 23% from P1 to P2, respectively. 100-year CDD and CDS decreased 22% and 34%, respectively. The increase in the occurrence of SN7day also indicates that the occurrence of drought has decreased. However, the occurrence of daily and 5-day 100-year flood events has decreased from the period 1962-1988 to the period 1989-2014, though the means of daily and 5-day maximum precipitation and streamflow have an increase.

The temperature increase is notably observed in the Kamo River basin. There is an obvious increase in the occurrence of extreme high temperature (TXx and TNx) and a decrease in the occurrence of extreme low temperature (TXn and TNn). Also, the hot days that daily maximum temperature is more than 30 °C in a year also have increased.

Finally, the goodness of fit test results show that the GEV distribution is adequate for most extreme indices, following by the LN3 and Gamma distributions. The GEV distribution is recommended as the first choice in extreme frequency analysis, when goodness of fit test is not conducted to determine the best distribution.

Reference

Alexander LV, Zhang X, Peterson TC, *et al.*, 2006. Global observed changes in daily climate extremes of temperature and precipitation. *Journal of Geophysical Research* 111, D05109.

Alias, N.E. (2014). Improving extreme precipitation estimates considering regional frequency analysis. Doctoral thesis, Kyoto University.

Allamano P, Claps P, Laio F and Thea C, 2009. A data-based assessment of the dependence of short-duration precipitation on elevation. *Physics and Chemistry of the Earth, Parts A/B/C* 34, 635-641.

Castillo E, Hadi AS, Balakrishnan N and Sarabia J-M, 2005. Extreme value and related models with applications in engineering and science. Wiley Hoboken, NJ.

Conover WJ and Conover W, 1980. Practical nonparametric statistics. New York: John Wiley.

Coumou D and Rahmstorf S, 2012. A decade of weather extremes. *Nature Climate Change* 2, 491-496.

Dai A, Trenberth KE and Qian T, 2004. A global dataset of Palmer Drought Severity Index for 1870-2002: Relationship with soil moisture and effects of surface warming. *Journal of Hydrometeorology* 5, 1117-1130.

Duan W, He B, Takara K, *et al.*, 2015. Changes of precipitation amounts and extremes over Japan between 1901 and 2012 and their connection to climate indices. *Climate Dynamics* 45, 2273-2292.

Field CB, 2012. Managing the risks of extreme events and disasters to advance climate change adaptation: special report of the intergovernmental panel on climate change. Cambridge University Press.

Fujibe F, Yamazaki N, Katsuyama M and Kobayashi K, 2005. The increasing trend of intense precipitation in Japan based on four-hourly data for a hundred years. *Sola* 1, 41-44.

Fujibe F, Yamazaki N and Kobayashi K, 2006. Long-term changes of heavy precipitation and dry weather in Japan (1901-2004). *Journal of the Meteorological Society of Japan* 84, 1033-1046.

Hirabayashi Y, Mahendran R, Koirala S, *et al.*, 2013. Global flood risk under climate change. *Nature Climate Change* 3, 816-821.

Japan Meteorological Agency (2015). "Report 2014 of climate change monitoring." EG: Electricity and gas 65(8): 17-19.

Hosking J and Wallis J, 2005. Regional frequency analysis: an approach based on L-moments. Cambridge University Press.

Kanae S, Oki T and Kashida A, 2004. Changes in hourly heavy precipitation at Tokyo from 1890 to 1999. *Journal of the Meteorological Society of Japan. . Ser. II* 82, 241-247.

Karl T, 2008. Weather and climate extremes in a changing climate: Regions of focus: North America, Hawaii, Caribbean, and US Pacific Islands. US Climate Change Science Program.

Katz RW, 2006. Hydrological Extremes. *Encyclopedia of Environmetrics.* John Wiley & Sons, Ltd.

Klein Tank AMG, Zwiers FW and Zhang X, 2009. Guidelines on analysis of extremes in a changing climate in support of informed decisions for adaptation. *Climate Data and Monitoring*, 1-52.

Krishnamurthy CKB, Lall U and Kwon H-H, 2009. Changing frequency and intensity of rainfall extremes over India from 1951 to 2003. *Journal of Climate* 22,

4737-4746.

Lehner B, Doll P, Alcamo J, Henrichs T and Kaspar F, 2006. Estimating the impact of global change on flood and drought risks in europe: A continental, integrated analysis. *Climatic Change* 75, 273-299.

Mann ME and Gleick PH, 2015. Climate change and California drought in the 21st century. *Proceedings of the National Academy of Sciences* 112, 3858-3859.

Milly PCD, Wetherald RT, Dunne KA and Delworth TL, 2002. Increasing risk of great floods in a changing climate. *Nature* 415, 514-517.

Miyajima J and Fujibe F, 2011. Climatology of extreme precipitation in Japan for different time scales. *Sola* 7, 157-160.

Murshudov GN, Vagin AA and Dodson EJ, 1997. Refinement of macromolecular structures by the maximum-likelihood method. *Acta Crystallographica Section D: Biological Crystallography* 53, 240-255.

Oguchi S and Fujibe M, 2012. Seasonal and regional features of long-term precipitation changes in Japan. *Papers in Meteorology and Geophysics* 63, 21-30.

Ohba M, Kadokura S, Yoshida Y, Nohara D and Toyoda Y, 2015. Anomalous Weather Patterns in Relation to Heavy Precipitation Events in Japan during the Baiu Season. *Journal of Hydrometeorology*, 688-701.

Parr D, Wang G and Ahmed KF, 2015. Hydrological changes in the U.S. Northeast using the Connecticut River Basin as a case study: Part 2. Projections of the future. *Global and Planetary Change* 133, 167-175.

Pokhrel Y, Hanasaki N, Koirala S, Kanae S and Oki T, 2010. Extreme river discharge under present and future climate conditions using high-resolution climate model data. *Methods* 1, 1-25.

Retchless D, Frey N, Wang C, Hung L-S and Yarnal B, 2014. Climate extremes in the

United States: recent research by physical geographers. *Physical Geography* 35, 3-21.

Sillmann J, Kharin VV, Zhang X, Zwiers FW and Bronaugh D, 2013a. Climate extremes indices in the CMIP5 multimodel ensemble: Part 1. Model evaluation in the present climate. *Journal of Geophysical Research: Atmospheres* 118, 1716-1733.

Sillmann J, Kharin VV, Zwiers FW, Zhang X and Bronaugh D, 2013b. Climate extremes indices in the CMIP5 multimodel ensemble: Part 2. Future climate projections. *Journal of Geophysical Research: Atmospheres* 118, 2473-2493.

Stephens MA, 1986. Tests based on EDF statistics. *Goodness-of-fit Techniques* 68, 97-193.

Tachikawa Y, Takino S, Fujioka Y, Yorozu K, Kim S and Shiiba M, 2011. Projection of river discharge of Japanese river basins under a climate change scenario. *J. Japan Soc. of Civil Eng.* 67, 1-15. [In Japanese]

Takara K, 2009. Frequency analysis of hydrological extreme events and how to consider climate change. *Water Resources and Water-Related Disasters under Climate Change,-Prediction, Impact Assessment and Adaptation, 19th UNESCO-IHP Training Course, Kyoto University*.

Takara K and Stedinger J, 1994. Recent Japanese contributions to frequency analysis and quantile lower bound estimators. *Stochastic and Statistical methods in hydrology and environmental engineering* 1, 217-234.

Takara K and Takasao T, 1988. Criteria for evaluating probability distribution models in hydrologic frequency analysis. *J. Japan Soc. of Civil Eng.* 393, 151-160. [In Japanese]

Takara K and Tosa K, 1999. Storm and flood frequency analysis using PMP/PMF

estimates. *Proceedings of the Proc. International symposium on floods and droughts, Nanjing, China*, 1999, 7-17.

Takasao T, Takara K and Shimizu A, 1986. A basic study on frequency analysis of hydrologic data in the Lake Biwa basin, Annual of Disas. *Prev. Res. Inst. Kyoto Univ* 29, 157-171.

Takeshita S, 2010. Influence on precipitation and the distribution in Miyazaki [Japan] Prefecture with climate changes. *Bulletin of the Faculty of Agriculture, Miyazaki University (Japan)*, 73-78.

Tanaka S and Takara K, 1999. Goodness-of-fit and Stability Assessment in Flood Frequency Analysis. *J. Japan Soc. of Civil Eng.* 43, 127-132. [In Japanese]

Yevjevich V, Engineer Y, Yevjevich V, Yevjevich V and Ingénieur Y, 1972. *Probability and statistics in hydrology*. Water resources publications Fort Collins, CO.

Zhang Q, Chen YD, Chen X and Li J, 2011a. Copula-based analysis of hydrological extremes and implications of hydrological behaviors in the Pearl River basin, China. *Journal of Hydrologic Engineering* 16, 598-607.

Zhang X, Alexander L, Hegerl GC, *et al.*, 2011b. Indices for monitoring changes in extremes based on daily temperature and precipitation data. *Wiley Interdisciplinary Reviews: Climate Change* 2, 851-870.

Zhou Y, Ma Z and Wang L, 2002. Chaotic dynamics of the flood series in the Huaihe River Basin for the last 500 years. *Journal of Hydrology* 258, 100-110.

Zolina O, Simmer C, Kapala A, *et al.*, 2014. Precipitation Variability and Extremes in Central Europe: New View from STAMMEX Results. *Bulletin of the American Meteorological Society* 95, 995-1002.

Chapter 7 Conclusion and Future Research

7.1 Conclusion

The relentless usage of fossil fuel, population growth, migration to urban areas and land use transition consequent global climate change have altered hydrological cycle, which might increase the risk of water-related disasters and bring challenges to water resource management. Due to the substantial spatial variability of climate and terrain characters, the hydrological processes and responses to climate change are regional dependent. Modern water management in Kyoto has begun about hundreds of years ago, which has great impact on the distribution of water resources. As an important cultural landscape and freshwater habitat, the streamflow variations of the Kamo River which flows through Kyoto city have significant impact on the water-related landscapes including freshwater ecosystem. In addition, due to Baiu front and typhoon, the basin of the Kamo River is vulnerable to water-related disasters. Understanding regional hydrological processes, in the context of climate change, land use change and present water management is necessary for sustainable water resources management in this basin. This study is conducted by focusing on the variations of long-term means and extreme events in hydro-climatic variables under the impact of climate and human activities using trend analysis, water balance analysis, hydrological simulation and frequency analysis. The main conclusions are summarized as follows:

1) According to the results of trend detection and anomaly analysis, the fluctuation in precipitation is frequent and intense since 1970s. Basin average precipitation has increased by 4.2 mm per year without statistical significance. And a significant upward trend was observed in winter, actually in February and December. In addition, the change in precipitation at a location is likely to be not in correspondence with regional average precipitation variations. The precipitation at Kyoto station presented different characteristics of changes compared with the data at other gauged stations and basin average precipitation.

2) A significant downward trend was found in river discharge at both annual and seasonal scales using non-parametric Mann-Kendall test and Sen's Slope estimator. The streamflow at Fukakusa station has decreased by 16.2 mm per year. In addition, the potential evapotranspiration generated by Penman-Monteith FAO 56 has increased due to the increases of temperature at annual, seasonal and monthly scales by using parametric linear regression t-test and non-parametric Mann-Kendall test. The potential evapotranspiration significantly increased by 1.3 mm per year from 1962 to 2014. The minimum temperature had the maximum increase per year (about 0.034℃). The magnitudes of the slope in maximum and air temperature were 0.020℃ and 0.027℃, respectively.

3) Based on water balance analysis and hydrological simulation, it was found that the impact of climate variability on river discharge varied at different time scales and the impact of land use on discharge was small. At annual scale, the effects of increase in precipitation diminished the effect of increase in evapotranspiration. The average annual natural streamflow increased by about 32.3mm from the period 1962-1976 to the period 1996-2010 due to climate variability. At seasonal and monthly scale, the combination effects of precipitation and evapotranspiration on streamflow are various. The changes

in natural discharge cannot be simply explained by the changes in the value of precipitation minus evapotranspiration.

4) Moreover, water management played a dominant role in the decrease of river discharge at different time scales. There was a decrease of 502.5 mm in annual average river discharge from the period 1962-1976 to the period 1996-2010 due to the impact of water management. The primary reasons in management for streamflow decreasing are the reduction of intake from Lake Biwa canal to Kamo River and the increase of drainage areas of the sewage system in Kyoto city. At the annual scale, about 72.2% of the reduction in streamflow was caused by the changes of water in Lake Biwa canal and 34.7% was induced by the variations sewage drainage areas.

5) There was an increase in the occurrence of flood and a decrease in the occurrence of drought according to the results of frequency analysis on extreme indices. It was observed that the magnitude of 100-year events of RX1hour, R10mm and SX1hour increased by 41%, 27% and 23% from the period 1962-1988 to the period 1989-2014, respectively. While 100-year CDD and CDS decreased by -22% and -34%, respectively. In addition, the changes in extreme streamflow are high correlated with the changes in extreme precipitation indicated by the similarities in the changes of magnitude and return period between the indices of extreme precipitation and river discharge.

6) Furthermore, maximum temperature have increased over 1962-2014. The hot days that daily maximum temperature is more than 30 °C in a year have increased 12% from the period 1962-1988 to the period 1989-2014. Also, there is an obvious increase in the occurrence of extreme high temperature (TXx and TNx) and a decrease in the occurrence of extreme low temperature (TXn and TNn).

7.2 Limitations and future work

There are still some limitations in this study. Probability distributions for extreme analysis and goodness of fit test requires more detailed studies because the SLSC test results show that the distribution functions used in the study have relatively low fit for some indices in certain period but good in the other period. In addition, the future probable changes in hydro-climatic variables in terms of long-term means and extremes will be considered. The prediction of future conditions is of merit for water recourse management. Beside these, the impact of statistical significant level, model performance improvement, probable maximum precipitation, and the extreme changes at the seasonal and monthly scales will be also considered in the future. Moreover, river discharge and water management database are needed to be improved. The streamflow data are unrealistic from 1978 to 1987. And the model calibration and validation are built based on the assumption that all the water from Biwa Lake (V_B) is either used by water treatment plant (V_S) or flows through Kamo River Canal (V_C) in the calibration and validation period. The distribution of water flows from Biwa Lake canal to the Uji River and Kamo River is unclear.

List of Publications

Papers in Journals

Maochuan Hu, Takahiro Sayama, Shusuke Takahashi and Kaoru Takara. Impact assessment of Human Activities and Climate Change on Annual Runoff in the Kamo River basin. *Annual Journal of Hydraulic Engineering, JSCE*, Vol.60, 2016.

Xingqi Zhang, Xinya Guo and **Maochuan Hu**. Hydrological effect of typical low impact development approaches in a residential district. *Natural Hazards*: 80(1): 389-400, 2016.

Maochuan Hu, Kaoru Takara, Weili Duan, Bin He and Pingping Luo. Integrated Assessment of Hydro-Climatology Variability in Kamo River Basin: Confronting Climate and Extremes. *International Journal of Sustainable Future for Human Security*, Vol.3, No.1, pp.46-55, 2015.

Maochuan Hu, Kaoru Takara, Pingping Luo, Bin He and Weili Duan, Climate Change and Land Use Change Impact Analysis in a Data Sparse Basin using a Hydrological Model, Annual Journal of Hydraulic Engineering, JSCE, Vol.58, pp.109-114, 2014.

Xingqi Zhang and **Maochuan Hu**, Effectiveness of Rainwater Harvesting in Runoff Volume Reduction in a Planned Industrial Park, China, Water Resources Management, Vol.28 (3), pp.671-682, 2014.

Weili Duan, Bin He, Kaoru Takara, Pingping Luo, Daniel Nover and **Maochuan Hu**, Modeling Suspended Sediment Sources and Transport in the Ishikari River Basin, Japan using SPARROW, Hydrology and Earth System Sciences Discussions, Vol.11 (10), pp.11037-11069, 2014.

Weili Duan, Bin He, Kaoru Takara, Pingping Luo, **Maochuan Hu**, Nor Eliza Alias, Masahito Ishihara and Yi Wang, Climate Change Impacts on Wave Characteristics along the Coast of Japan from 1986 to 2012, Journal of Coastal Research, Vol.68 (sp1), pp.97-104, 2014.

Maochuan Hu, Kaoru Takara and Xingqi Zhang, Analysis of Optimum Rainwater Tank Size in a Multi-building, Kyoto University Disaster Prevention Research Institute Annuals, Vol.56 (B), pp.53-58, 2013.

Xingqi Zhang, **Maochuan Hu**, Gang Chen and Youpeng Xu, Urban Rainwater Utilization and its Role in Mitigating Urban Waterlogging, Water Resources Management, Vol.26 (13), pp.3757-3766, 2012.

Papers in review

Maochuan Hu, Takahiro Sayama, Weili Duan, Kaoru Takara, Bin He and Pingping Luo, 2016. Assessment of hydrological extremes in the Kamo River Basin, Japan. *Hydrological Science Journal*. Revised

Book Chapter

Maochuan Hu, Bin He, Pingping Luo, Kaoru Takara and Weili Duan, 2015. Modeling the Effects of Land Use Change and Climate Change on Stream Flow Using GIS and Hydrological Model, Monitoring and Modeling of Global Changes: A Geomatics Perspective, Springer.

Proceedings of Conference

Maochuan Hu, Kaoru Takara, Weili Duan and Bin He, Assessment of Hydrological Extremes at a River Basin Scale, 12th Annual Meeting of the Asia Oceania Geosciences Society (AOGS 2015) and 7th Asia Pacific Association of Hydrology and Water Resources (APHW 2015), Suntec city, Singapore, August 02-07, 2015.

Maochuan Hu, Xingqi Zhang, Bin He, Kaoru Takara and Han Xue, Water Reuse and Flood Mitigation beneath Low Impact Development in an Urbanized Watershed: a Case Study in Nanjing, 3rd Water Research Conference, Shenzhen, China, January 11-14, 2015.

Maochuan Hu, Bin He and Kaoru Takara, Water and Nutrient Assessment in a Rural Data Sparse Catchment in South China: Set-up and Evaluation of HYPE Model, International Conference on Ecohydrology (ICE 2014), Yogyakarta, Indonesia, November 10-14, 2014.

Maochuan Hu, Kaoru Takara, Bin He, Xingqi Zhang, Pingping Luo, Weili Duan and Han Xue, Flood Mapping and the Variation of Inundation Area with the application of LID using Flo-2D model, 6th International Conference on Flood Management (ICFM), Sao Paulo, Brazil, September 16-18, 2014.

Maochuan Hu, Kaoru Takara, Bin He and Pingping Luo, Integrated Assessment of Stream Flow in Kamo River Basin: Confronting Land-use Change, GCOE-ARS Final Symposium 2013—Sustainability Science for Survivable Societies Coping with Extreme Weather and Water Conditions, Uji city, Japan, December 1-3, 2013.

Maochuan Hu, Bin He, Pingping Luo and Kaoru Takara, HYPE (Hydrological predictions for the Environment) Model Application in Kamo River Basin, Japan, 6th Asia Pacific Association of Hydrology and Water Resources (APHW 2013), Seoul, Korea, August 19-21, 2013.

Xingqi Zhang, **Maochuan Hu**, Gang Chen and Youpeng Xu, Urban rainwater utilization and its role in reducing of urban Waterlogging Disasters, 5th International Conference on Flood Management (ICFM), Tokyo, Japan, September 27-29, 2011.